Universidade de Lisboa
Faculdade de Ciências
Departamento de Química e Bioquímica

Organometallic Complexes of Tc(I) and Re(I) for radiometalation of biologically active peptides

Mariana Nogueira Pinto

Mestrado em Química Tecnológica
2014

Universidade de Lisboa
Faculdade de Ciências
Departamento de Química e Bioquímica

Organometallic Complexes of Tc(I) and Re(I) for radiometalation of biologically active peptides

Mariana Nogueira Pinto

Dissertação de Mestrado orientada pela Prof.ª Doutora Maria Helena Garcia

Mestrado em Química Tecnológica
2014

Esta tese foi realizada no âmbito do Mestrado em Química Tecnológica, ministrado pela Faculdade de Ciências da Universidade de Lisboa. O Mestrado foi aprovado pela deliberação nº 1068/2009, publicado em Diário da República, 2.ª série — N.º 69 — 8 de Abril de 2009.

O trabalho experimental foi efectuado no Grupo de Ciências Radiofarmacêutica, no Centro de Ciências e Tecnologias Nucleares (C^2TN) sediado nas instalações do Campus Tecnológico e Nuclear (CTN), do Pólo de Loures do Instituto Superior Técnico (IST), sob supervisão da Doutora Maria Paula Cabral Campello.

AGRADECIMENTOS

Os agradecimentos que tenho a fazer são genuínos e pequenos demais para esta página, uma vez que se estendem para além desta folha.

Primeiramente quero agradecer à minha Orientadora de coração, à Dra. Paula Campello, pela sua ajuda incessante, pela disponibilidade, pela simpatia e compreensão, pela motivação e por todos os ensinamentos. Sem ela, esta Tese seria praticamente impossível de concretizar.

À minha Orientadora, Prof. Dra. Helena Garcia, pelo acompanhamento, conselhos e interesse demonstrado.

Sem esquecer o apoio e incentivos importantes por parte da coordenação do Mestrado, nomeadamente à Prof. Dra. Maria José Lourenço, que sempre exigiu dos seus alunos o melhor que eles podem dar.

Ao Prof. Dr. António, agradeço por me ter introduzido o gosto pela área Radiofarmacêutica e ter sugerido o Tema desta Tese. Para além disso, por me ter apresentado ao Grupo de Ciências Radiofarmacêuticas do C²TN (IST-UL) e ainda por ter seguido de perto o meu trabalho, com discussões científicas importantes para o desenvolvimento do mesmo.

À Prof. Dra. Isabel Santos, agradeço por me ter recebido no Grupo de Ciências Radiofarmacêuticas

À Dra. Célia Fernandes agradeço a disponibilidade para resolver questões relacionadas com o HPLC e o facto de ter realizado todos os espectros de massa envolvidos neste trabalho.

À Dra. Paula Raposinho, estou grata pela realização dos estudos de biodistribuição e pelas incalculáveis discussões científicas acerca dos estudos de internalização e de uptake celular relativos aos péptidos.

Tenho de agradeçer à Inês Rodrigues a constante ajuda e companhia no laboratório, e também toda a paciência para me explicar as bases essenciais de todos os laboratórios e principalmente as dicas para poupar tempo e neurónios.

Agradeço ao Grupo de Ciências Radiofarmacêuticas (C²TN, IST-UL), em geral pela forma agradável como me receberam e pela constante ajuda ao longo do ano. De salientar a Susana Cunha, uma caixinha de surpresas, cheia de conhecimentos e experiência para partilhar, além de saber sempre onde encontrar tudo no laboratório.

Ainda quero destacar os momentos de trabalho, mas também de pausa, partilhados com a Leticia Quental, o Filipe Vultos e a Vera Ferreira.

À Maria Belo quero agradecer tudo. Algo difícil de colocar em palavras. Todas as conversas e desabafos, os incentivos e a boa companhia. No fundo, agradeço a amizade demonstrada e que certamente não acabará aqui.

Gostaria de agradeçer aos meus colegas do Mestrado de Química Tecnológica, ao Diogo Magalhães e à Rita Rosado, os "monos mais fixes" que eu conheço e com quem partilhei as experiências dos trabalhos de Tese e do Mestrado.

E por fim, os agradecimentos mais importantes. À minha família, pais e irmão, que me apoiaram sempre incondicionalmente e me proporcionaram manter o meu bem-estar emocional ao longo desta etapa.

Concluo de igual forma ao agradeçer aos meus amigos e ao Nuno, que me ajudaram na parte da descontração, na diversão e muito mais ao longo da vida.

Resumo

O desenvolvimento de Radiofármacos específicos capazes de detectar e/ou tratar neoplasias continua a ser uma das mais importantes áreas de investigação, uma vez que o cancro tem grandes taxas de incidência na população mundial. A utilização de péptidos biologicamente activos é uma estratégia para direccionar os radiofarmacos aos tumores de uma forma específica, já que os receptores que os reconhecem estão sobreexpressos numa grande variedade de tumores.

A introdução dos precursores organometálicos *fac*-$[M(H_2O)_3(CO)_3]^+$ (M=Re, ^{99m}Tc) permitiu explorar novas metodologias na marcação de péptidos com radioisótopos de Tc ou Re, com base numa química bem definida e facilmente adaptavél a diferentes estratégias de bioconjugação. Apesar desta vantagem, o uso de complexos de tricarbonilo de Tc(I)/Re(I) na marcação de péptidos tem conduzido a radiopéptidos com uma farmacocinética pouco favorável. Mais do que uma limitação intrinseca da aproximação tricarbonilo, esta tendência reflecte a utilização de ligandos bifuncionais (LBF) que originam péptidos radiomarcados com caracter lipofílico, com uma excreção hepatobiliar indesejável. Assim, a concepção de novos LBF para marcação de péptidos com a unidade *fac*-$[M(CO)_3]^+$ ainda se reveste de grande importância de modo a aproveitar a elevada estabilidade *in vitro/in vivo* dos complexos tricarbonilo.

Nesta tese, estudou-se a utilidade e influência de diferentes LBF tridentados na radiometalação de péptidos, com base na aproximação tricarbonilo. O péptido avaliado é um análogo de um Antagonista da Bombesina designado por AR. Este péptido é reconhecido pelos receptores do péptido libertador da Gastrina (GRP-r; Gastrin releasing peptide-receptor), sobreexpressos em vários cancros, nomeadamente no cancro da próstata.

Neste contexto, o objetivo a longo prazo do trabalho descrito nesta tese foi contribuir para a concepção de novos radiofármacos específicos baseados em $[^{99m}Tc(CO)_3]^+$ para a visualização *in vivo* dos receptores da GRP, nomeadamente nas neoplasias da próstata. Para alcançar este objetivo, foram sintetizados três quelantes bifuncionais diferentes e caracterizados pelas técnicas usuais em química, incluindo ESI-MS, RMN e HPLC, tendo sido posteriormente conjugados ao AR. Os ligandos bifuncionais estudados contêm pirazolilo (**L1 e L2**) e imidazolilo (**L3**) como grupos coordenantes e têm o mesmo número e tipo de átomos coordenantes (N,N,N). Esperava-se que conduzissem a

complexos estáveis de Re(I)/Tc(I), cuja farmacocinética fosse facilmente optimizada por introdução de grupos hidrofílicos nos anéis de pirazolilo e imidazolilo.

Os dois LBF derivados do pirazolilo que foram estudados contêm espaçadores diferentes entre o grupo carboxílico terminal a usar para ligação ao péptido e a amina central do ligando: **L1** contém um braço do tipo propilo e o **L2** um braço metilo. Desta forma, esperava-se avaliar a influência da distância do péptido biologicamente activo ao centro metálico no perfil biocinético dos radioconjugados resultantes. O **L1** é um quelante do tipo pirazolilo que já se encontra bastante estudado pelo Grupo de Ciências Radiofarmacêuticas (C²TN-IST) e tem excelentes propriedades de coordenação face ao centro metálico tricarbonilo, bem como fácil conjugação a biomoléculas, nomeadamente a péptidos.

Foi avaliada a capacidade de coordenação de um novo ligando (**L5**), contendo um grupo coordenante do tipo imidazolilo, face à unidade $[M(CO)_3]^+$(M = Re, ^{99m}Tc). No caso do ^{99m}Tc, este estudo conduziu a um complexo hidrofílico que foi obtido com rendimento e pureza radioquímica elevados. Este complexo apresenta ainda uma elevada estabilidade *in vitro* e *in vivo* e estudos de biodistribuição em ratinho mostraram que tem um perfil biocinético favorável. Assim, concluimos que este ligando tem características favoráveis para conjugação com péptidos biologicamente activos.

Os análogos peptidicos sintetizados basearam-se na seguinte sequência: DPhe^1-Gln^2-Trp^3-Ala^4-Val^5-Gly^6-His^7-Sta^8-Leu^9-NH_2 (**AR**), a qual foi acoplada a um espaçador de polietilinoglicol (PEG) por forma a aumentar a distância entre o centro metálico e a BM e conferir um carácter mais hidrofílico aos conjugados. Para a síntese destes péptidos foi utilizada a estratégia de sintese em fase sólida (resina) e aminoácidos protegidos com o grupo protector Fmoc. Após cada síntese e/ou conjugação a derivados dos ligandos **L1**-**L3**, os péptidos e conjugados peptídicos (**AR**, **ARPEG$_2$**, **L4**, **L6** e **L7**) foram purificados e caracterizados por ESI-MS e HPLC.

No caso do conjugado peptídico **L4**, resultante da conjugação de **ARPEG$_2$** a um derivado de **L1**, iniciou-se o estudo da sua radiomarcação com ^{99m}Tc. São necessários mais estudos para melhorar as condições de marcação e continuar com os necessários estudos de captação celular em células tumorais de cancro da próstata e de biodistribuição e farmacocinética em ratinhos com tumores induzidos. Esses estudos deverão ser alargados aos restantes bioconjugados de modo a investigar quais são os mais promissores para a concepção de novos radiofármacos para detecção de cancro da próstata.

Abstract

The development of radiopharmaceuticals for imaging/therapy of cancer remains an important issue. Biologically active peptides are used as specific carriers for the targeting of tumors, as many peptide receptors are overexpressed in tumors.

The organometallic precursors *fac*-$[M(H_2O)_3(CO)_3]^+$ (M=Re, ^{99m}Tc) allow the labeling of peptides based on a well-defined and easily adaptable chemistry. However, the resulting complexes are often lipophilic and show unfavorable pharmacokinetics. Improving this issue is still crucial, which requires the design of new BFC's (bifunctional chelator) for coordination of *fac*-$[M(CO)_3]^+$ and aiming to obtain radiopeptides with more favorable *in vivo* profile.

In this context, the goal of this thesis was to contribute for the development of radiopharmaceuticals based on $[^{99m}Tc(CO)_3]^+$ for *in vivo* imaging of tumors overexpressing the Gastrin Releasing Peptide-receptor (GRP-r,), particularly prostate cancer. To accomplish this goal, three different BFC's were synthesized, characterized and conjugated to a bombesin antagonist peptide, with known ability to target GRP-r.

The investigated BFC's contain pyrazolyl (**L1**, **L2**) and imidazolyl (**L3**) coordinating groups and can lead to hydrophilic complexes of Re(I)/Tc(I). Pyrazolyl-diamine chelators like **L1** and **L2** are known to have excellent properties to stabilize the $[M(CO)_3]^+$ core.On contrary, imidazolyl-diamine chelators like **L3** were not explored so far. Therefore, a model imidazolyl-diamine ligand, **L5**, was synthesized its coordination capacity towards the $[^{99m}Tc(CO)_3]^+$ evaluated. **L5** forms a hydrophilic complex, in high radiochemical yield and purity, which presents high stability *in vitro/in vivo* and a favorable biokinetic profile.

The synthesized peptide analogs were based on the following sequence: $DPhe^1$-Gln^2-Trp^3-Ala^4-Val^5-Gly^6-His^7-Sta^8-Leu^9-NH_2 (**AR**). A spacer of polyethyleglycol (PEG) was conjugated to **AR**, to impart a more hydrophilic character. For the synthesis of peptides, a solid phase (resin) and Fmoc strategy were used. These studies led to the synthesis of several peptide conjugates (**AR, ARPEG$_2$** and **L4**). It was inititated the study of the radiolabeling of **L4** with$[^{99m}Tc(CO)_3]^+$. This preliminary results indicated that more studies are needed to improve the labeling and proceed with the evaluation of cellular uptake and biodistribution/pharmacokinetics in mice with induced prostate tumors.

Palavras-Chave

Radiofármacos
Complexos de Tc(I) e Re(I)
Péptidos biológicamente activos
Antogonista da bombesina

Keywords

Radiopharmaceuticals
Tc(I) and Re(I) Complexes
Biologically active peptides
Bombesin antagonist

TABLE OF CONTENTS

Table of content of Figures

Table of content of Schemes

Table of content of Tables

Symbols and Abbreviations

A

AA – amino acid

ACN – Acetonitrile

ALA – Alanine

AR – Bombesin antagonist peptide

ARG – Arginine

ASN – Asparagine

ASP – Aspartic acid

Avg - Average

B

BFC - bifunctional chelator

BM - Biomolecule

BN - Bombesin

Boc - t-Butyloxycarbonyl

C

CT – computed tomography

Cys – Cysteine

D

d – Doublet

DCM – Diclomethane

dd – doublet of doublets

DMF - N,N-Dimethylformamide

DNA - Deoxyribonucleic acid

dt- doublet of triplets

E

ESI – MS Electrospray ionization–Mass spectroscopy

EtOAc – Ethyl acetate

G

GCC - gravity column chromatography

Gln – Glutamine

Glu – Glutamic acid

GRP-r – Gastrin realesing peptide receptor

Gly – Glycine

H

HATU - 1-[Bis(dimethylamino)methylene]-1*H*-1,2,3-triazolo[4,5-*b*]pyridinium 3-oxid hexafluorophosphate, *N*-[(Dimethylamino)-1*H*-1,2,3-triazolo-[4,5-*b*]pyridin-1-ylmethylene]-*N*-methylmethanaminium hexafluorophosphate *N*-oxide

HCL – Hidrocloridric acid

His – Histidine

I

Ile – Isoleucine

K

K_2CO_3 – Potassium carbonate

KCN - Potassium cyanide

KeV - kiloelectron volt

L

Leu – Leucine

LET – linear energy transfer

Lys – Lysine

M

mRNA – menssager ribonucleic acid

MeOH - Methanol

Met – Methionine

MBHA - 4-methylbenzhydrylamine

MS – Mass spectroscopy

m – multiplet

mTOR – mammalian target of rapamycin

^{m} – metastable isotope

MRI – magnetic resonance imaging

MHz – megahertz

N

^{nat} – Natural isotope

N_2 – Nitrogen

$NaBH_4$ – Sodium tetrahydridoborate

NaOH – Sodium hydroxide

NMR - Nuclear Magnetic Resonance Spectrometry

P

PC – Prostate Cancer

PRRT - peptide receptor radionuclide therapy

PEG – Polyehtilene Glycol

Phe – Phenylalanine

ppm – parts per million

PSA- Prostate-Specific Antigen

Pro – Proline

p.i. – post injection

Pd/C – Palladium on carbon

Q

q – quartet

QIT – quadrupole

quint – quintet

R

R.T. – Room Temperature

Rf- Retention fraction

RP-HLPC - Reversed-Phase High Performance Liquid Chromatography

S

s – Singlet

SCLCs - Small cell lung carcinomas

Ser – Serine

SPECT - Single Photon Emission Computed Tomography

SPPS - Solid Phase Peptide Synthesis

T

t – triplet

$T_{1/2}$ – Half-life

TFA - Trifluoroacetic acid

THF – Tetrahydrofurane

Thr – Threonine

TIS - Triisopropylsilane

TLC - Thin-layer chromatography

Tyr – Tyrosine

Trp – Tryptophan

Trt – Tripheylmethyl

U

US - Ultrasons

UV – Ultraviolet

V

Val – Valine

Vis – Visible

others

α – Alpha

β – Beta

γ – Gama

η – Yield

λ - wave lengh

y - years

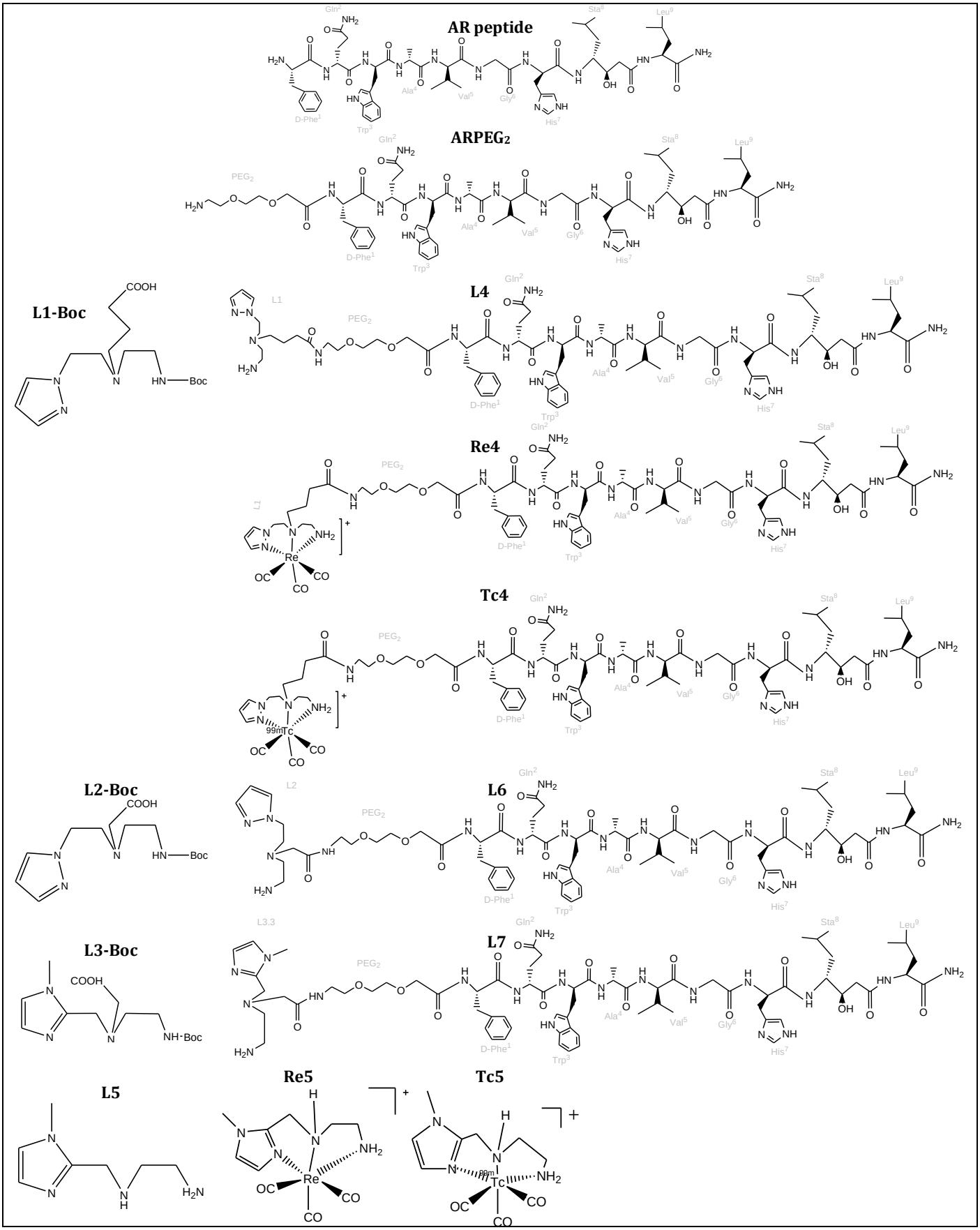

Figure A.1 - Main compounds described in this thesis.

Scope and Aim

Cancer remains one of the most devastating diseases with more than 10 million new cases each year world-wide, which is estimated to increase to 20% by 2020. However, due to a better understanding of cancer, and improved diagnostics equipment and treatment strategies, the mortality is decreasing.(1)

Prostate cancer (PC) has been the most frequently diagnosed noncutaneous cancer and is the second cause of cancer-related mortality after lung and bronchus cancers in men. (2,3) An optimal PC treatment is guided by a clinically staging of the cancer and selecting treatment options based on the stage. The treatment options for men with prostate cancer may include an expectant management (watchful waiting) or an active surveillance, that included surgery; radiation therapy; cryosurgery (cryotherapy); hormone therapy; chemotherapy; vaccine treatment and bone directed treatment. These treatments are generally used one at a time, although in some cases, they may be combined. (1)

Prostate cancer continues to be the second leading cause of cancer-related deaths for men in developed countries. Although the 5-year disease-specific survival rate of localized disease treated by surgery or radiotherapy is more than 90%. The effectiveness of systemic therapy for advanced prostate cancer is limited. Currently, depleting or blocking the action of androgens is the standard of care for men with advanced prostate cancer, but the response to treatment is not durable and with time prostate-specific antigen concentrations increase, indicating reactivated androgen-receptor signaling. (2)

Over the last years an emerging area in nuclear oncology deals with the evaluation of radiolabeled bioactive peptides for the diagnostic and therapy of tumors, due to overexpression of many peptide receptors in human tumors. Comparatively to other biomolecules, small peptides have many advantages. Namely, they can be easily synthesized and manipulated molecularly to optimize their in vivo half-life, receptor binding affinity and subsequently, pharmacokinetics. Peptide-based radiopharmaceuticals for therapeutic applications offer the ability to exploit the radioactive chelate as a radiocytotoxic unit and the bioactive molecule as a vector to localize the tumor.

Bombesin-like peptides such as gastrin-releasing peptide (GRP) have been shown to play a role in cancer promoting growth factors that stimulate tumor growth through specific receptors. The GRP receptor shows high over-expression in invasive prostatic neoplasias and also, although in less cases, in bone metastases of androgen-independent

prostate cancers. This represents the potential clinical basis for GRP receptor imaging of prostate cancer with radioactive compounds for early tumor diagnosis, followed by radiotherapy with radiolabeled bombesin analogues.

Despite the remarkable advances, the design of specific probes for targeted imaging or therapy still remains a great challenge and a demanding task within the field of radiopharmaceutical sciences. This is a multidisciplinary research area, which profits from the input of chemists, radiochemists, radiopharmacists and clinicians. Due to its chemical and nuclear properties, associated with the low cost and easy availability, ^{99m}Tc is among the most attractive radionuclides for SPECT imaging. In addition, rhenium, the congener 2nd row d-transition element from the 7th group, forms isostructural complexes with Tc and displays two radioisotopes (^{186}Re and ^{188}Re) suitable for targeted antitumor therapy.

Within this framework, the long term goal of the work described in this thesis was to contribute for the design of new specific radiopharmaceuticals based on the $^{99m}Tc(CO)_3$ core for *in vivo* visualization of GRP receptors overexpressed in prostatic cancer. To accomplish this goal, three different bifunctional chelators (BFC's) were synthesized and conjugated to a bombesin analog peptide. This peptide was chosen because it was already established its usefulness as a targeting vector for GRP receptors. It was intended to radiolabel the different bioconjugates with ^{99m}Tc, to evaluate the *in vitro* stability of the resulting complexes, as well as its *in vivo* profile in mice, to have an insight on their relevance in the design of specific radiopharmaceuticals for prostate cancer imaging. Finally, the most promising radiopeptides would be evaluated using imaging and biodistributions studies in mice bearing prostatic tumors. In summary, this work comprised the synthesis and characterization of BFC's; synthesis and characterization of the peptide analogues; conjugation of peptide analogues to the BFC's (figure A.1); Synthesis of organometallic complexes of ^{99m}Tc and ^{nat}Re, and finally *in vitro* and *in vivo* studies for some of the ^{99m}Tc complexes.

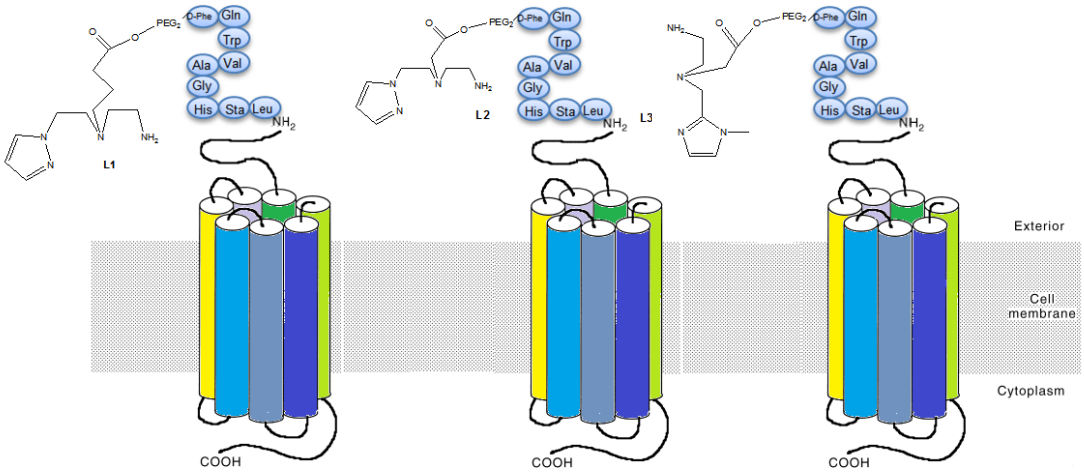

Figure A.1 - Representation of peptide conjugates studied in this Thesis**.**

This thesis is organized in five chapters. **Chapter 1** comprises a general introduction on nuclear imaging in oncology and radiopharmaceuticals. It covers also peptide related matters, such as the relevance of Gastrin Releasing Peptide-receptors (GRP-r) as a target for tumor imaging and therapy, and the use of radiolabeled Bombesin (BN) analogues for in vivo imaging of GRP-r. **Chapter 2** is dedicated to the description of all materials and methods used, namely the synthetic procedures.

The **3rd chapter** reports the results and discussions, and is divided into the synthesis of bifunctional chelators (BFC's), peptide synthesis and conjugation, radiolabeling studies and biodistribution evaluation.

Concluding remarks are presented in **chapter 4**, where is also scrutinized the options for the future work.

1. Introduction

1.1 NUCLEAR MEDICINE AND RADIOPHARMACEUTICALS

1.1.1 General Considerations

Nuclear medicine is a medical speciality that uses radiopharmaceuticals for diagnosis and/or therapy of several diseases. Radiopharmaceuticals are drugs with no pharmacological effect that contains in its composition a radionuclide. A radiopharmaceutical can be a small organic (e.g. ^{18}F-FDG), inorganic (e.g. Na^{131}I and Na^{18}F), or organometallic compound with defined composition, or can also be a small peptide, inhibitors or substrates of enzymes or large molecules such as antibody fragments, among others. (3–5)

1.1.2. Radionuclides

A nuclide is an atomic nucleus identified by a unique combination of a given number of protons and neutrons and the energy state of its nucleus. A nuclide can be specified by the notation: ${}^{A}_{Z}X_{N}$; where X is the chemical element symbol, Z is the atomic number (number of protons in the nucleus), N is the neutron number (number of neutrons in the nucleus), A is the mass number (A=N+Z, total number of nucleons in the nucleus). A radionuclide is an unstable form of a nuclide, due the unsuitable composition of the nucleus. Radionuclides disintegrate emitting gamma ray(γ) and/or particles α, β^-, β^+ or Auger electrons. They may occur naturally, but most of them are artificially produced in cyclotrons or reactors. It is also possible to have indirect production routes like radionuclide generators. In this case a radionuclide (parent), produced in a reactor or cyclotron, is immobilized in a chromatographic column, allowing the elution of another radionuclide (daughter) with shorter half-life. The advantage of this process is to deliver very short-lived radionuclides (daughter) to hospitals or medical institutions that don't have cyclotron or reactor facilities. (6–8)

1.1.3. Diagnosis *Vs.* Therapy in Nuclear Medicine

Depending on the medical application, diagnosis or therapy, different physical properties are required for the radionuclide. Among these properties, the type and energy of the emitted radiation as well as the half-life of the radionuclide (time necessary for half of the original atoms of the radionuclide to decay - $t_{1/2}$) of the nuclide are the most important for selection of a suitable radionuclide to the desired medical application. A **radiopharmaceutical for diagnosis** contains a positron- (β^+) or gamma- (γ) emitting radionuclide of sufficiently high energy (>50 keV) in their composition, whereas **therapeutic radiopharmaceuticals** have in their composition a radionuclide that emits

ionizing radiation with a high linear energy transfer (LET), to destroy selectively cells or tissues. The most used radionuclides for therapeutic purposes are β^-, but intense research involving α and Auger electron emitters is also underway, like the Phase III Study of Radium-223 Dichloride in Patients With Symptomatic Hormone Refractory Prostate Cancer With Skeletal Metastases (ALSYMPCA). (9)

1.1.4. Nuclear Imaging

Medicinal imaging is a key tool for improving the diagnosis of a large variety of diseases. Nowadays, the imaging techniques can be included into two large non-invasive categories: Structural and functional imaging techniques. X-ray, CT (Computed Tomography) and MRI (Magnetic Ressonance Imaging) are the three most important techniques that can primarily provide structural and anatomical imaging such as tumor location, size, morphology, and structural changes to adjacent tissues. (10–12)

Functional imaging, rather than anatomical, aims at the visualization and characterization of biochemical pathways, molecular interactions, drug pharmacokinetic and pharmacodynamics. Positron Emission Tomography (PET) and Single Photon Emission Computed Tomography (SPECT) are currently accepted as the most important functional imaging techniques, used in nuclear medicine. (13,14)

Examples of typical instruments available for small-animal molecular imaging are shown in Figure 1.2 and Table 1.1; they summarize the most relevant characteristics of imaging modalities mentioned above, including the major strengths and weaknesses. (13)

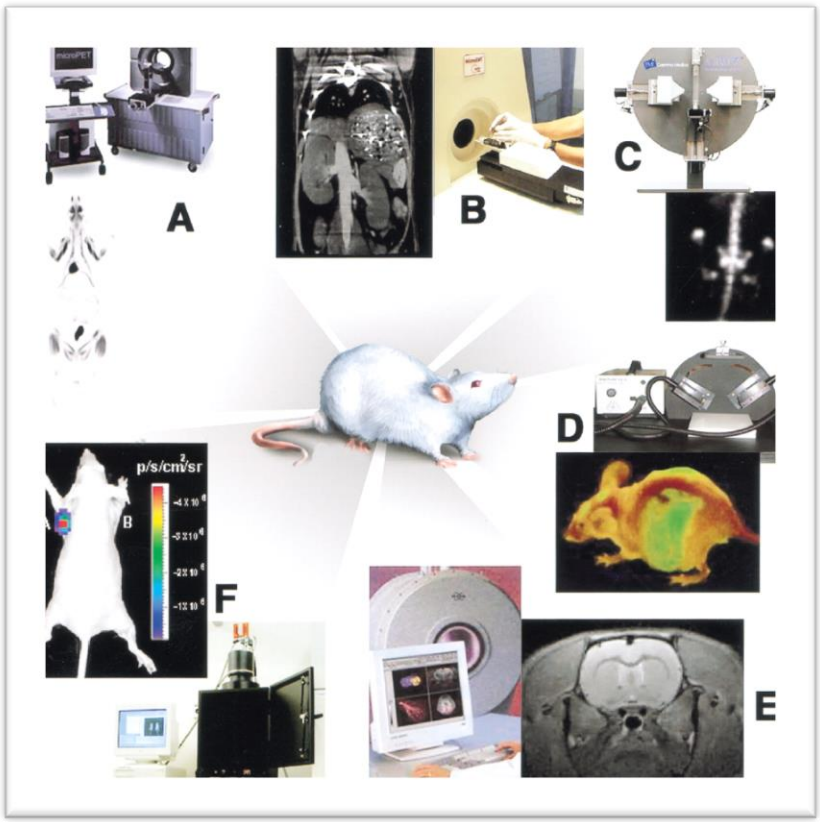

Figure 1.2 - Multiple imaging modalities are available for small-animal molecular imaging. There are views of typical instruments available, and illustrative examples of the variety of images that can be obtained with these modalities.(A) microPET whole-body coronal image of a rat injected with ^{18}F-FDG; (B) microCT coronal image of a mouse abdomen after injection of intravenous iodinated contrast medium. (C) microSPECT coronal image of a mouse abdomen and pelvic regions after injection of ^{99m}Tc methylene diphosphonate, (D) Optical reflectance fluorescence image of a mouse (E) microMRI coronal T2-weighted image of a mouse brain. (F) Optical bioluminescence image of a mouse. (*adapted from(13)).

Table 1.1 - Relevant characteristics of the imaging modalities used in clinical set.

	Technique	Spacial resolution	Amount of molecular probe used	Main use	Advantages	Disadvantages
Structural imaging	MRI	25-100 μm	mg-g	Morphological / Metabolic	Higher spatial resolution, combines morphological and functional imaging	Low sensitivity, amount of probe
	CT	50-200 μm	Not applicable	Morphological	Bone and tumor imaging, anatomical imaging	Limited soft tissue resolution
	US (ultrasons)	50-500 μm	mg-μg		Real time imaging, low cost	Limited spatial resolution
Functional Imaging	SPECT	1-2 mm	ng	Metabolic	Highest sensitivity, quick, easy, low cost, relatively high throughput	Low spatial resolution
	PET	1-2 mm			High sensitivity, isotopes can substitute naturally occurring atoms	Cyclotron or generator needed

From the nuclear imaging modalities, SPECT requires a radiopharmaceutical containing a radionuclide that emits gamma (γ radiation with energies between 80 and 300 KeV and a gamma camera for patient imaging). PET requires a radiopharmaceutical labeled with a positron-emitting radionuclide (β^+) and a PET camera. (15)

SPECT Imaging - The gamma rays are emitted by the radionuclide present in the injected radiopharmaceutical. These rays are detected by a gamma camera and an image of localized radioactivity is produced. In SPECT, the gamma camera rotates around the patient's body and the image is reconstructed to produce image slices.

Figure 1.3 – SPECT device from Philips.

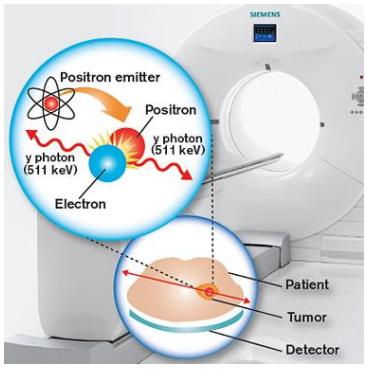

Figure 1.4– PET principle of detection. (108)

PET Imaging - The nucleus of the radionuclide decays by the emission of a positron (Positive electron) which will then combine with an electron from the surroundings tissues and annihilate to produce two characteristic γ-rays of energy equivalent to the rest mass energy of an electron (511keV). These are emitted at approximately 180º degrees away from each other. The PET scanner, used to detect the two photons, consists of a ring of scintillation detectors of which opposing detectors are in coincidence so that the

radionuclide can be determined to be in the region between the detector pair. Reconstruction of events between these multiple detector pair leads to a functional image of the brain.

Although SPECT imaging has lower sensitivity in the detector and less quantitative accuracy than PET, it has broader clinical applications. In fact, the radioisotopes used in SPECT have longer half-life ($t_{1/2}$) and therefore can be produced away from the site of administration and transported whenever required.(16) Moreover, the detection period can be widened, allowing the observation of biological processes *in vivo* over several hours or days after the administration of the radioactive probe.(17)

The γ-emitting radionuclides with the most suited characteristics for SPECT imaging are ^{99m}Tc ($t_{1/2}$ = 6.02 h, Eγ(max) = 140 keV), ^{123}I ($t_{1/2}$ = 13.20 h, Eγ(max) = 159 keV), ^{67}Ga ($t_{1/2}$ = 78.26 h, Eγ(max) = 296 keV), ^{201}Tl ($t_{1/2}$ = 72 h, Eγ(max) = 167 keV) and ^{111}In ($t_{1/2}$ = 67.9 h, Eγ(max) = 245 keV).

The β^+-emitting radioisotopes used in PET imaging are in general short-lived nonmetallic isotopes, such as ^{18}F ($t_{1/2}$ = 109.8 min, E_{β^+} (max) = 202 keV), ^{11}C ($t_{1/2}$ = 20.4 min, E_{β^+} (max) = 326 keV), ^{15}O ($t_{1/2}$ = 2.03 min, E_{β^+} (max) = 650 keV), and ^{13}N ($t_{1/2}$ = 9.98 min, E_{β^+} (max) = 432 keV). [^{18}F]-2-fluoro-2-deoxy-D-glucose (^{18}F-FDG) is the most widely used positron-emitting radiopharmaceutical for PET imaging, making ^{18}F the most used radionuclide in this nuclear imaging technique. ^{18}F-FDG has also shown clinical usefulness in cardiology and neurology, but it is used mainly in oncology, in the diagnosis, staging and post-therapy evaluation. (18,19)

Most PET radionuclides have the disadvantage of requiring costly technology, namely cyclotrons for their production and sophisticated automated methods for the radiosynthesis of the radiopharmaceuticals. Owing to the short half-life of most β^+-emitting radioisotopes, the production and synthesis must occur close to the administration site. A few β^+-emitting radiometals such as ^{64}Cu ($t_{1/2}$ = 12.7 h, E_{β^+}(max) = 660 keV) and ^{68}Ga ($t_{1/2}$ = 1.1 h, E_{β^+}(max) = 1899 keV) are also of great interest in developing new PET radiopharmaceuticals. In particular, ^{68}Ga is emerging as a PET radionuclide with clinical relevance, due not only to its physical and chemical properties, but mostly to its availability from a long-lived ^{68}Ge/^{68}Ga generator system. (3,5,7,20–22)

1.1.5. Nuclear Therapy

As mentioned before, radiopharmaceuticals for systemic radiotherapy have in their composition a radionuclide that emits ionizing radiation with a high LET to destroy selectively cells or tissues (β^- emitters, α- and Auger electron emitters). (7) These particles have different ranges in the tissues and can be described by the amount of transferred kinetic energy as a function of distance.

The selection of a radionuclide for therapy depends not only on the type, energy, half-life and range of emitted particles, but also on the size of the tumor or tissue to irradiate and treat. Since the penetration depth range of β^- particles in biological tissues is relatively long (0.1 – 10 mm), radiopharmaceuticals containing β^--emitting radionuclides can be used for the treatment of large solid tumors. (9,23)

Among **β^--emitting radionuclides** with potential application, ^{131}I ($t_{1/2}$ = 8.0 d, E_{β^-} (max) = 0.81 MeV, Eγ(max) = 0.364 MeV), ^{90}Y ($t_{1/2}$ = 2.7 d, E_{β^-} (max) = 2.27 MeV), ^{186}Re ($t_{1/2}$ = 3.8 d, E_{β^-}(max) = 1.07 MeV, Eγ(max) = 0.137 MeV), and, more recently, ^{188}Re ($t_{1/2}$ = 0.7 d, E_{β^-} (max) = 2.10 MeV, Eγ(max) = 0.155 MeV), are used in the clinical onset for the treatment of different tumor types. Moreover, the radiolanthanides ^{153}Sm ($t_{1/2}$ = 1.9 d, E_{β^-} (max) = 0.8 MeV, Eγ(max) = 0.103 MeV), ^{166}Ho ($t_{1/2}$ = 1.1 d E_{β^-} (max) = 1.86 MeV, Eγ(max) = 0.081 MeV) and ^{177}Lu ($t_{1/2}$ = 6.7 d, E_{β}- (max) = 0.497 MeV, Eγ(max) = 0.208 MeV) have been fully explored both at the preclinical and clinical levels as bone palliative agents (^{153}Sm, ^{166}Ho) and for peptide receptor radionuclide therapy in the case of ^{177}Lu-labeled somatostatin analogs. (23–27)

The **α particles** are heavy and charged helium nuclei with high LET. These particles “travel” only short distances and cause the most ionizing damage over a small distance (30 – 80 μm). Hence, α-emitting radionuclides are appropriate for the treatment of small tumors and/or metastasis. (9) Most of the α-emitters have a half-life that is too long to be compatible with *in vivo* applications. As a result, only a few of these radioisotopes have received serious attention for radiotherapeutic applications, namely, ^{211}At ($t_{1/2}$ = 7.2 h, $E_{\alpha(avg)}$ = 6.8 MeV), ^{212}Bi ($t_{1/2}$ = 1 h, $E_{\alpha(avg)}$ = 7.8 MeV) and ^{223}Ra ($t_{1/2}$ = 11.4 d, $E_{\alpha(avg)}$ = 5.65 MeV). (23,24,28,29) It is worth mentioning that $^{223}RaCl_2$ (Alpharadin®) was explored in the treatment of skeletal metastases and due to the promising results obtained this compound is currently under clinical evaluation for the treatment of bone metastases resulting from prostate cancer.

The **Auger electrons** are less energetic particles with a very short range of penetration (< 1 μm), having a LET similar to that of α particles, which makes them potentially interesting for therapy. Unlike α and β^- particles, treatment based on Auger electron-emitters requires the targeting of individual cells, specifically the DNA in the nucleus. Despite the multiple obstacles that have to be overpass, Auger electron therapy approaches remain very appealing. Among the available Auger electrons-emitting radionuclides, ^{125}I ($t_{1/2}$ = 57 d, 24 electrons/decay), ^{111}In ($t_{1/2}$ = 67 h, 14 electrons/decay), ^{67}Ga ($t_{1/2}$ = 78 h, 4 electrons/decay) and ^{99m}Tc ($t_{1/2}$ = 6.02 h, 4 electrons s/decay) are the most interesting for potential clinical applications. (9,24,30–32)

Perfusion and Specific Radiopharmaceuticals

The radiopharmaceuticals can be classified according to their biodistributions profile as **perfusion** or first generation radiopharmaceutical and **specific** or second generation radiopharmaceutical. Most of the radiopharmaceuticals in clinical use are perfusion agents, but nowadays most of the research efforts are directed to specific radiopharmaceuticals for diagnostic and/or therapy. The biodistribution of perfusion agents depends mainly on their lipophilicity, size and charge. These agents are transported in the blood and delivered to the target organ in the proportion of the blood flow. A wide variety of compounds were successfully developed for imaging organs, such as liver, kidney, heart or brain, giving information on a pathologic condition. (6,33,34)

In the last decade, due to the advances in molecular biology and the consequent identification and comprehension of molecular mechanisms that are the base of several diseases, the most recent radiopharmaceuticals in the market are specific radiopharmaceuticals. The targeting capability of these compounds depends on a biologically active biomolecule (BM), which can be a small organic BM, a small peptide, an antibody, a nanobody, sugars, inhibitors or substrates of enzymes, nucleotides or oligonucleotides. The capacity of the BM to recognize a certain molecular target (receptor, antigen, enzyme, DNA, mRNA, etc) will determine the radiopharmaceutical uptake in the target organ or tissue.

Since the end of 1980's, an intensive research for developing specific radiopharmaceuticals is being carried out, but only some cases were successful in getting to clinical use. (4,6) In fact, this is a challenging task, since it is necessary to conjugate the radionuclide to a biomolecule without interfering with its biological properties. For the design of specific radiopharmaceuticals there are three general strategies: the integrated, the hybrid and the bifuncional approach (Figure 1.5). (6,23,34–36)

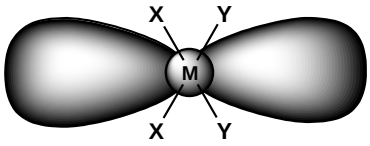

Figure 1.5– Representation of the integrated approach.

The integrated approach involves the substitution of a part of a biologically active molecule by a metal unit. This replacement must minimize changes in the structure, molecular size and conformation. Figure 1.5 presents the basis of the integrated approach and figure 1.6 shows examples of this approach. So far, integrated approach did not provide good results, as the resulting molecules presented low specificity and biological affinity for the receptors.(36,37)

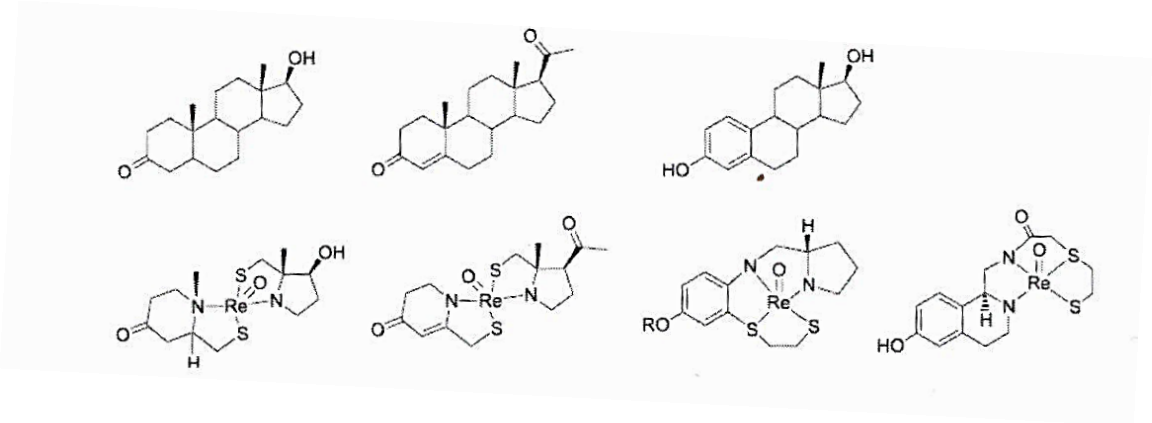

Figure 1.6 – Exemples of the Integrated approach. Rhenium complexes which mimic the structure of dihydrotestoterone, progesterone and estradiol. (36)

In the hybrid approach, the metal is stabilized by functional groups naturally occurring or synthetically introduced in the BM. These groups are usually tripeptides, such as GLY-GLY-GLY, CYs- GLY-GLY or CLYs-GLY-CYs. The small peptide sequence can be part of a linear or cyclic polypeptide. In some cases, the coordination of the radiometal to such amino acids can promote the cyclization of the polypeptide, improving the affinity for the receptors and increasing the *in vivo* stability. An example of such approach is the ^{99m}Tc(V)-Depreotide (NeoTect®) (Figure 1.7) a radiopharmaceutical for imaging of somatostatin receptors pulmonary masses, in clinical use. (4,6)

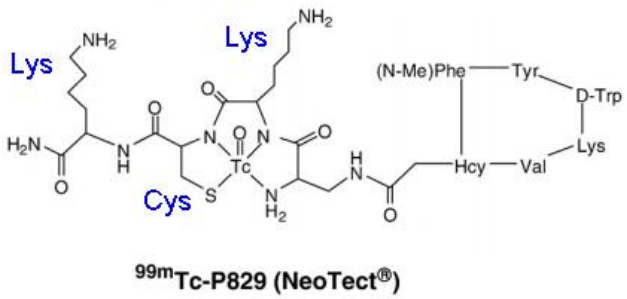

Figure 1.7 – Molecular configuration of NeoTect®. (38)

The bifunctional approach (Figure 1.8) has been the most exploited for the development of specific radiopharmaceuticals.

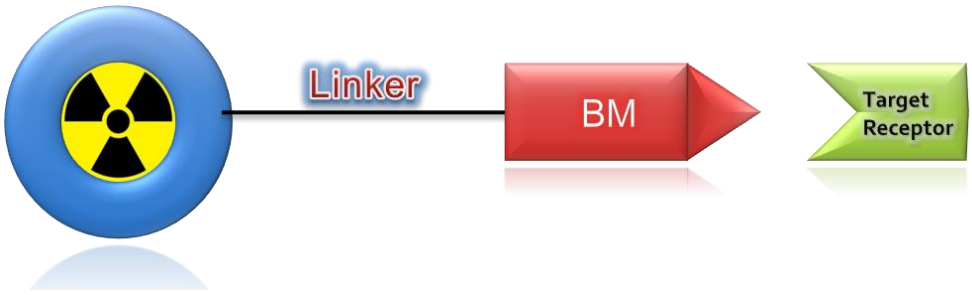

Figure 1.8 – Representation of the Bifuntional Approach (BFA); BM= biomolecule

This approach uses a bifunctional chelator (BFC) that strongly coordinates the metal ion, through appropriate coordinating groups, and is covalently attached to the biomolecule, which much interact specifically with the desired target. The nature of the BFC depends on the metal and its oxidation state. A spacer/linker between the metal and the biomolecule may exist, to modulate either the pharmacokinetics of the compound and/or its biological activity. This approach has been successfully used for the development of some radiopharmaceuticals, as it is for example the case of Octreoscan®, a radiopharmaceutical based on ^{111}In in clinical use for the imaging of neuroendocrine tumors. (39)

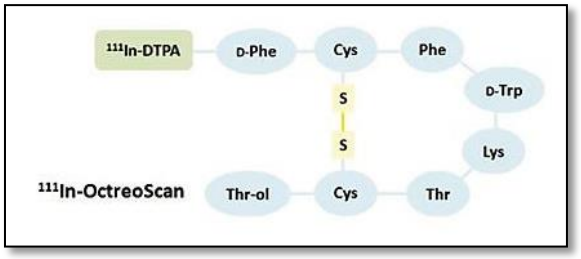

Figure 1.9 – ^{111}In-OctreoScan. In this case, the BFC used is 2-[Bis[2-[bis(carboxymethyl)amino]ethyl]amino]acetic acid (DTPA).

1.2. TECHNETIUM AND RHENIUM COORDINATION CHEMISTRY RELEVANT FOR NUCLEAR MEDICINE

Technetium was discovered in 1937 by Perrier and Segrè in a sample of molybdenium, which was irradiated by deuterons. The new element received its name from the Greek word *technetos*, meaning artificial, because technetium was the first element previously unknown on earth to be made artificially. In 1939 Seaborg and Segrè observed that molybdenum-98 irradiated with slow neutrons gave rise to ^{99}Tc through decay of the metastable isomer, ^{99m}Tc. Eventually 21 isotopes of technetium were discovered ranging from ^{90}Tc to ^{110}Tc, with technetium-110 having the shortest half life (0.86 Sec) and ^{97}Tc the longest (2.6 x 106 y). All technetium isotopes are radioactive. In the 1950s, a purification work on the tellurium-132 / iodine-132 generator at Brookhaven National Laboratory (BNL) turned up a contaminant which was proved to be technetium. The technetium contaminant was due to the presence of ^{99}Mo in the chemical separation, which was also present, because it had followed tellurium in the chemical separation process. This discovery eventually led to the production of the ^{99}Mo/^{99m}Tc generator in 1957 at BNL. Final improvements were made by Powell Richards. (40)

Rhenium, first detected by Noddack, Tacke and Berg in 1925 in the X-ray spectra of certain mineral concentrate, was the last of the stable elements to be discovered. Rhenium occurs naturally as a mixture of two isotopes: ^{185}Re(37.4%) and ^{187}Re(62.6%) and has two radioactive isotopes with an interest in nuclear medicine: ^{186}Re and ^{188}Re, two β^- emitters that can be used in therapy. Due to its availability from the generator (^{188}W/^{188}Re) and favorable nuclear properties, ^{188}Re is being intensively studied for the design of therapeutics radiopharmaceuticals.

Technetium (Tc) and rhenium (Re) are group 7 transition metals, belonging respectively to the 2nd and 3rd transition series, with atomic numbers 43 and 75 and

electronic configurations [Kr]$4d^5 5s^2$ and [Xe]$4f^{14} 5d^5 6s^2$, respectively. Tc complexes can have the metal in the oxidation states -I (d^8) to +VII (d^0), whereas for Re complexes the metal presents oxidation states -III (d^{10}) to +VII (d^0). These metals present very similar atomic radius (Tc, 1.36 Å; Re, 1.37 Å), forming structurally analog complexes. For that reason, the characterization of ^{99m}Tc complexes (obtained at very low concentration, 10^{-10}-10^{-7}M) is usually supported by the synthesis of analogs rhenium complexes. However, there are differences between both metals that must be taken into consideration in the preparation of Tc and Re complexes. The most striking difference is related to the higher kinetic inertness and easier oxidation associated to Re complexes. (7,41)

1.2.1. Radiochemistry of Technetium

The growth and wide application of diagnostic nuclear medicine have been mainly driven by the coordination chemistry and unique features of technetium. Among the 21 known artificial isotopes, ^{99m}Tc is the most useful radioisotope in nuclear medicine. The importance of ^{99m}Tc in nuclear medicine is related to its almost ideal characteristics: (4,34)

- Half-life of 6.02h is optimal for diagnostic, which is long enough to examine metabolic processes and yet short enough to minimize the radiation dose to the patient;
- γ-emitter (140 keV) with energy sufficiently high to penetrate easily the human body and to be detected externally by a gamma camera, and sufficiently low to minimize the dose to the patient;
- Available at reduced prices from a commercial ^{99}Mo/^{99m}Tc generator, being one of the greatest advantages of this radionuclide;
- Diverse coordination chemistry, which enables the preparation of a wide variety of complexes with different physicochemical and biological properties.

The prominence achieved by ^{99m}Tc as a useful radioisotope in nuclear medicine is directly related to the design and development of a ^{99}Mo/^{99m}Tc generator in the late 1950's. (42–44)

Molybdenium-99 (^{99}Mo), with a half-life of 66h, undergoes a radioactive decay, emitting β^- particles, in which 87% of the ^{99}Mo atoms is converted directly into the metastable state ^{99m}Tc, whereas 13% pass directly to the fundamental state ^{99}Tc (Fig 1.10)

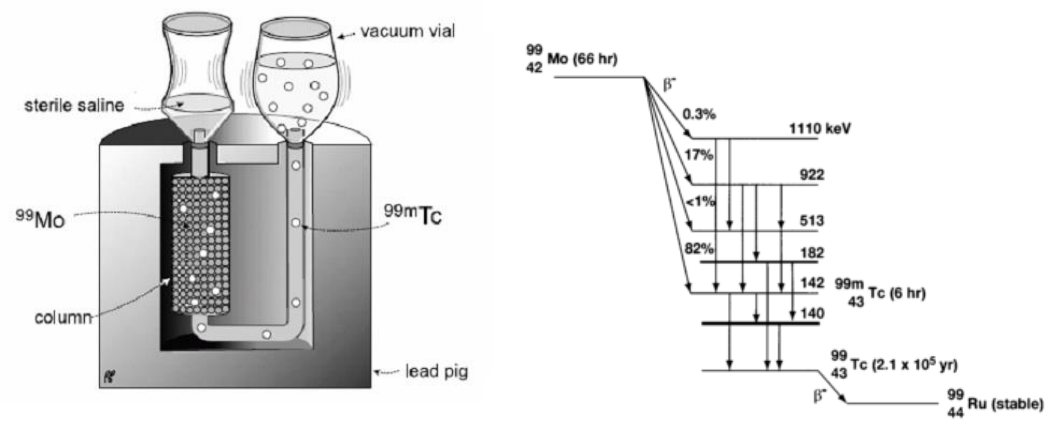

Figure 1.10 – Left: illustration of the contents of a $^{99}Mo/^{99m}Tc$ generator;Right: Decay scheme of ^{99}Mo. There is a 2-keV isomeric transition from the 142-keV level to the 140-keV level, which occurs by internal conversion. Approximately 87% of the total ^{99}Mo ultimately decays to ^{99m}Tc and the remaining 13% decays to ^{99}Tc. (7)

1.2.2. Coordination chemistry of ^{99m}Tc

The design of ^{99m}Tc-radiopharmaceuticals depends on the understanding of the coordination chemistry of ^{99m}Tc. Factors such as stable oxidation states and core structures are crucial in the design of effective target-specific ^{99m}Tc-radiopharmaceuticals.

The $[^{99m}TcO_4]^-$ anion, also known by pertechnetate, presents the metal in the highest oxidation state possible (+VII) being an easily accessible precursor in the synthesis of all ^{99m}Tc-based complexes for imaging application. It is the most stable form of technetium in aqueous solution, however, does not bind directly to any ligand and thus, for the synthesis of a ^{99m}Tc-radiopharmaceutical, reduction of $^{99m}Tc(VII)$ to a lower oxidation state in the presence of a suitable ligand is a prerequisite. Several reducing agents such as tin salts ($SnCl_2$, tin citrate, tin tartrate) or sodium borohydride, as well as different reaction conditions (pH, temperature, concentration) are used to reduce $[TcO_4]^-$ in aqueous solution, yielding a technetium core in a lower oxidation state that is stabilized by a suitable chelator. (5,9) When reduced in the presence of a ligand, the $[^{99m}TcO_4]^-$ usually does not release all the oxygen atoms, leading to complexes with different ^{99m}Tc cores.(45)

^{99m}Tc is usually used in the oxidation state +V as $[^{99m}TcO]^{3+}$ or $[^{99m}TcO_2]^+$ cores.(6) The coordination chemistry of the $[^{99m}TcO]^{3+}$ core has been explored for a long time but, more recently, a lot of attention has been focused on the use of organometallic cores for the radiolabelling of BMs. In fact, the $^{99m}Tc(I)$- and Re(I)-tricarbonyl core $[M(H_2O)_3(CO)_3]^+$

(M = ^{99m}Tc/^{188}Re), or simply the $[M(CO)^3]^+$ core, has been adopted as an alternative strategy to the ^{99m}Tc(V) complexes for the synthesis of ^{99m}Tc-radiopharmaceuticals. Nowadays, the research is focused on the synthesis of new chelators that can coordinate strongly to the $[M(CO)_3]^+$ core. (6,20,33,45)

1.2.2.1. The $[M(CO)_3]^+$ core (M = ^{99m}Tc, Re)

The $[M(CO)_3]^+$ core (M = ^{99m}Tc, Re) has been adopted as an alternative strategy to the ^{99m}Tc(V) complexes for the synthesis of ^{99m}Tc-radiopharmaceuticals. Nowadays, the research is focused on the synthesis of new chelators that can coordinate strongly to the $[M(CO)_3]^+$ core. (6,20,33,45)

Alberto et al. were the first to report the one-step synthesis of an organometallic Tc(I) aqua-ion, $[^{99m}Tc(H_2O)_3(CO)_3]^+$, useful as a precursor for the radiolabelling of BMs for diagnostic purposes. The Tc(I)-tricarbonyl precursor was synthesized by direct reduction of the $[^{99m}TcO_4]^-$ from the oxidation state +VII to +I, using sodium boranocarbonate ($Na_2[H_3BCO_2]$) as reductant and also as an in situ source of carbon monoxide. (46) Nowadays, the precursor $[^{99m}Tc(H_2O)_3(CO)_3]^+$ can be obtained in quantitative yield by directly adding $[^{99m}TcO_4]^-$ in 0.9% NaCl to a lyophilized commercial kit (IsoLink® kit, Mallinckrodt-Covidien, Petten, The Netherlands), followed by incubation at 100 °C for 20 minutes. The ready availability of the precursor directly from the $[^{99m}TcO_4]^-$ constitutes one advantage of the use of this ^{99m}Tc(I)-tricarbonyl precursor. The preparation of the Re homolog $[^{188}Re(H_2O)_3(CO)_3]^+$ was also accomplished, although using a procedure slightly different from that envolved the preparation of the Tc(I)-tricarbonyl precursor, since Re is more difficult to reduce and reacts, in general, much slower, as previously mentioned. (45,47)

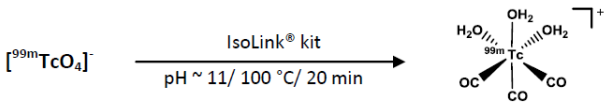

Figure 1.11 - Synthesis of the organometallic precursor $[^{99m}Tc\ (H_2O)_3(CO)_3]^+$.

The $[M(CO)_3]^+$ core is stable, even at high temperature and extended reaction time.(48) Complexes of $[M(CO)_3]^+$ exhibit a d^6 low-spin electronic configuration and, for that reason, are kinetically inert. The core contains three tightly coordinated CO ligands and three water molecules, which are very labile and can be readily replaced by mono-, bi- or tridentate chelators.(49) The tridentate chelators form ^{99m}Tc(I)-tricarbonyl complexes

with the highest *in vivo* stability, which is essential for medical applications.(50) The $[M(CO)_3]^+$ core is very compact, being significantly smaller than the complexes in the oxidation state (+V). This fact can be an advantage since it is thought that the smaller the complex, the higher the possibility that the biological activity will not be altered.(17,49)

The three water molecules in the precursor *fac*-$[^{99m}Tc(CO)_3(H_2O)_3]^+$ are labile with respect to substitution, and the precursor can interact with potential coordination sites in proteins in human serum (e.g. histidine and cysteine residues). Therefore, the precursor itself is not suitable for diagnostic purposes, displaying a very unfavorable biological profile as demonstrated by biodistribution studies in mice. (51) Hence, to develop suitable radiopharmaceuticals based on this core, it is necessary to replace the water molecules by mono, bi, or tridentate ligands to form stable complexes. A wide variety of organometallic complexes have already been described, with those stabilized by tridentate chelating systems displaying the highest stability both in vitro and vivo. (52) In Figure 1.12 are represented selected complexes, stabilized by tridentate bifunctional chelators, bearing or not pendant targeting moieties. The diverse coordination chemistry of the $[M(CO)_3]^+$ core offers an opportunity for the development of new chelators.

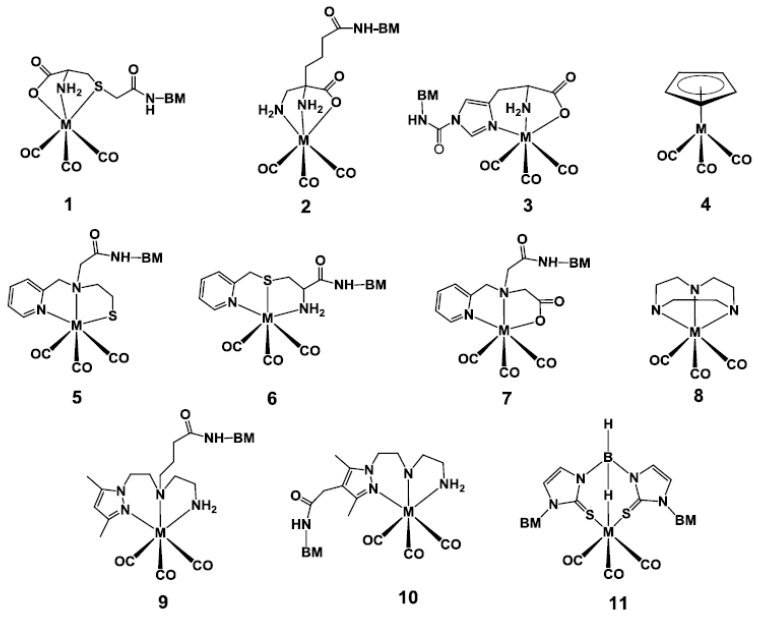

Figure 1.12 - Examples of $M(CO)_3$-complexes stabilized by various types of chelating agents (BM = biomolecule; M = Re/^{99m}Tc). 1 - Functionalized cysteine (53); 2 - Funcionalized 2,3-diamino propionic acid derivatives (51); 3-Functionalized histidine derivatives (54,55); 4 – Cyclopentadienyl (56) ; 5, 6 and 7 - Functionalized picolinic acid derivatives (57,58); 8 – Triazacyclononane(59) ; 9 and 10 - Functionalized pyrazolyl-diamine containing ligands (60–64); 11 – Functionalized bis(mercaptoimidazolyl)borates.(65)

1.2.3. ^{99m}Tc Radiopharmaceuticals

The ^{99m}Tc-based radiopharmaceuticals are roughly divided into two general categories, as mentioned before. Examples of the perfusion agents, commercially available and respective clinical application are presented in Figure 1.13. (4,7,66)

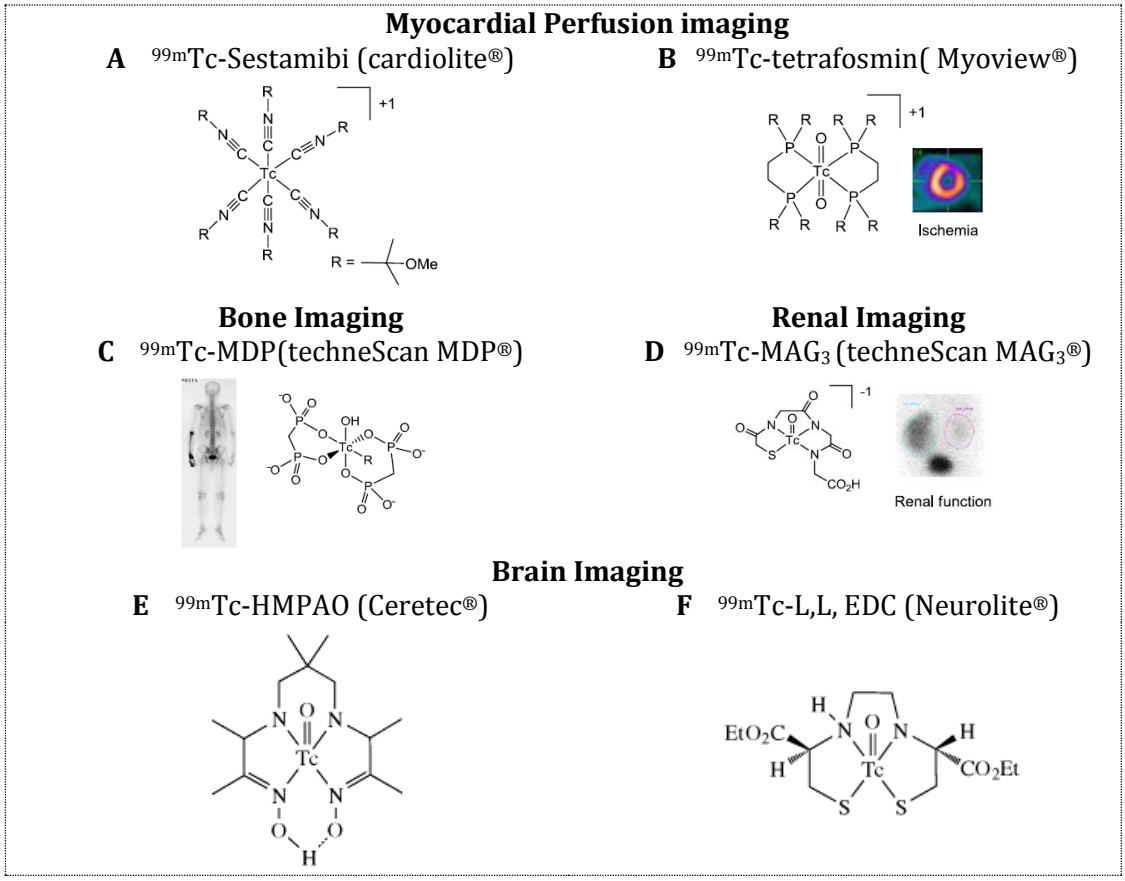

Figure 1.13 - ^{99m}Tc-based radiopharmaceuticals for diagnosis in clinical use. (MDP = methylenediphosphonate, MAG3 = mercaptoacetyl-triglycine, HMPAO = hexamethylpropyleneamine oxime, EDC = cysteinate dimer).

The growing demand for more specific ^{99m}Tc-radiopharmaceuticals has prompted the development of targeted radiopharmaceuticals mainly based on the BFC approach (Figure 1.8). As mentioned before, the targeting ability of specific radiopharmaceuticals relies on the capacity of the pendant biologically active molecule in the metal complex to recognize its target *in vivo* (e.g. membrane receptor, antigen or enzyme). (67–69) Besides the targeting moiety, also the spacer/linker between the metal and the biomolecule has a decisive influence in the overall biological properties of the radiopharmaceutical. (36) The modulation of the metal coordination environment with different chelators is a imperative parameter that opens great opportunities towards the design of innovative target specific radiopharmaceuticals with improved biological properties. Indeed, the design and

selection of the most appropriate BFC are the cornerstone for the development of clinically relevant imaging agents. Figure 1.14 shows selected Tc cores, which have been used for labeling different type BM with ^{99m}Tc.

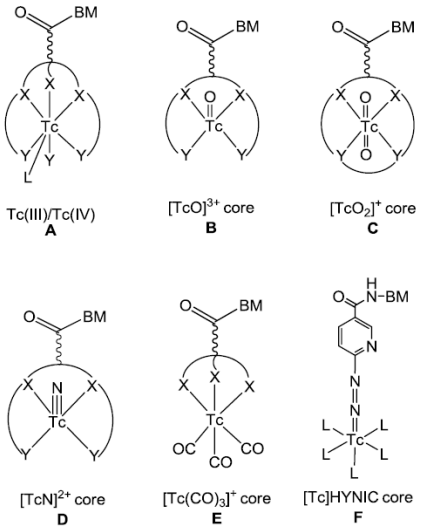

Figure 1.14 – Examples of Tc cores useful fort the labeling of biomolecules (BM) (6)

The BM can be an antibody, a small peptide or a nonpeptidic molecule that can act as an agonist or antagonist of a specific receptor. (70) The most relevant examples of specific ^{99m}Tc-based radiopharmaceuticals approved for SPECT imaging are radiolabeled peptides: ^{99m}Tc-Depreotide (see figure 1.7) and ^{99m}Tc-Apcitide, figure 1.15.

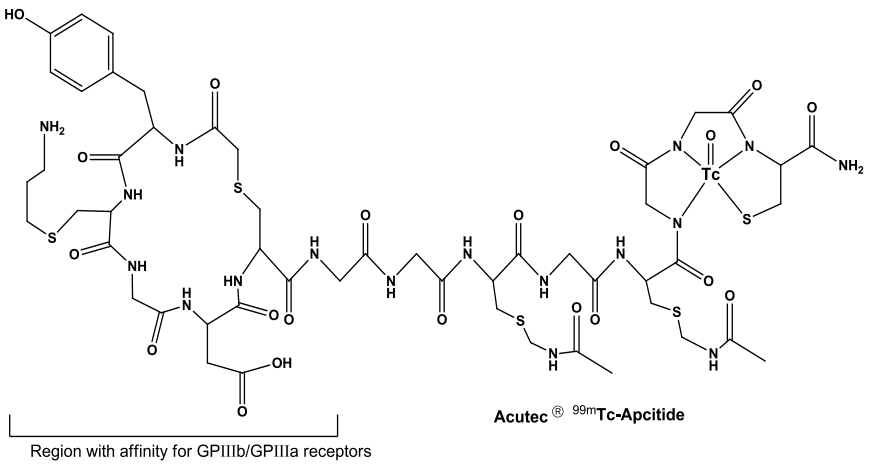

Figure 1.15 - ^{99m}Tc-Apcitide (Acutec®)

1.3. Peptides in Molecular imaging

To understand the role of peptides in molecular imaging is necessary to recognize how does a tumor cell and how is made the interaction between cells receptors and

peptides. The conformation of a tumor cell permits targeting different structures for imaging and therapy in oncology, see figure 1.16.

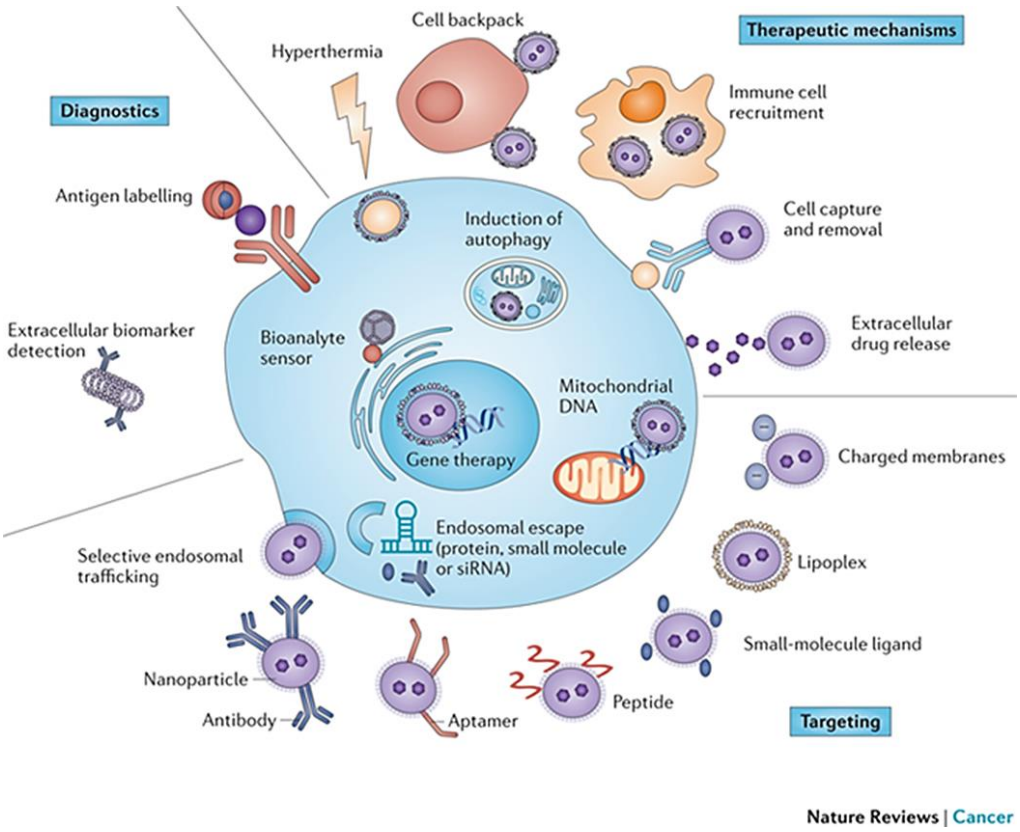

Figure 1.16 – Summary of all unique targeting, diagnostic and therapeutic mechanisms as they relate to cancer cells.(67)

Since the late 1980's, peptides were synthesized to mimic natural ligands of receptors, and are being developed as tools for specific tumor cell targeting. Different kinds of receptors, e.g. hormone-, growth factor- or folate receptors, are often overexpressed in tumor cells, enabling discrimination between malignant and normal tissues. The much smaller size of tumor-specific peptide analogues compared to that of antibodies reveals several advantages: rapid tissue penetration combined with a rapid clearance; no antigenicity; easy synthesis and simple to be modified chemically. Moreover, peptides can be easily conjugated with chelates to enable radiolabelling with metallic radionuclides. (71) The overexpression of peptide receptors in human tumors has been of considerable clinical interest for the past 10 years. The most successful example is the overexpressed somatostatin receptors in human neuroendocrine tumors that can be targeted successfully. (72)

Somatostatin receptors are overexpressed in neuroendocrine tumors. There are different subtipes of somastatin receptors built from 5 subtypes of somastotatin receptors

belonging to the G-protein coupled receptors; subtype 2 is the most widely overexpressed by tumors. (figure 1.17)

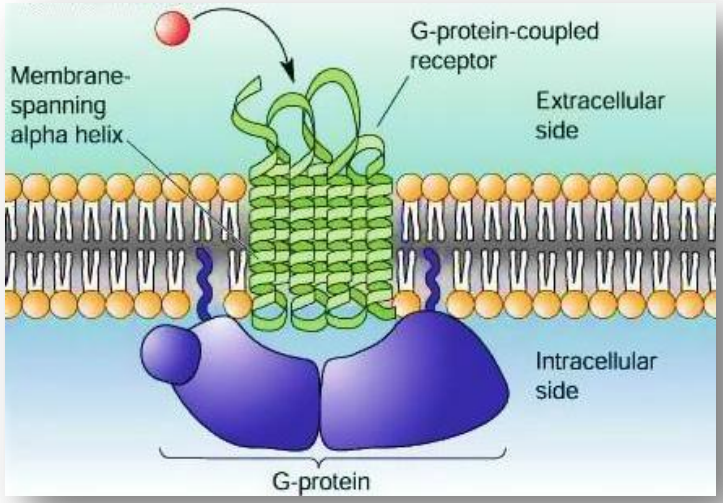

Figure 1.17 - G-Protein-coupled receptor conformation in the cellular membrane.(73)

Bombesin (BN), is a tetradecapeptide originally isolated from the skin of the European frog, Bombina bombina. It belongs to a large family of structurally related amphibian and mammalian peptides. BN has been shown to have potent physiological and behavioral effects in mammals, including the ability to suppress food intake. (74)

Although BN itself is not present in mammals, gastrinreleasing peptide (GRP) and neuromedin B (NMB) are two homologs that have been isolated from mammalian tissue and their receptors cloned and characterized. Structural and pharmacological differences have led to the identification of two BN receptor subtypes referred to as BB2 or GRP-preferring (GRP-r) and BB1 or NMB-preferring (NMB-r). The GRP-r subtype preferentially binds GRP but has a low affinity for NMB, whereas the NMB-R subtype has a high affinity for the NMB and a lower affinity for GRP. BN binds with equal and high affinity to both receptor subtypes. (75)

BN and its human counterpart GRP2 belong to a family of brain-gut peptides, shown, in addition to physiological effects, to play also an important role in cancer. It has been observed several years ago that cancer cell lines as well as primary human tumors can synthesize bombesin and GRP. (75) More recently, it has been shown that the GRP receptor proteins can be overexpressed in a large variety of human tumors, including prostate cancers, breast carcinomas, Small cell lung carcinomas (SCLCs), and non-SCLCs,

as well as renal cell carcinomas. Most of the studies up to now have been able to primarily identify the GRP receptor subtype, although it is known that the bombesin receptor family includes at least four different subtypes, namely the GRP receptor subtype (BB2), the NMB receptor subtype (BB1), and the BB3 and BB4 subtypes (16 –19). Except for the GRP receptor, the other three subtypes have been poorly characterized, in particular in regard to their distribution and function in human tissues. (76)

There have been several studies about bombesin analogues in the past few years. Different research groups have studied these peptides, and there are new studies being published every year. (table 1.2) These studies involved a variety of approaches with the use of different chelators, linkers and peptide sequences for specific targeting of GRP-r.

Table 1.2 - Sequences of various bombesin analogs. (76)

Analogs	Chelator	Linker	Sequences		
			1-6	7-13	14
Bombesin	-	-	pGlu-Gln-Arg-Leu-GLy-Asn-	-Gln-Trp-Ala-Val-Gly-His-Leu-	-Met-NH_2
Demo-besin-1	N4	-BzDig-	-D Phe-	-Gln-Trp-Ala-Val-Gly-His-Leu-NHEt	
BBS-1	(N^xHis)Ac-	-βAla-βAla-		-Gln-Trp-Ala-Val-Gly-His-Nle	
BBS-2	(N^xHis)Ac-	-Lys(sha)-βAla-βAla-		-Gln-Trp-Ala-Val-Gly-His-Nle	
BBS-3	(N^xHis)Ac-	-Lys(Amd)-βAla-βAla-		-Gln-Trp-Ala-Val-Gly-His-Nle	
BBS-4	(N^xHis)Ac-	-Ala(^{N}TG)-βAla-βAla-		-Gln-Trp-Ala-Val-Gly-His-Nle	
MP2653	DOTA		-aCMpip-Tha-	-Gln-Trp-Ala-Val-βAla-His-Tha-	-Nle-NH_2
MP2346	DOTA		-Pro-Gln-Arg-Tyr-Gly-Asn-	-Gln-Trp-Ala-Val-Gly-His-Leu-	-Met-NH_2
Pesin	DOTA	-$dPEG_4$-		-Gln-Trp-Ala-Val-Gly-His-Leu-	-Met-NH_2
AMBA	DOTA	-CH_2CO-Gly-4-aminobenzyl		-Gln-Trp-Ala-Val-Gly-His-Leu-	-Met-NH_2
RM 1	DOTA	-CH_2CO-Gly-4-aminobenzyl	-Phe-	-Gln-Trp-Ala-Val-Gly-His-Sta-	-Leu-NH_2
Lys(sha) = lysine-coupled shikimic acid, Lys(Amd) = Amadori-Product; Ala(^{N}TG) = triazole-coupled glucose, Sta= statyl					

The first proof of concept of the clinical relevance of radiolabeled BN peptides for imaging and therapy of tumors was develop by Van de Wiele et al. (77), in year 2000. Following these studies, Lantry et al. (78) demonstrated that ^{177}Lu-AMBA (DO3A-CH_2CO-G-(4-aminobenzoyl)-QWAVGHLM-NH_2) binds with low nanomolar affinity to GRP-r. This compound showed good radiotherapeutic efficacy in PC-3 tumor bearing nude mice and effective targeting of primary prostate cancer in humans. (78)

The analogues that have been studied are agonist and antagonist, as GRP-r can be targeted both by agonist and antagonist that belong to the family of bombesin peptides.

Whereas antagonists bind to GRP-r and remain on the surface of the tumor cells, typical agonists bind to GRP-r and are then internalized into the cells. (figure 1.18) (79)

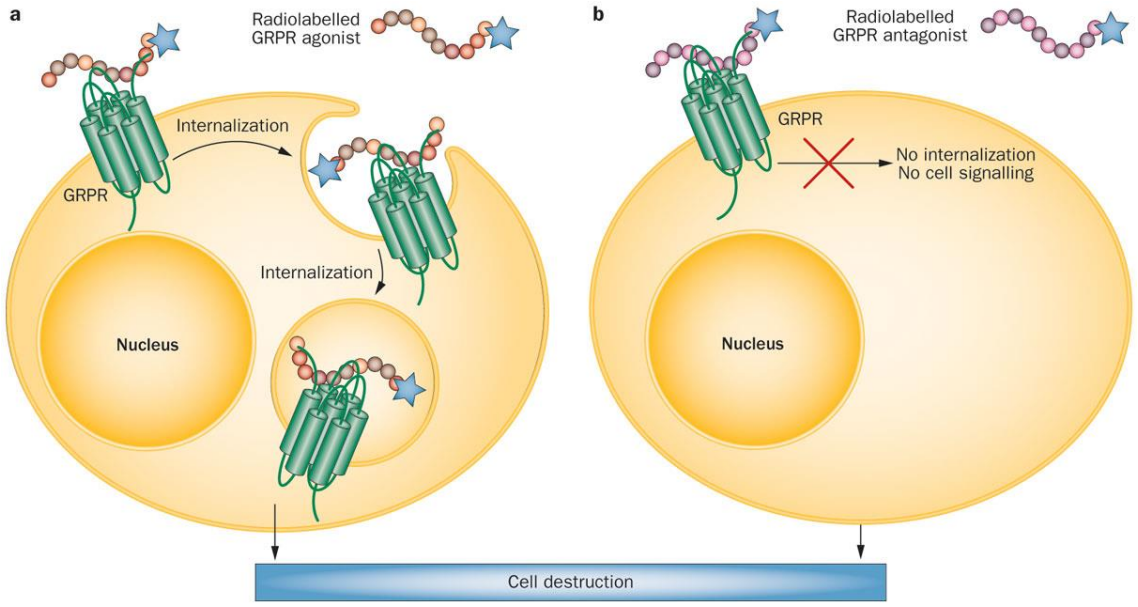

Figure 1.18 – Difference of agonists(a) and antagonists(b) of GRP-r. (80)

In 2007, it was published a study using a pegylated bombesin agonist, DOTA-PESIN (DOTA-PEG4-BN (7–14)). In that study, it was shown that this radiopeptide has suitable pharmacokinetic properties for a potential use as diagnostic and therapeutic agent (81). However, the use of bombesin agonists in clinical studies is limited by the possible mitogenic properties of these compounds and by the side effects observed in patients undergoing escalation study. (82)

Different classes of bombesin based antagonists were evaluated for their potential as targeting agents for diagnostic applications, such as PET, SPECT, and targeted peptide receptor radionuclide therapy (PRRT) of GRP-r positive tumors.(83–86) A first clinical study using the ^{64}Cu-labeled statine-based bombesin antagonist ^{64}Cu-CBC-AR-06 was recently reported by Wieser et al. showing suitable pharmacokinetics and good tracer accumulation in primary prostate cancer, in the four patients studied. (81)

From 2013, there is a study of the effective potential of the statine-based bombesin antagonist RM2 in the treatment of PC-3 tumor bearing nude mice. Animals treated with ^{177}Lu-RM2 showed a significant inhibition of tumor progression leading to an increasing survival rate without treatment-related toxicity. (2)

There are many reports on the study of the influence of spacer, chelator and/or radiometal on the pharmacology of radiolabeled bombesin analogs, highlighting the importance of choosing the right combination of these factors in order to obtain suitable radiopeptides for diagnostic and therapeutic applications.(81,82,87) Rogers et al. showed that a DOTA-PEG-Bombesin(7-14) derivative (PEG having a molecular weight of 3500kDa) lost about a factor of 10^3 in regard to GRP-r affinity but still showed good tumor uptake and pharmacokinetics. The importance of N-terminal charges and in particular of different spacer compositions were also demonstrated by Zhang et al. (81) and Yang et al. (88)

Several ^{99m}Tc-labeled bombesin analogues have been investigated using the bifuntional approach and the tricarbonyl methodology, as exemplified in figure 1.19 for the conjugates [^{99m}Tc(CO)$_3$-DTMA-(X)-BBN(7-14)NH$_2$] obtained using the chelator DTMA (2-(*N,N'*-Bis(*tert*-butoxycarbonyl)diethylenetriamine) acetic acid). (89)

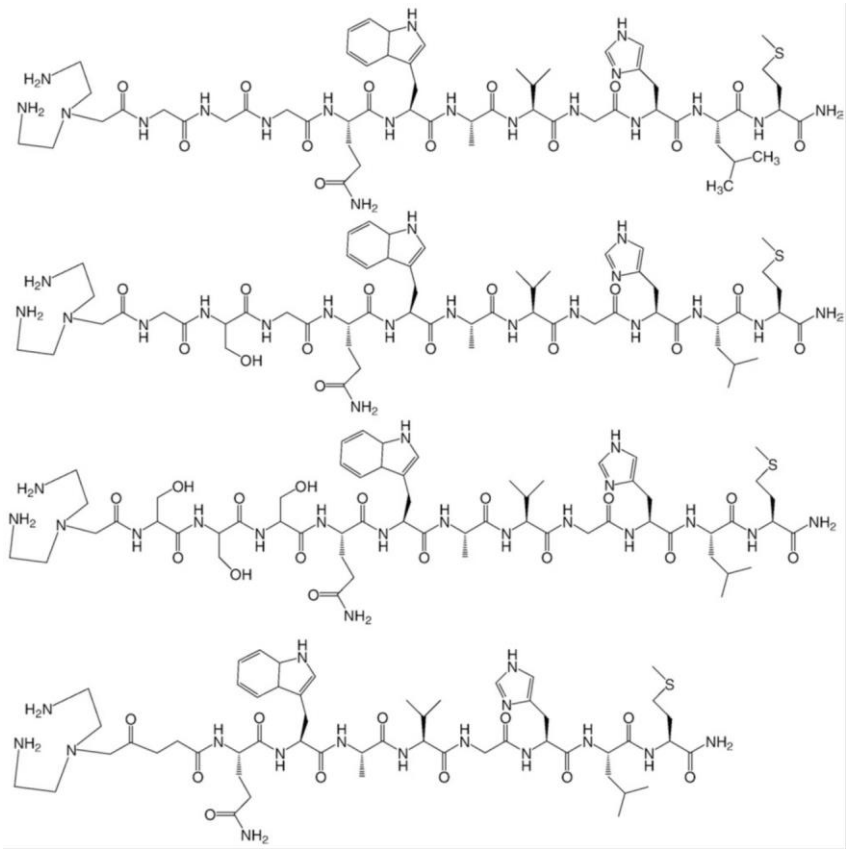

Figure 1.19 - Struture of DTMA-(X)-BBN(7-14)NH$_2$, where X=GGG(top), GSG, SSS and β-Ala (bottom). *GGG= AA Gly-Gly-Gly; GSG= Gly-Ser-Gly; SSS= Ser-Ser-Ser;

In general the radioconjugates [^{99m}Tc(CO)$_3$-DTMA-(X)-BBN(7-14)NH$_2$] showed good results in terms of affinity to the GRP-r. However, as reported for other ^{99m}Tc/^{188}Re-tricarbonyl-based bombesin derivatives, they were predominantly cleared via the

hepatobiliary excretion pathway because of tricarbonyl's inherent lipophilicity. Increasing the hydrophilicity of radiolabeled GRP-targeting peptide conjugates is necessary to avoid accumulation of radioactivity in the liver and intestinal tract, which would compromise their capacity to effectively image solid tumors and metastatic lesions in the abdomen. Therefore, the finding of ^{99m}Tc-$(CO)_3$ labeled BN derivatives with improved biodistribution profile still is an important issue in modern Radiopharmaceutical Sciences.

1.4. Objective

This thesis aimed to evaluate organometallic complexes of Tc(I) and Re(I) useful for the radiometalation of biologically active peptides. Due to the large spectrum of GRP receptor–expressing tumors, the bombesin receptor system is a clinically relevant target receptor system. Therefore, one of the goals was to investigate the radiolabeling of bombesin derivatives using the tricarbonyl approach. It was anticipated that the resulting radiopeptides should act as antagonists of GRPr. To accomplish this goal, we have synthesized different BFC's for peptide conjugation and complexation of the (radio)metal. To evaluate the effect on the biological profile of the final radioconjugates, linkers of different length were used between the BFC's backbone and the carboxylic function used for conjugation of the peptide.

By exploring the pair Tc(I)/Re(I), is was taken into consideration the potential therapeutic applications of ^{186}Re and ^{188}Re. To concretize the strategy of development of a theranostic radiolabeled peptide, having at the same time imaging and therapeutic properties, it is necessary to improve the pharmacokinetic of the conjugates in order to have high ratio between target and non-target organs. Hence, as it is known that most of the ^{99m}Tc/^{188}Re-tricarbonyl-based bombesin derivatives are very lipophilic, a PEG was attached to the N-terminal of the bombesin analogue, trying to enhance the hydrophilicity of the final compounds.

In the following chapters, it will be described the different steps to realize the aforementioned objectives, namely the strategies, synthetic procedures and studies involved in the synthesis and evaluation of the proposed compounds.

2. Materials and Methods

2.1 SOLVENTS AND REAGENTS

All chemicals from commercial suppliers were of reagent grade or higher.

The dry solvents used in this project were dried by distillation processes in C²TN laboratory and used for reactions under inert atmosphere. Tetrahydrofuran (THF) was freshly distilled from the sodium benzophenone ketyl radical ion. Acetonitrile (ACN), dichloromethane (DCM) were distilled from calcium hydride. Other solvents used in the experimental work were used as received. (90)

The compound (2-Amino-ethyl)-carbamic acid tert-butyl ester (**c4**) and the organometallic precursor *fac*-$[Re(CO)_3(H_2O)_3]^{Br}$ were prepared in the Radiopharmaceutical Sciences Group of C²TN (RSG-IST/C²TN) according to published methods. (91)Also the radioactive precursor $[^{99m}Tc(CO)_3(H_2O)_3]^+$ was prepared in the RSG-IST/C²TN, according to the IsoLink manufacturer's insert. (47)

Table 2.1 - List of main solvents, reagents, AAs, and chemicals used in this work.

	Products	*Molecular Formula*	Manufacturer	*Cas-number*
Solvents	*Diclomethane(DCM)*	CH_2Cl_2	*Sigma-Aldrich*	75-09-2
	1,4-Dioxane	$C_4H_8O_2$	*Sigma-Aldrich*	123-91-1
	Acetone	$(CH_3)COCH_3$	Carlo-Erba	67-64-1
	Acetonitrile (ACN)	CH_3CN	*Sigma-Aldrich*	75-05-8
	Chloroform	$CHCl_3$	*Scharlau*	67-66-3
	Diethylether	$(CH_3CH_2)_2º$	Sigma-Aldrich	60-29-7
	Ethanol (EtOH)	CH_3CH_2OH	*Panreac*	64-17-5
	Ethyl Acetate(EtOAc)	$CH_3COOC_2H_5$	Carlo-Erba	141-78-6
	Methanol (MeOH)	CH_3OH	*Carlo-Erba*	67-56-1
	N,N-Diisopropylethylamine (Dipea)	$[(CH_3)_2CH]_2NC_2H_5$	Sigma-Aldrich	7087-68-5
	N,N-Dimethylformamide (DMF)	$HCON(CH_3)_2$	*Carlo-Erba*	68-12-2
	n-hexane	$CH_3(CH_2)_4CH_3$	Sigma-Aldrich	110-54-3
	Petroleum ether	C_7H_7BrMg	Sigma-Aldrich	8032-32-4
	Piperidine	$C_5H_{11}N$	*Sigma-Aldrich*	110-89-4
	Tetrahydrofurane (THF)	C_4H_8O	Carlo-Erba	109-99-9
	Triethylamine	$(C_2H_5)_3N$	*Sigma-Aldrich*	121-44-8
	Trifluoroacetic acid (TFA)	CF_3COOH	*Sigma-Aldrich*	76-05-1
	Water	H_2O	*In house*	.
Deuteraded solvents	*Deuterochloroform*	$CDCl_3$	*Sigma-Aldrich*	865-49-6
	Tetradeuteromethanol	CD_3OD	*Euriso-top*	811-98-3
Reagents	Benzyl Bromoacetate	$C_9H_9BrO_2$	*Sigma-Aldrich*	5437-45-6
	1,2-dibromoethane	$BrCH_2CH_2Br$	*Sigma-Aldrich*	106-93-4
	1-Methyl-2-imidazolecarboxaldehyde	$C_5H_6N_2O$	*Sigma-Aldrich*	13750-81-7
	Di-*tert*-butyl dicarbonate (Boc protective group)	$[(CH_3)_3COCO]_2O$	*Sigma-Aldrich*	24424-99-5
	Ethyl 4-bromobutyrate	$C_6H_{11}BrO_2$	*Sigma-Aldrich*	2969-81-5
	Ethylenediamine	$NH_2CH_2CH_2NH_2$	*Sigma-Aldrich*	107-15-3
	Hydrochloric acid	HCl	*Sigma-Aldrich*	7647-01-0
	Magnesium sulfate anhydrous 96%	$MgSO_4$	*Panreac*	7487-88-9
	Potassium Carbonate	K_2CO_3	*Sigma-Aldrich*	584-08-7
	Potassium Iodide	KI	*Sigma-Aldrich*	7681-11-0
	Pyrazol	$C_3H_4N_2$	*Sigma-Aldrich*	288-13-1
	Sodium borohydride	NaBH4	*Sigma-Aldrich*	16940-66-2
	Sodium Hidroxide	NaOH	*Sigma-Aldrich*	1310-73-2

	sodium triacetoxyborohydride	$(CH_3COO)_3BHNa$	*Sigma-Aldrich*	56553-60-7
	Tetrabutylammonium bromide (TBAB)	$(CH_3CH_2CH_2CH_2)_4N(Br)$	*Sigma-Aldrich*	1643-19-2
Peptide Synthesis	HATU	$C_{10}H_{15}F_6N_6OP$	*Sigma-Aldrich*	148893-10-1
	FMOC-Ala-OH	$C_{18}H_{17}NO_4$	*Novabiochem*	35661-39-3
	FMOC-D-Phenylanine-OH	$C_{24}H_{21}NO_4$	*Novabiochem*	86123-10-6
	FMOC-Gln(Trt)-OH	$C_{39}H_{34}N_2O_5$	*Sigma-Aldrich*	132327-80-1
	FMOC-Gly-OH	$C_{17}H_{15}NO_4$	*Novabiochem*	29022-11-5
	FMOC-His(Trt)-OH	$C_{10}H_{15}NO_4$	*Sigma-Aldrich*	109425-51-6
	FMOC-Leu-OH	$C_{27}H_{23}NO_4$	*Novabiochem*	35661-60-0
	FMOC-NH-PEG-COOH (9 atoms)	$C_{21}H_{23}NO_6$	*Novabiochem*	166108-71
	FMOC-Sta-OH	$C_{23}H_{27}NO_5$	*Novabiochem*	158257-40-0
	FMOC-Trp(Boc)-OH	$C_{31}H_{30}N_2O_6$	*Sigma-Aldrich*	143824-78-6
	FMOC-Val-OH	$C_{20}H_{21}NO_4$	*Novabiochem*	68858-20-8
	Rink Amide-MBHA Resin		*Novabiochem*	431041-83-7
	Triisopropylsilane (TIS)	$[(CH_3)_2CH]_3SiH$	*Sigma-Aldrich*	6485-79-6

Table 2.2 - List of main devices used in this project.

Device Name	Description	Manufacturer
0.22 µm filters	Sample preparation for HPLC system	Millipore, Billerica, MA, USA
300 or 400 MHz spectrometer	NMR	Varian Unity 300 or 400 MHz spectrometer
^{99}Mo/^{99m}Tc generator	Elution of ^{99m}Tc	Drytec®, GE Healthcare
Automatic analyzer EA 110	Elementary analysis	CE Instruments, Ltd. Hindley Green Wigan. United Kingdom
Buchi® R-210 Rotavapor® Evaporator	Evaporation of Solvents	Bunchi® Flawil Switzerland
C18 reversed phase column (Nucleosil 10 µm, 250 x 4 mm)	HPLC System	Macherey-Nagel
CEM 12-Channel Automated Peptide Synthesizer	Peptide synthesizer	CEM corporation. Qlabo Lda. Lisboa
Discover and Explorer SP	Microwave device	CEM corporation. Qlabo Lda. Lisboa
Discovery bio® wide pore C-18 Column	HPLC column	Supelco. Sigma-Aldrich Co. LLC
ionization chamber	Radiation reader	Curiemeter IGC-3, Aloka, Tokyo, Japan
Lyophilizer Alpha I-12	Lyophilizer	BODE & Co. Hamburg
Mass Spectrometer	MS	Bruker HCT, Bilerica, MA, USA
PerkinElmer Series 200 LC pump	HPLC system	PerkinElmer, Waltham, MA, USA
Pump	Vacuum line system	Acatel, New Jersey, USA
ultraviolet/visible (UV/Vis) detector	HPLC system	Shimadzu SPD-10AV, Shimadzu, Kyoto, Japan
Vacuum Line	Vacuum Lines system	Rotaflo, England
γ detector	HPLC system	Berthold-LB 509, Berthold Technologies, Bad Wildbad, Baden-Württemberg, Germany

2.2 PURIFICATION AND CHARACTERIZATION TECHNIQUES

The purification and characterization methods used in this project are presented in this section and includes procedures of purification and characterization of organic compounds, as well as methods used to characterize the ^{99m}Tc radiolabeled compounds.

2.2.1. Gravity Column chromatography (GCC)

When necessary, compounds were purified by gravity column chromatography (GCC) performed by using open glass columns loaded with silica gel (ASTM Merck 70-230 mesh granulometry, 0.063-0.200mm). Columns with appropriate dimensions were used, depending on the amount of compound to purify; small vials were used to collect and separate the different fractions. The presence of the desired compound in the elution fractions was monitored by TLC and confirmed by ^{1}H-NMR spectroscopy.

2.2.2. Reversed-Phase High Performance Liquid Chromatography (RP-HLPC)

RP-HPLC analysis of compounds were performed on a PerkinElmer Series 200 LC pump coupled to an UV/VIS detector (PerkinElmer LC 290 or Shimadzu SPD-10AV) and to a γ detector (Berthold-LB 509). The organic eluents were of HPLC grade and the water was bidistilled in a quartz distillation unit. All solvents were purged with helium prior to use. The samples injected were pre-filtered with 0.22 μm filters (Millipore).

Two different elution methods (method 1 and 2) were used, according to the characteristics of the analyzed compounds.

Method 1

- Used in purification runs for peptide conjugates;
- Discovery bio® wide pore C-18 (25cmx4,6mm; 5μm) reverse-phase column;
- Flow: 1.0 mL/min or 2.0 mL/min;
- U.V. detection: λ = 220 nm and 280nm
- Eluents: A - TFA 0.1 % in H_2O; B - TFA 0.1% in ACN

Table 2.3 – RP-HPLC **method 1.**

Step	Time (min)	%A	%B
0	5	90	10
1	0-45	90→0	10→100
2	47	90	10

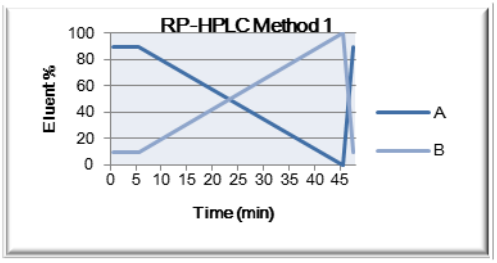

Figure 2. 1 – RP-HPLC **method 1** graphic profile.

Method 2

- used in analytical runs for Re complexes and radiolabelling with ^{99m}Tc ;
- Macherey-Nagel C18 reversed phase column (Nucleosil 10 µm, 250 x 4 mm);
- Flow: 0.5 mL/min;
- U.V. detection: λ = 220 nm
- γ detection suited for ^{99m}Tc
- Eluents: A - TFA 0.1% in H_2O; B - CH_3OH

Table 2.4 – RP-HPLC **method 2.**

Step	Time (min)	%A	%B
0	5	100	0
1	0-3	100	0
2	3-3.1	100→75	0→25
3	3.1-9	75	25
4	9-9.1	75→66	25→34
5	9.1-20	66→0	34→100
6	20-25	0	100
7	25-25.1	0→100	100→0
8	25.1-30	100	0

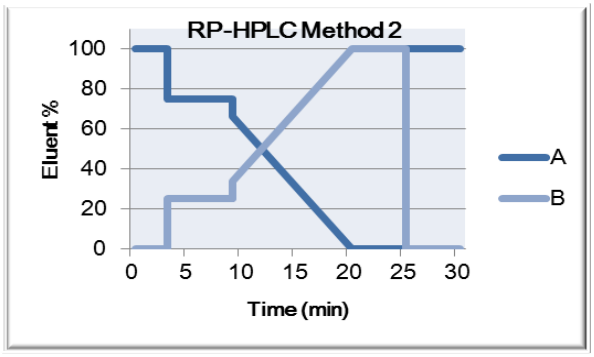

Figure 2.2 – RP-HPLC **method 1** graphic profile.

2.2.3. Thin-layer chromatography (TLC)

Reactions were monitored by using thin layer chromatography (TLC) plates precoated with silica UV254 (60 F_{254} Merck silica gel, 0.2 mm). Visualization of the plates was carried out using UV light (254 or 365 nm) and/or iodine container, or a solution of 2% ninhydrin (2,2-Dihydroxyindane-1,3-dione) in EtOH, followed by heating.

2.2.4. Nuclear Magnetic Resonance (NMR) Spectroscopy

The ^{1}H, ^{13}C or ^{19}F-NMR (1D-NMR) and ^{1}H-^{1}H g-COSY (2D- NMR) spectra were recorded in a Varian Unity 300 or 400 MHz spectrometer.

^{1}H and ^{13}C chemical shifts (δ) were referenced to the residual solvent resonances relative to tetramethylsilane ($SiMe_4$). The data are presented in ppm relative to the $CDCl_3$ solvent (^{1}H, δ 7.26; ^{13}C, δ 77.16) as internal standard or to the CD_3OD solvent (^{1}H δ 3.31; ^{13}C, δ 49.00). (92)

2.2.5. Mass Spectrometry (MS)

The electrospray-mass spectrometry (ESI-MS) analysis of compounds were obtained using an electrospray ionization/quadrupole ion trap (ESI/QIT) mass

spectrometer (Bruker HCT, Bruker, Billerica, MA, USA) and were performed by Dr. Célia Fernandes from the C²TN.

2.2.6. Spectrophotometry

UV-vis absorption measurements were performed in a Shimadzu UV-1800 Spectrophotometer (range: 200 – 1100 nm) at 280 nm, which the maximum absorption wavelength of the aminoacid triptofan.(93)

2.2.7. Measurements of Radioactivity

The radioactivity of the ^{99m}Tc solutions was measured in an ionization chamber (Aloka, Curiemeter IGC-3). The samples with activity less than 2 μCi were measured in a Gamma Counter (Berthold LB 2111).

2.2.8. Partition coefficient

The partition coefficient was evaluated by the ''shakeflask'' method.(94) The radioconjugate was added to a mixture of octanol (1 mL) and 0.1 M PBS, pH 7.4 (1 mL) which had been previously saturated with each other by stirring. This mixture was vortexed and centrifuged (3,000 rpm, 10 min) to allow phase separation. Aliquots of both octanol and PBS were counted in a γ-counter. The partition coefficient in octanol/ water (log Po/w) was calculated by dividing the counts in the octanol phase by those in the buffer, and the results were expressed as log $P_{o/w}$ ± the standard deviation (S.D).

2.2.9. Biodistribution studies

All animal experiments were performed in compliance with national and European regulations for animal treatment. The animals were housed in a temperature- and humidity-controlled room with a 12 h light/12 h dark schedule.

The biodistribution of the ^{99m}Tc complex **Tc4** was evaluated in groups of 3 CD-1 female mice (Charles River outbred strain, from IFFA CREDO, Barcelona, Spain). Mice were intravenously injected with 100 μl of complex **Tc4** (3 - 10 MBq) via the tail vein and the animals were kept in normal diet *ad libitum*. Animals were sacrificed by cervical dislocation at 1 and 4 h after injection. The administered dose and the radioactivity in the sacrificed animals were measured with a dose calibrator (Curiemeter IGC-3, Aloka, Tokyo, Japan). The difference in radioactivity between the injected animal and the sacrificed animal was assumed to be due to excretion. Tissues and organs of interest were dissected,

rinsed to remove excess blood, weighted, and their radioactivity was measured using the dose calibrator. The uptake in the tissues or organs was calculated and expressed as percent injected dose per gram of tissue or organ (% IA/g). For blood, bone, muscle, and skin, total activity was estimated assuming that they represent 6, 10, 40, and 15 % of the total body weight, respectively.

2.2.10. *In Vivo* stability studies

The *in vivo* stability of the ^{99m}Tc(I) complexes was evaluated by RP-HPLC analysis of urine and blood.

Urine: The urine collected at the sacrifice time was centrifuged at 3000 rpm for 15 min and the supernatant was analyzed by RP-HPLC.

Blood: The blood was collected at the sacrifice time, centrifuged at 3000 rpm for 15 min at 4 °C, and the serum was separated. 100 µl aliquots of serum were sampled and treated with 200 µl of EtOH to precipitate the proteins. Samples were then centrifuged at 3000 rpm for 15 min at 4 °C. The supernatant was analyzed by RP-HPLC.

2.3. SYNTHESIS OF LIGANDS

2.3.2. Synthesis and characterization of ***N*-2-bromoethyl-pyrazole - c1**

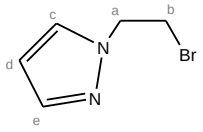

The percursor **c1** was prepared as described in the literature. (97)

To a solution of pyrazole (10.51 g; 0.15 mol) in 1,2-dibromoethane (95 mL; 1.10 mol) was added a solution of 40% NaOH (45 mL; 2.38 mol) and tetrabutylammonium bromide (TBAB) (1.20 g; 3.70 mmol) as a catalytic compound. After 24h of stirring at room temperature, the aqueous phase was extracted with $CHCl_3$. The organic phase was dried over $MgSO_4$, filtered and the solvent evaporated under vacuum. The resulting product was purified by distillation, under reduced pressure, and **c1** was obtained as a colorless oil (19.03 g, 0.11 mol).

Yield (η) = 70%

R_f (Retention Factor) ($CHCl_3$/ MeOH; 9:1) = 0.42

^{1}H-NMR (300 MHz, $CDCl_3$; δ/ppm): 7.87 (s, 1H, $CH^{c/e}$), 7.79 (s, 1H, $CH^{c/e}$), 6.57 (s, 1H, CH^{d}), 4.80 (t, J = 6.2 Hz, 1H, CH_2^{a}), 4.03 (t, J = 6.2 Hz, 1H, CH_2^{b}).

2.3.3. Synthesis and characterization of Synthesis and characterization of **[2-(2-Pyrazol-1-l-ethylamino)-ethyl]-carbamic acid tert-butyl ester - c2**

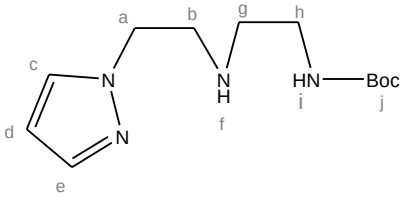

Compound **c2** was prepared as described in the literature. (63)

To a solution of **c1** (1.01 g; 5.70 mmol) and triethylamine (1.73 g; 0.68 mL 6.70 mmol) in dry ACN (25 mL) was added (2-Amino-etil)-carbamic acid *tert*-butyl ester (**c4**) (1.89 g, 4.68 mmol), which was synthetized as described in 2.3.6. After overnight reflux, the suspension was cooled down to r.t. and extracted with DCM. The organic phase was

dried over $MgSO_4$, filtered and the solvent evaporated under vacuum. The resulting product was purified by silica gel column chromatography, using $CHCl_3$/MeOH (90/10) as eluent. After solvent evaporation of the collected fractions, **c2** was obtained as pale yellow oil.

η = 77%

R_f ($CHCl_3$/MeOH; 9:1) = 0.63

^{1}H NMR (300 MHz, $CDCl_3$; δ/ppm): 7.51 (s, 1H, $CH^{c/e}$), 7.41 (s, 1H, $CH^{c/e}$), 6.24 (s, 1H, CH^{d}), 5.01 (s, 1H, NH^{f}), 4.22 (t, *J* = 5.5 Hz, 2H, CH_2^{a}), 3.16 (d, *J* = 5.0 Hz, 2H,CH_2^{h}), 3.04 (t, *J* = 5.4 Hz, 2H, CH_2^{b}), 2.70 (t, *J* = 5.4 Hz, 2H,CH_2^{g}), 1.81 (s, 2H, NH^{i}), 1.43 (s, 9H, $(CH_3)_3^{j}$, *Boc*).

2.3.4. Synthesis and characterization of **4-[(2-tert-Butoxycarbonylamino-ethyl)-(2-pyrazol-1-yl-ethyl)-amino]-butyric acid ethyl ester - c3**

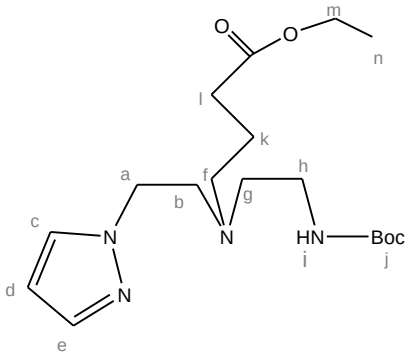

The percursor **c3** was prepared as described in the literature. (63)

To a solution of **c2** (0.93 g; 3.6 mmol) in dry ACN (30 mL) were added ethyl 4-bromobutyrate (1.03 mL; 7.20 mmol; 1.4 g), K_2CO_3 (1.01 g; 7.2 mmol) and KI (0.1 mmol). After overnight reflux, the suspension was cooled down to r.t. and the solvent evaporated under vacuum. The resulting product was purified by silica gel column chromatography, using DCM/MeOH (95/5) as eluent. After solvent evaporation from the collected fractions, **c3** was obtained as yellow oil.

η = 75%

R_f ($CHCl_3$/MeOH; 9:1) = 0.73

^{1}H-NMR (300 MHz, $CDCl_3$; δ/ppm): 7.42 (s, 2H, $CH_2^{c,e}$), 6.61 (s, 2H, CH_2^{m}), 6.15 (s, 1H, CH^{d}), 4.10 (s, 2H, CH_2^{a}), 2.98 (s, 2H, CH_2^{b}), 2.79 (s, 2H, CH_2^{h}), 2.43 (s, 2H, CH_2^{f}), 2.37 (s,

2H, CH_2^g), 2.17 (s, 1H, NH^i), 2.04 (s, 2H, CH_2^l), 1.54 (s, 2H, CH_2^k), 1.38 (s, 9H, $(CH_3)_3^{j=Boc}$), 1.25 (t, J = 7.1 Hz, 3H, CH_3^n).

2.3.5 Synthesis and characterization of **4-[(2-*tert*-Butoxycarbonylamino-ethyl)-(2-pyrazol-1-yl-ethyl)-amino]-butyric acid – L1-Boc**

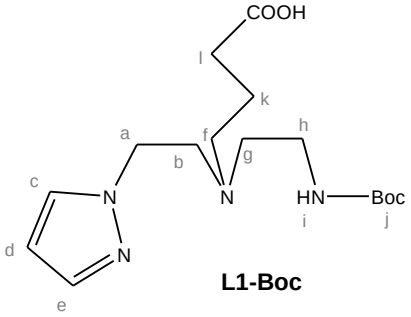

L1-Boc

The ligand **L1-Boc** was prepared as described in the literature. (63)

Compound **c3** was dissolved in THF (15 mL) and to the resulting solution was added an excess of NaOH (8.07 mmol) in H_2O (5 mL). After overnight reflux, the suspension was cooled down to r.t., neutralized with 1M HCL (7 mL) and the solvent evaporated. The obtained residue was extracted with DCM. The organic phase was dried over $MgSO_4$, filtered and the solvent evaporated. The resulting product was purified by silica gel column chromatography, using $CHCl_3$/MeOH (80/20) as eluent. After evaporation of the solvent from the collected fractions, **L1-Boc** was obtained as yellow oil.

η = 78%

Rf ($CHCl_3$/MeOH; 9:1) = 0.71

^{1}H-NMR (300 MHz, $CDCl_3$; δ/ppm): 7.42 (s, 2H, $CH_2^{c,e}$), 6.61 (s, 2H, CH_2^m), 6.15 (s, 1H, CH^d), 4.10 (s, 2H, CH_2^a), 2.98 (s, 2H, CH_2^b), 2.79 (s, 2H, CH_2^h), 2.43 (s, 2H, CH_2^f), 2.37 (s, 2H, CH_2^g), 2.17 (s, 1H, NH^i), 2.04 (s, 2H, CH_2^l), 1.54 (s, 2H, CH_2^k), 1.38 (s, 9H, $(CH_3)_3^{j=Boc}$).

^{13}C NMR (300 MHz, $CDCl_3$, δ/ppm): 184.7 (CO), 173.2 (CO), 142.9 (C^c), 135.6 (C^e), 122.4 (C^d), 83.1 ($C(CH_3)$) 55.2 (C^l), 54.6 (C^g), 52.3 (C^b), 50.1 (C^a), 39.1 (C^h), 37.1 (C^f), 29.7 ($C(CH_3)$), 24.3(C^k).

2.3.6. Synthesis and characterization of **(2-Amino-etil)-carbamic acid *tert*-butyl ester – c4**

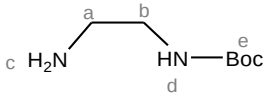

The percursor **c7** was prepared as described in the literature. (109)

A solution of di-*tert*-butyl dicarbonate ($(Boc)_2O$) (13.93 g, 63.80 mmol) in 1,4-dioxane (100 mL) was drop wise added to ethylenediamine (22.47 g, 0.37 mol) in 1,4-dioxane (80 mL). After overnight with strong stirring at r.t., the solvent was evaporated and the residue extracted with $CHCl_3$. The organic phase was filtered, dried with $MgSO_4$ and evaporated. After evaporation, **c4** was obtained as pale white oil.

η = 74%

Rf ($CHCl_3$/MeOH; 9,8:0,2) = 1 (solvent front)

^{1}H NMR (400 MHz, $CDCl_3$; δ/ppm): 5.59 (s, 1H, NH^d), 2.87 (s, 2H, $CH_2{}^a$), 2.50 (s, $CH_2{}^b$), 1.21 (s, 2H, $NH_2{}^c$), 1.16 (s, 9H, $(CH_3)_3{}^{j=Boc}$).

^{13}C NMR (400 MHz, $CDCl_3$; δ/ppm): 28,03 ($(CH_3)_3$, Boc); 41,49 ($CH_2{}^a$); 43,06 ($CH_2{}^b$); 78,51 (C-Boc);156,00 (C=O, Boc)

2.3.7. Synthesis and characterization of **(2-(1-Methyl-1*H*-imidazol-2-ylmethyl)-amino)-ethyl)-carbamic acid *tert*-butyl ester – c5**

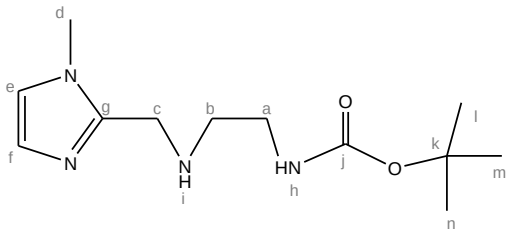

To a solution of **c4** (3.1 mmol) in dried MeOH (20 mL) was added 1-methyl-2-imidazolecarboxaldehyde (3.1 mmol). The solution was refluxed during 3h and then stirred overnight at r.t., under N_2 atmosphere. Then, a solution of $NaBH_4$ (9.3 mmol) in MeOH (10 mL) was added to the mixture. After one more night of stirring at r.t., the

solvent was evaporated and the residue extracted with DCM. The organic phase was filtered, dried with $MgSO_4$ and evaporated. After solvent evaporation, the residue was extracted with diethyl ether and the obtained suspension was separated by centrifugation (3500 rpm, 8 min) and the organic phase evaporated to afford **c5** as white oil.

η = 97%

Rf ($CHCl_3$/MeOH; 9,8:0,2) = 0.31

^{1}H-NMR (300 MHz, $CDCl_3$; δ/ppm): 6.94 (s, 1H, CH^e), 6.83 (s, 1H, CH^f), 5.18 (s, 1H, NH^i), 3.90 (s, 2H, $CH_2{}^c$), 3.68 (s, 3H, $CH_3{}^d$), 3.46 (t, *J* = 9.4 Hz, 1H, NH^h), 3.33 – 3.17 (m, 2H, $CH_2{}^a$), 2.83 (t, *J* = 5.8 Hz, 2H, $CH_2{}^b$), 1.43 (s, 9H, $(CH_3)_3{}^{m,n,l}$, Boc).

^{13}C-NMR (300 MHz, $CDCl_3$; δ/ppm): 156.21 (C=O^j, Boc), 146.33 (C^g), 127.12 (C^e), 121.26 (C^f), 79.13 (C^k), 48.83 (C^b), 45.19 (C^a), 32.70 (C^c), 28.45 ($C^{l,m,n}$, Boc), 28.39 ($CH_3{}^d$).

ESI-MS (+) (mass/charge-m/z): 255.3 $[M+H]^+$, calculated for $C_{12}H_{22}N_4O_2$ = 254.17

2.3.8. Synthesis and characterization of **N-(1-metyl-1H-imidazol-2ylmethyl)-ethane-1,2-diamine – L5**

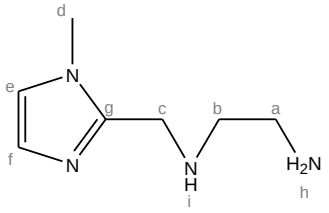

To a solution of **c5**(0.79 mmol) in DCM (10 mL) was added TFA (1 mL, 13.06 mmol)**.** The reaction mixture was stirred overnight at room temperature. The solvent was removed under vacuum and the resulting product, **L5**, was obtained as white oil.

η = 64% (for L5·TFA)

Rf ($CHCl_3$/MeOH; 9,8:0,2) = 0,43

^{1}H-NMR (400 MHz, CD_3OD; δ/ppm): 6.86 (s, 1H, $CH^{e/f}$), 6.74 (s, 1H, $CH^{e/f}$), 3.71 (s, 2H, $CH_2{}^c$), 3.59 (s, 1H, NH^i), 3.57 (s, 3H, $CH_3{}^d$), 2.61 (t, *J* = 5.7 Hz, 2H, $CH_2{}^a$), 2.55 (t, *J* = 5.7 Hz, 2H, $CH_2{}^b$).

^{13}C-NMR (400 MHz, CD_3OD; δ/ppm): 163.41 (C^d), 120.07 (C^f), 116.19 (C^e), 56.53 (C^b), 45.06 (C^a), 41.00 (C^c), 33.09 (C^d).

^{19}F-NMR (400 MHz, CD_3OD; δ/ppm): -77.05 (TFA)

ESI-MS (+) (mass/charge-m/z): 155.8 $[M+H]^+$, 177.3 $[M+Na]^+$, 269.3 $[M+TFA+H]^+$, calculated for $C_7H_{14}N_4$ = 154.12

2.3.9. Synthesis and characterization of **benzyl 2-(2-(*tert*-butoxycarbonylamino)ethylamino)acetate – c6**

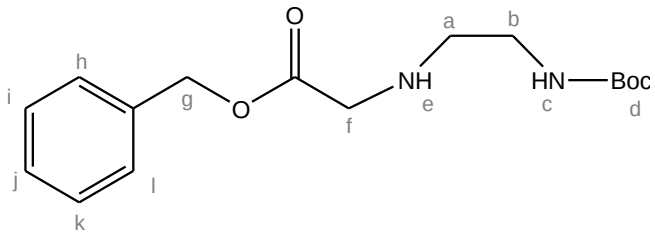

The precursor **c6** was prepared as described in the literature. (110)

To a solution of **c4** (0.95 g, 5.9 mmol) and triethylamine (0.59 g; 0.83 mL; 5.92 mmol) in ACN (20.0 mL) was added benzyl bromoacetate (1.28 g; 0.88 mL; 5.91 mmol) via syringe over 3 min. After 3h, the reaction mixture was diluted with 40 mL of EtOAc and washed with 40 mL of 2M K_2CO_3 (aq.). The organic phase was separated, then brine was added and the organic phase separated again. The organic phase was dried with Na_2SO_4, filtered and the solvent evaporated. The resulting product was purified by silica gel column chromatography, using $CHCl_3$/MeOH (98/2) as eluent. After solvent evaporation from the collected fractions, **c6** was obtained as yellow oil.

η = 38%

Rf ($CHCl_3$/MeOH; 9,8:0,2) = 0,55

^{1}H-RMN (300 MHz, $CDCl_3$; δ/ppm): 7.35 (s, 5H, $(CH)_5{}^{h-l}$, Benzyl), 5.17 (s, 2H, $CH_2{}^g$), 5.02 (s, 1H, NH^e), 3.49 (s, 2H, $CH_2{}^f$), 3.23 (s, 2H, $CH_2{}^a$), 2.79 (s, 2H, $CH_2{}^b$), 2.18 (s, 1H, NH^c), 1.44 (s, 9H, $(CH_3)_3{}^d$, Boc).

2.3.10. Synthesis and characterization of **[(2-tert-Butoxycarbonylamino-ethyl)-(1-methyl-1H-imidazol-2-ylmethyl)-amino]-acetic acid benzyl ester – c7**

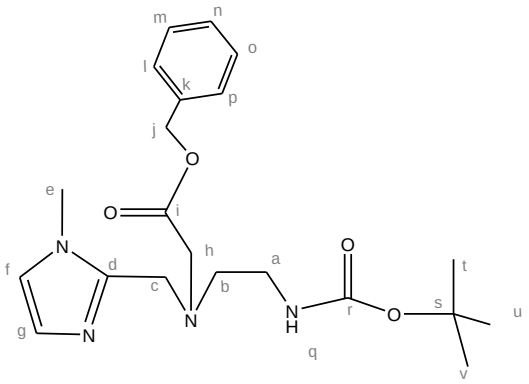

To a solution of **c6** (0.23 g, 0.723 mmol) in dried DCM (20 mL) was added 1-methyl-2-imidazolecarboxaldehyde (79.63 mg; 0.723 mmol) and sodium triacetoxyborohydride (0.21 g; 1.01 mmol). After overnight reflux under N_2, a saturated aqueous sodium hydrogen carbonate solution was added, and the mixture stirred for 15 min prior to extraction with ethyl acetate. The organic phase was filtered, dried with $MgSO_4$ and evaporated. The resulting product was purified by silica gel column chromatography, using $CHCl_3$/MeOH (98/2) as eluent. After solvent evaporation from the collected fractions, **c7** was obtained as transparent oil.

η = 55%

Rf ($CHCl_3$/MeOH; 9,8:0,2) = 0.24

^{1}H NMR (400 MHz, $CDCl_3$; δ/ppm): 7.28 (s, 5H, $(CH)_5^{l-p}$, Benzyl), 6.85 (s, 1H, $CH^{f/g}$), 6.77 (s, 1H, $CH^{f/g}$), 5.39 (s, 1H, NH^q), 5.06 (s, 2H, CH_2^j), 3.81 (s, 2H, CH_2^c), 3.61 (s, 3H, CH_3^e), 3.36 (s, 2H, CH_2^h), 3.09 (d, J = 4.4 Hz, 2H, CH_2^a), 2.68 (t, J = 5.3 Hz, 2H, CH_2^b), 1.38 (s, 9H, $(CH_3)_3^{t,u,v}$, Boc).

^{13}C NMR (400 MHz, $CDCl_3$; δ/ppm): δ 169.47($C=O^r$, Boc), 154.35 ($C=O^i$), 142.90 (C^d), 133.80 (C^k), 126.87 ($C^{o,m}$), 126.65 (C^n), 126.58 ($C^{l,p}$), 125.16 (C^f), 120.16 (C^g), 75.76 (C^j), 64.67 (C^h), 52.97 (C^b), 51.98 (C^c), 49.17 (C^a), 36.57 (C^s), 31.05 (C^e), 26.73 ($C^{t,u,v}$, Boc).

ESI-MS (+) (mass/charge-m/z): 403.4 $[M+H]^+$, 425.2 $[M+Na]^+$ calculated for $C_{21}H_{30}N_4O_4$= 402,23.

2.3.11. Synthesis and characterization of **{(2-tert-Butoxycarbonylamino-ethyl)-[2-(2H-pyrazol-1-yl)-ethyl]-amino}-acetic acid benzyl ester – c8**

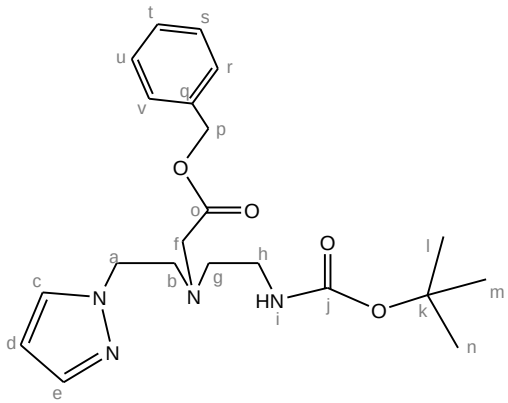

To a solution of **c6** (0.19 g; 0.62 mmol) in dried ACN (30 mL) were added compound **c1** (0.12 g; 0.62 mmol), K_2CO_3 (85.6 mg, 0.62 mmol) and KI (0.01 mmol). After 100h of reflux, the suspension was cooled down to r.t. and the solvent evaporated. The resulting product was purified by silica gel column chromatography, using $CHCl_3$/MeOH (98/2) as eluent. After solvent evaporation from the collected fractions, **c8** was obtained as an yellow oil.

η = 81%

Rf ($CHCl_3$/ MeOH; 9,5:0,5) = 0.59

^{1}H-RMN (400MHz, CD_3OD; δ/ppm): 7.32 (s, 1H, CH, C^e), 7.33 (s, 1H, C^c), 7,34 (m, 5H, $(CH)_5^{r\text{-}v}$, Benzyl), 6.27(s,1H, CH^d), 5.14 (s, 2H, CH_2^p), 4.49 (m, 2H, CH_2^a), 3.43 (m, 4H, $(CH_2)_2^{b,g}$), 3.23 (s, 4H, $(CH_2)_2^{f,h}$), 1.53 (s, 1H, CH^i), 1.44 (s, 9H, $(CH_3)_3^{l,m,n}$, Boc)

^{13}C NMR (400 MHz, $CDCl_3$; δ/ppm): 171.12 ($C{=}O^j$, Boc), 156.06 ($C{=}O^o$), 139.43 (C^c), 135.53 (C^q), 129.83 (C^e), 128.60 ($C^{u,s}$), 128.40 (C^t), 128.34 ($C^{v,r}$), 105.36 (C^d), 77.36 78.85 (C^p), 66.34 (C^f), 54.71 (C^g), 54.27 (C^b), 53.64 (C^a), 50.66 (C^h), 38.35 (C^k), 28.45 ($C^{l,m,n}$, Boc).

2.3.12. Synthesis and characterization of **4-(2-tert-Butoxycarbonylamino-ethylamino)-butyric acid ethyl ester – c9**

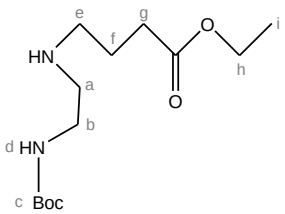

To a solution of **c4** (0.19 g; 0,62 mmol), K_2CO_3 (85.60 mg, 0.62 mmol) and KI (0.01 mmol) in dried ACN (20 mL) was added drop-wise 4-bromo- ethyl butyrate (0.12 g; 0.62 mmol). After 48h reflux, under N_2 atmosphere, the suspension was cooled down to r.t. and the solvent evaporated. The resulting product was purified by silica gel column chromatography, using $CHCl_3$/MeOH (98/5) as eluent. After solvent evaporation, the purified compound wasn't isolated and it was performed other column chromatography with silica gel, using EtOAc/n-hexane (90/10). After solvent evaporation from the collected fractions, **c9** was obtained as an brown oil.

η = 9%

Rf (EtOAc/n-hexane; 9:1) = 0,48

^{1}H-RMN (400MHz, CD_3OD; δ/ppm): 4.87 (s, 1H, NH), 4.13 (p, J = 7.1 Hz, 2H, CH_2^h), 3.45 (dd, J = 12.9, 5.9 Hz, 2H, CH_2^b), 3.42 – 3.34 (m, 4H, $CH_2^{a,f}$), 3.34 – 3.24 (m, 2H, CH_2^e), 2.38 (t, J = 8.1 Hz, 2H, CH_2^g), 1.44 (s, 3H,CH_3^i), 1.42 (s, 9H, $(CH_3)_3^c$), 1.25 (dd, J = 13.9, 6.7 Hz, 1H, NH^d).

ESI-MS (+) (mass/charge-m/z): 275.4 $[M+H]^+$ calculated for $C_{21}H_{30}N_4O_4$= 274,36.

2.3.13. Synthesis and characterization of **[(2-tert-Butoxycarbonylamino-ethyl)-(1-methyl-1H-imidazol-2-ylmethyl)-amino]-acetic acid – L3.3-Boc**

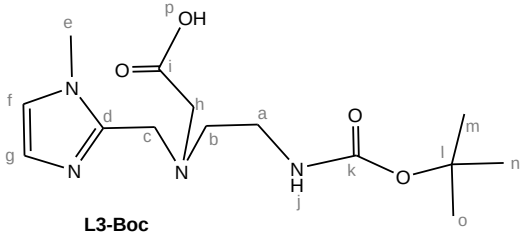

L3-Boc

The percursor **L3.3-Boc** was prepared as described in the literature. (111)

A solution of **c7** (0.16 g, 0.51 mmol) and 10% Pd/C (54.20 mg, 0.41 mmol) in MeOH (50 mL) at r.t. was placed under an atmosphere of hydrogen. After 7h, the mixture was filtered through Celite using MeOH as eluent, and concentrated under reduced pressure, to afford compound **L3-Boc** as orange oil.

η = 94%

Rf ($CHCl_3$/MeOH; 9,5:0,5) = 0.30

^{1}H NMR (400 MHz, $CDCl_3$; δ/ppm): 6.88 (s, 1H, $CH^{f/g}$), 6.87 (s, 1H, $CH^{f/g}$), 6.69 (s, 1H,OH^{p}), 3.64 (s, 2H, CH_2^{b}), 3.56 (s, 2H, CH_2^{a}), 3.33 (s, 3H, CH_3^{e}), 2.95 (s, 2H, CH_2^{c}), 2.95 (s, 1H, NH^{j}), 2.48 (s, 2H, CH_2^{h}), 1.33 (s, 9H, $(CH_3)_3^{m,n,o}$, Boc).

^{13}C NMR (400 MHz, $CDCl_3$; δ/ppm): 176.85 ($C=O^{i}$), 156.42 ($C=O^{k}$, Boc), 146.04 (C^{d}), 127.01(C^{f}), 121.10 (C^{g}), 78.59 (C^{e}), 77.36 (C^{h}), 53.83 (C^{a}), 49.90 (C^{b}), 32.78 (C^{c}), 28.68 (C^{e}), 28.57 ($C^{m,n,o}$, Boc).

ESI-MS (+) (mass/charge-m/z): 313.4 $[M+H]^+$ and 351.3 $[M+K]^+$ calculated for $C_{14}H_{24}N_4O_4$= 312,18.

2.3.14. Synthesis and characterization of **[(2-tert-Butoxycarbonylamino-ethyl)-(2-pyrazol-1-yl-ethyl)-amino]-acetic acid – L2-Boc**

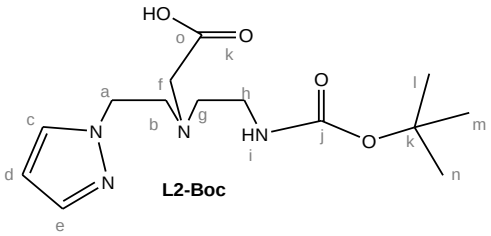

The ligand **L2-Boc** was prepared using a similar procedure described in the literature. (111)

A solution of **c8** (192 mg; 0.47 mmol) and 10% Pd/C (50 mg; 0.47 mmol) in MeOH (50 mL) at r.t. was placed under hydrogen atmosphere. After 7 h, the mixture was filtered through Celite using MeOH as eluent, and concentrated under reduced pressure, to afford compound **L2-Boc** as a orange oil.

η = 94%

Rf ($CHCl_3$/MeOH; 9,5:0,5) = 0.59

^{1}H NMR (400 MHz, $CDCl_3$; δ/ppm) : 9.31 (s, 1H, OH), 7.46 (d, J = 15.6 Hz, 2H, $(CH)_2^{c,e}$), 6.20 (s, 1H, CH^{d}), 5.39 (s, 1H,NH^{i}), 4.20 (s, 2H, CH_2^{a}), 3.29 (s, 2H, CH_2^{f}), 3.07 (s, 4H,$(CH_2)_2^{b,g}$), 2.72 (s, 2H, CH_2^{h}), 1.38 (s, 9H, $(CH_3)_3^{l,m,n}$, Boc).

^{13}C NMR (400 MHz, $CDCl_3$; δ/ppm): 173.65($C=O^{j}$), 156.29 ($C=O^{o}$), 139.49 (C^{c}), 130.23(C^{e}), 105.68 (C^{d}), 79.10 (C^{k}), 77.36 (C^{f}), 54.50 (C^{g}), 54.16 (C^{a}), 49.49 (C^{b}), 37.92 (C^{h}), 28.43 ($C^{m,n,l}$, Boc).

ESI-MS (+) (mass/charge-m/z): 313.4 $[M+H]^+$ calculated for $C_{14}H_{24}N_4O_4$= 312,18.

2.4. SYNTHESIS AND CHARACTERIZATION OF BOMBESIN ANTAGONIST PEPTIDES AND CONJUGATES

Table 2.5 – Summary of procedures in Solid Phase Peptide Synthesis (SPPS).

Procedure	Addition	Time	Cycles
Swelling	2.0 mL DMF	15 min	1
	2.0 mL DMF	60 min	1
Fmoc Deprotection	2.0 mL 25% piperidine/DMF	3 min	1
	2.0 mL 25% piperidine/DMF	12 min	1
Washing	2.0 mL DMF	1 min	5
To store the resin dry	2.0 mL DCM	5 min	2
Cleavage	2.0 mL 95%TFA, 2.5% Tis and 2.5% H_2O	2-3h	1
Coupling	1eqv of Resin 3 eqv of coupler 4 eqv of Activator (HBTU or HATU) 7 eqv of Base (Dipea)	3h	2x

2.4.1. Synthesis of Bombesin Antagonist (**AR**) peptide

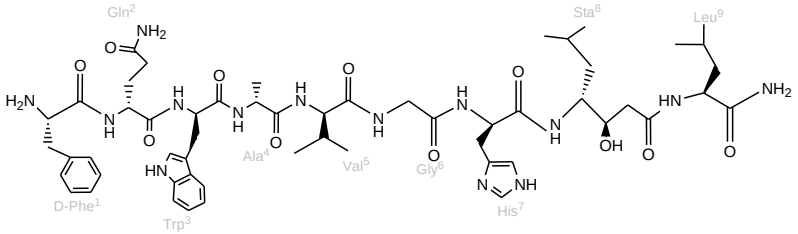

The **AR** peptide was prepared using a similar procedure to that described in the literature. (87)

The fully protected AR peptide (DPhe[1]-Gln[2]-Trp[3]-Ala[4]-Val[5]-Gly[6]-His[7]-Sta[8]-Leu[9]-NH_2.) was prepared by Fmoc-based Solid Phase Peptide Synthesis in a CEM 12-Channel Automated Peptide Synthesizer (scale 0.1 mM), using a Rink Amide-MBHA resin 100 – 200 mesh (0.97g; substitution: 0.65 mmol/ g) and the following side chain protecting groups: Boc for Trp and Trt for His and Gln.

The peptide was cleaved from the resin. The cleavage solution was separated from the resin by filtration and concentrated under N_2. The crude peptide was precipitated and washed with ice-cold diethylether, vacuum-dried, and dissolved in water before lyophilization.

ESI-MS (+) (m/z): 557.7 $[M+2H]^{++}$, 976.9 [M-His], 1130.4 $[M+NH_4]^+$, 1130.4 $[M+H_2O]^+$ calculated for $C_{55}H_{80}N_{14}O_{11}$ = 1112.61

2.4.2. Synthesis of AR peptide conjugated with polyethyleneglycol (PEG_2) (**$ARPEG_2$**)

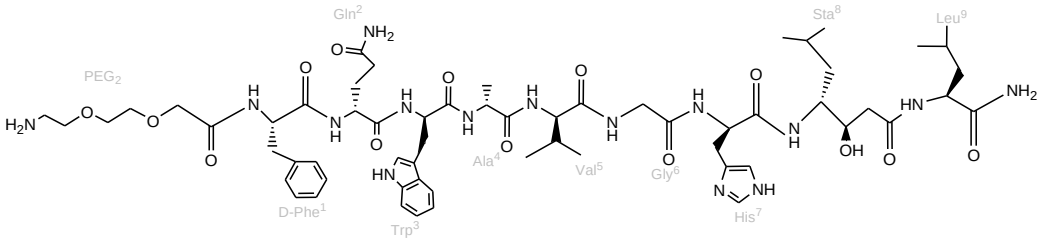

The **AR** peptide in solid phase, obtained as described in section 2.4.1, (0.39 g; 0.25 mmol), was suspended in DIPEA (342 µL)/DMF (250 µL) and added to the commercial reagent PEG_2 (0.39 g; 1.01 mmol) pre-incubated during 15 min with HATU (0.29 g; 0.76 mmol) in DMF. The pH was followed and the reaction mixture was left under stirring at room temperature for 3 hours. Then, another coupling cycle was repeated using the same conditions. The kaiser test (see section 2.4.9) was performed with a negative result for free amine groups. After cleavagefrom the resin using the standard cocktail mixture (95% TFA, 2.5% TIS, 2.5% H_2O) the compound, **$ARPEG_2$**, was precipitated with ice-cold diethylether. The precipitate was dried under N_2 flow and dissolved in water before lyophilization.

ESI-MS (+) (mass/charge-m/z): 1123.1 $[M\text{-His}]^+$, 1258.9 $[M+H]^+$ and 1298.5 $[M+ACN]^+$ calculated for $C_{61}H_{91}N_{15}O_{14}$ = 1257.9

RP-HPLC (Method 2): Rt=15.84 min.

2.4.3. Synthesis of **L4**

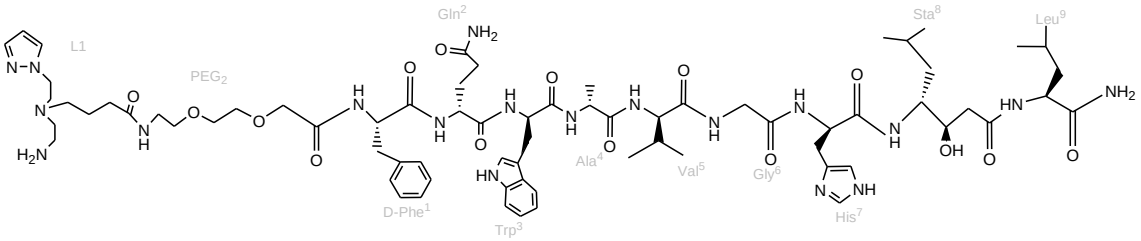

The FMOC group of **$ARPEG_2$** in solid phase, not submitted to any purification, was deprotected with a solution of 25% piperidine/DMF. After 15 min. stirring, the **$ARPEG_2$** containing resin (0.05 g;, 0.03 mmol) was suspended in DIPEA (200 µL)/DMF (250 µL) and added to the Boc-protected bifunctional chelator **L1-Boc** (0.08 g; 0.24 mmol) pre-incubated during 30 min with HATU (0.13 g; 0.35 mmol) in dry DMF. The solution was

submitted to three cycles of microwave irradiation (40 W, 75ºC, 5 min). The residue was deprotected with the standard cocktail mixture (95% TFA, 2.5% TIS, 2.5% H_2O) and precipitated with ice-cold diethylether. The precipitate was dried under nitrogen flow and dissolved in water before lyophilization. The reaction mixture was purified by semi-preparative RP-HPLC (Method 1). The HPLC fraction corresponding to the compound was collected and evaporated. After analytical purification and evaporation of solvents from the corresponding fractions, **L4** was obtained as a white solid.

ESI-MS (+) (mass/charge-m/z): 1481.5 $[M+H]^+$ calculated for $C_{72}H_{109}N_{19}O_{15}$ = 1479.84

RP-HPLC (Method 1): Rt = 34.2 min; (Method 2) 98.5 % Rt=20.00

2.4.4. Attempted synthesis of **L6**

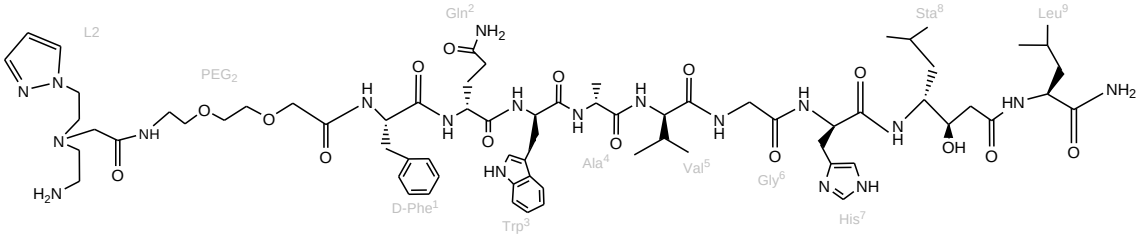

The coupling of the peptide conjugate **L6** was done using the same procedure as for the synthesis of **L4**, described in section 2.4.3. The ligand, **L2-Boc** (52.40 mg; 0.17 mmol) was pre-incubated with the activator HATU (63.95; 0.17mmol) was coupled with the peptide conjugated **$ARPEG_2$** in resin, pre-deprotonated with Dipea (80µL; 0.45 mmol) by microwave technology (40 W, 75ºC, 5 min).

ESI-MS (+) (mass/charge-m/z): calculated for $C_{70}H_{105}N_{19}O_{15}$ = 1451,8.

2.4.5. Attempted synthesis of **L7**

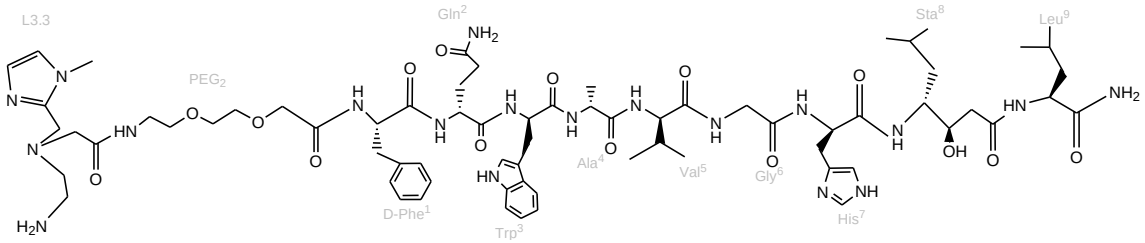

The coupling of the peptide conjugate **L7** was done as the same procedure for the synthesis of **L4**, described in section 2.4.3. L3.3-Boc (50.90 mg; 0.16 mmol) was pre-activated with the activator HATU (62.10; 0.16 mmol) and coupled to **ARPEG$_2$** in resin, with Dipea as base (80µL; 0.43 mmol) by microwave technology (40 W, 75ºC, 5 min).

ESI-MS (+) (mass/charge-m/z): calculated for $C_{70}H_{105}N_{19}O_{15}$ = 1451,8.

2.4.6. Cleavage of Bombesin Antagonist and Resin

The AR and derivatives were cleaved and removed from the resin and remaining lateral protection groups, using a deprotection cocktail of 2mL TFA:TIS:H_2O (v/v) (95 : 2.5:2.5), mixed for 2h-3h.

2.4.7. Precipitation of Bombesin Antagonist Derivatives

Diethyl ether at -18^0 C was added to the collected product and centrifuged at 3,500 rpm at 4^{0}C during 10 min. The solvent was disposed of and this procedure repeated twice. The product was liophilizated overnight, and the dry product was stored at -18^{0}C.

2.4.8. HPLC analysis and Purification of Bombesin Antagonist Derivatives

The synthesized product was analyzed and purified by RP-HPLC, Method 1, described in section 2.2.2 .

For all tested compounds, HPLC runs were performed with detection at 220 nm (wavelength of peptide bond absorption) and 280 nm (wavelength of tryptophan absorption). (93)

After purification the collected fractions were evaporated and then freeze dried in the lyophilizer then the dry product was stored at -18^{0}C.

2.4.9. Kaiser Test

SPPS when performed manually is necessary to assess the coupling with the formation of the amide bond and also the deprotection reactions. This evaluation is done through a Kaiser Test (Ninhydrin Test). Kaiser Test consist in testing a small sample of resin with a solution of 5% ninhydrin in ethanol, 80% phenol in ethanol and potassium cyanide (KCN) in pyridine (2mL 0.001 KCN in 98mL pyridine), followed by heating. (95)

This qualitative test involve the comparison of the color with reference solutions. (Table 2.7). The appearance of the color blue when the α-AA is deprotected is due to formation of Ruhemann complex.

Table 2.6 – Color patterns of Kaiser test.

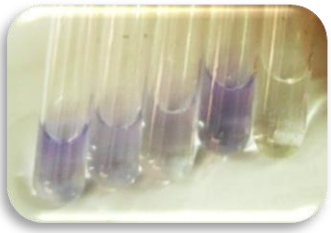	**Colorless or faint blue color**	• **complete coupling,** • **proceed with synthesis**
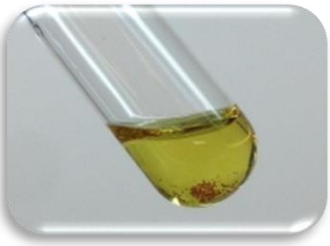	**Solution yellow**	
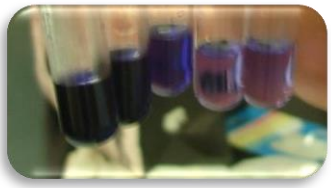	**Dark blue solution but beads are colorless**	• nearly complete coupling, • extend coupling or capunreacted chains
	Solution is light blue but beads are dark blue	• coupling incomplete, • recouple
	Solution is intense blue and all beads are blue	• failed coupling, • check amino acid, reagents, then recouple

2.4.10. Handling and Storage of Peptides

Peptides have widely varying solubility properties. The main problem associated with the dissolution of a peptide is secondary structure formation. This formation is likely to occur with all, but the shortest of peptides and is even more pronounced in peptides containing multiple hydrophobic amino acid residues. Secondary structure formation can be promoted by salts. It is recommended first to dissolve the peptide in sterile distilled or deionized water. Sonication can be applied if necessary to increase the rate of dissolution. If the peptide is still insoluble, addition of a small amount of dilute (approximately 10%) acetic acid (for basic peptides) or aqueous ammonia (for acidic peptides) can facilitate dissolution of the peptide.

For long-term storage of peptides, lyophilization is highly recommended. Lyophilized peptides can be stored for years at temperatures of -20°C or lower with little or no degradation. Peptides in solution are much less stable. Peptides are susceptible to degradation by bacteria so they should be dissolved in sterile, purified water.

Peptides containing methionine, cysteine, or tryptophan residues can have limited storage time in solution due to oxidation. These peptides should be dissolved in oxygen-free solvents. To prevent the damage caused by repeated freezing and thawing of peptides, dissolving the amount needed for the immediate experiment and storing the remaining peptide in solid form is recommended.(96)

All the peptides used in this project follow the previous recommendations.

2.5. SYNTHESIS AND CHARACTERIZATION OF THE $Re(CO)_3$-COMPLEXES

2.5.1. Rhenium complex *fac*-[$Re(CO)_3(\kappa^3$-**L4**$)$]+ (**Re4**)

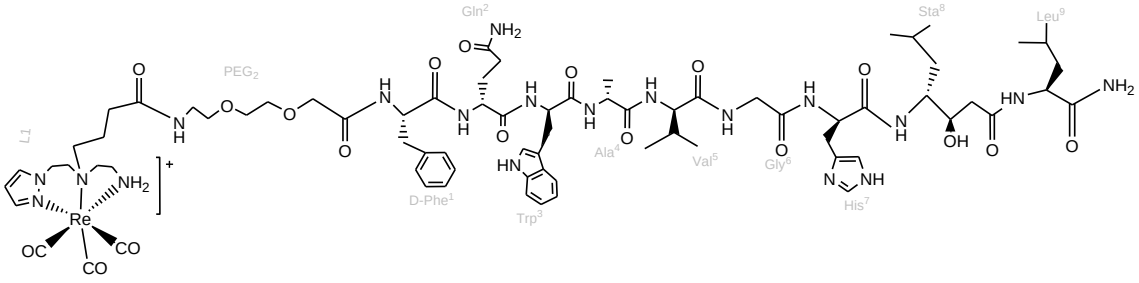

Briefly, **L4** (0.60 mg, 0.4x10^{-3} mmol) reacted with the organometallic precursor [$Re(CO)_3(H_2O)_3$]^{Br} (0.30 mg, 0.7x10^{-3} mmol) in MeOH in reflux for 72 h and with pH adjustment with NaOH from 5 to 9-10. After evaporation of the solvent the resulting residue was purified by preparative RP-HPLC (Method 2).

ESI-MS (+) (mass/charge-m/z): 1751 $[M+H]^+$, calculated for $C_{75}H_{109}N_{19}O_{18}Re^+$ = 1749,84 .

RP-HPLC (Method 2): Rt = 23,17 min

2.5.2. Rhenium complex *fac*-[$Re(CO)_3(\kappa^3$-**L5**$)$]+ (**Re5**)

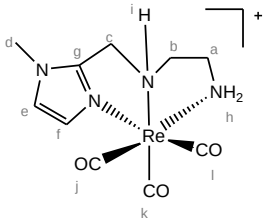

The complex was prepared according to the methodology described in **2.5.1** Briefly, **L5** (18 mg, 0.12 mmol) reacted with the organometallic precursor $[Re(CO)_3(H_2O)_3]^{Br}$ (50 mg, 0.12 mmol) in MeOH reflux for 3 h. After evaporation of the solvent the resulting residue was purified by preparative RP-HPLC (Method 2, section 2.2.2). After that, the complex **Re5** was isolated as a white solid.

η = 75%

^{1}H-NMR (300MHz, CD_3OD; δ/ppm): 7.23 (s, 1H, CH^e), 7.10 (s, 1H, CH^f), 4.40 (d, J = 1.5 Hz, 2H, CH_2^c), 3.76 (s, 3H, CH_3^d), 3.09 – 2.75 (m, 4H, $CH_4^{a,b}$)

^{13}C-NMR (300MHz, CD_3OD; δ/ppm): 153.88(C^g), , 129.36(C^e), 125.13 (C^f), 57.42 (C^b), 51.52(C^c), 41.54(C^a), 34.97(C^d).

ESI-MS (+) (mass/charge-m/z): 425.2 $[M+H]^+$, calculated for $C_{10}H_{14}N_4O_3Re^+$ = 424.45.

RP-HPLC (Method 2): Rt = 18.57 min

2.6. SYNTHESIS AND CHARACTERIZATION OF ^{99m}TC-COMPLEXES

2.6.1. *fac*-$[^{99m}Tc(H_2O)_3(CO)_3]^+$ precursor

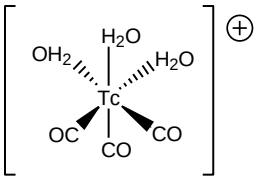

To prepare the precursor, the following reagents were weighted in a glass vial (of 10mL capacity) and purged with N_2: sodium tartrate dihydrate (8.50 mg), sodium tetraborate decahydrate (2.85 mg), sodium carbonate (7.15 mg) and sodium boranocarbonate (4.50 mg). Then, $Na[^{99m}TcO_4]$ was eluted from a $^{99}Mo/^{99m}Tc$ generator with a solution of 0.9% (w/v) NaCl. From that eluate, 3.0 mL (~ 8.5 mCi) were added to the reaction vial, which was incubated at 100 °C for 30 min. After cooling the vial to r.t., the solution was neutralized with 1 M HCl (140 – 160 μL) to decompose any residual boranocarbonate.

RP-HPLC (Method 2): Rt = 8.87 min

2.6.2. ^{99m}Tc complex *fac*-[^{99m}Tc(CO)$_3$(κ^3-**L5**)]$^+$ (**Tc5**)

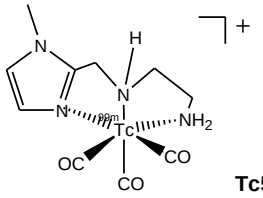

Tc5

In a capped nitrogen purged glass vial, 500 µL of a 10^{-4} M solution of the ligand **L5,** were added to a solution of *fac*-[^{99m}Tc(CO)$_3$(H$_2$O)$_3$]$^+$ (500 µL, 1.80 mCi, pH 7). The vial was incubated at 100 °C for 30 min and the resulting complex was analyzed by RP-HPLC (Method 2) using the same method of the rhenium surrogate.

RP-HPLC (Method 2): Rt = 19.20 min

2.6.3. ^{99m}Tc complex *fac*-[^{99m}Tc(CO)$_3$(κ^3-**L4**)]$^+$ (**Tc4**)

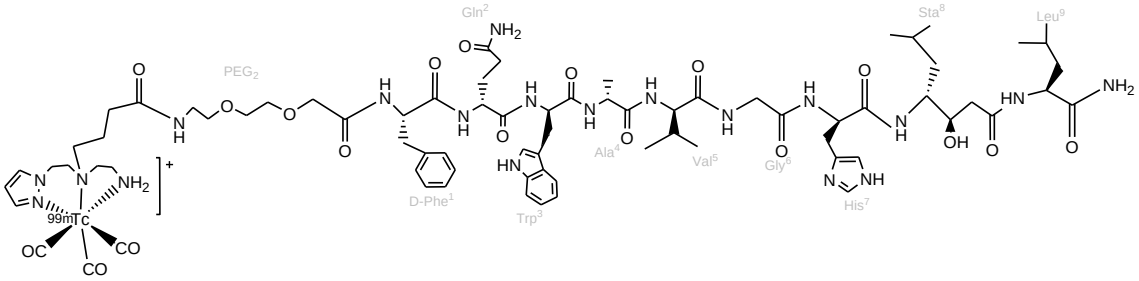

In a capped nitrogen purged plastic vial, 40µL of **L4** (1,65x10^{-4} M, dissolved in water) were added to a solution of *fac*-[^{99m}Tc(CO)$_3$(H$_2$O)$_3$]$^+$ (360 µL; 2.60 mCi) at pH 7. The vial was incubated at 90 °C for 30 min and **Tc4** was analyzed by RP-HPLC (Method 2) and in comparison with the corresponding Rhenium complex.

RP-HPLC (Method 2): Rt = 24.07 min

3. Results and Discussion

3.1. Synthesis of Ligands and Bifuncional Chelators (BFC's)

As mentioned before, the main goal of this work was to contribute for the design of new target-specific radiopharmaceuticals useful for *in vivo* imaging of GRP receptors overexpressed in prostatic neoplasias. To achieve such goal, we have explored the radiolabelling of a bombesin analogue peptide (AR) with the *fac*-$[^{99m}Tc(CO)_3]^+$ moiety. The bifuncional chelators contain pyrazolyl- and imidazolyl coordination groups, and present N,N,N donor atom sets. Both types of chelators contain a pendant arm with a terminal CO_2H group for conjugation to the AR peptide. In all the BFC's, the free terminal primary amine is protected with a Boc protecting group (Boc, tert-butyloxycarbonyl), in order to avoid undesirable side-reaction, namely lactamization, that will hamper the conjugation of the AR peptide. As it is shown in figure 3.1, the two pyrazolyl-containing BFC's present spacers of different length, between the carboxylic acid group and the chelating backbone. In this way, we expected to assess the influence of the chelating unit and/or spacer on the biological profile of the final radiolabeled bioconjugates.

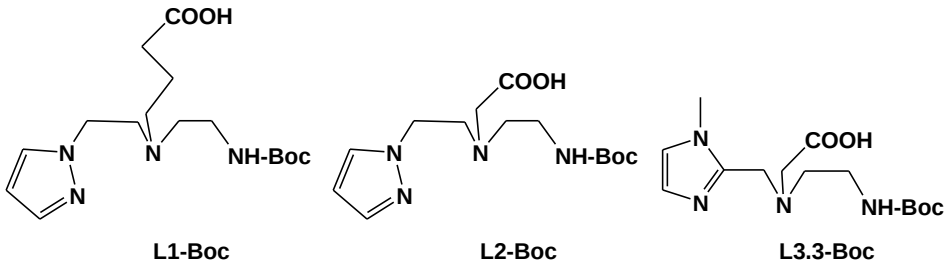

Figure 3.1 –Boc-protected pyrazolyl and imidazolyl bifuncional chelators.

3.1.1. Pyrazolyl-Based BFC's

The synthesis of the pyrazolyl-based BFC (**L1-Boc**) containing a propylenic spacer between the chelating unit and the carboxylic acid group has been performed as previously reported (62,97), using a multistep synthesis as depicted in scheme 3.1. The characterization of **L1-Boc** by ^1H and ^{13}C NMR gave data consistent with those described in the literature for this compound. (63)

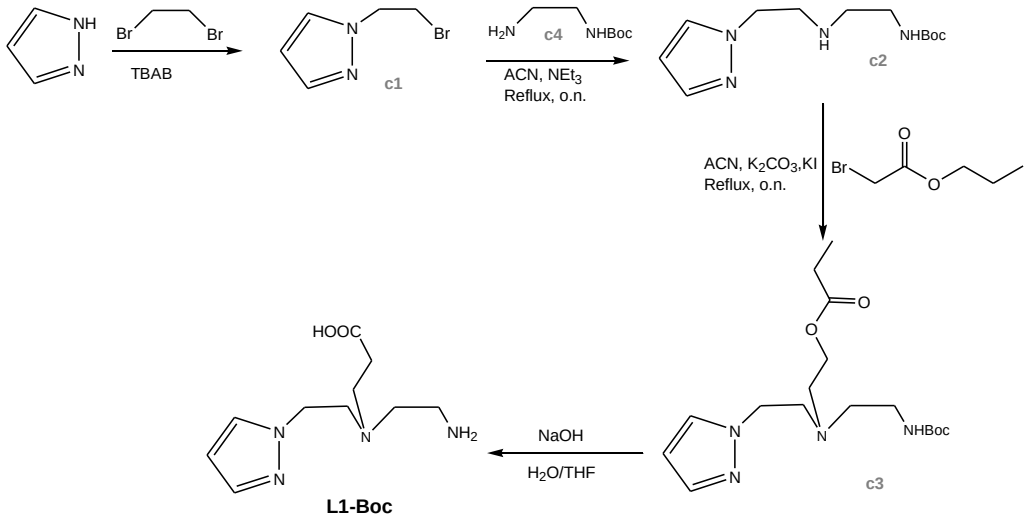

Scheme 3.1 - Synthesis of L1-Boc; **TBAB= tetrabutylammonium bromide**

The new BFC **L2-Boc**, containing a methylenic linker between the chelating unit and the carboxylic acid, was synthesized in moderate yield (61%), using a similar procedure to the one involved in the synthesis of **L1-Boc**(scheme 3.2); briefly, after alkylation of the central secondary amine in the Boc-protected pyrazolyl precursor, with benzyl bromoacetate, the ester group was hydrolyzed with Pd/C in the presence of H_2 (scheme 3.2).

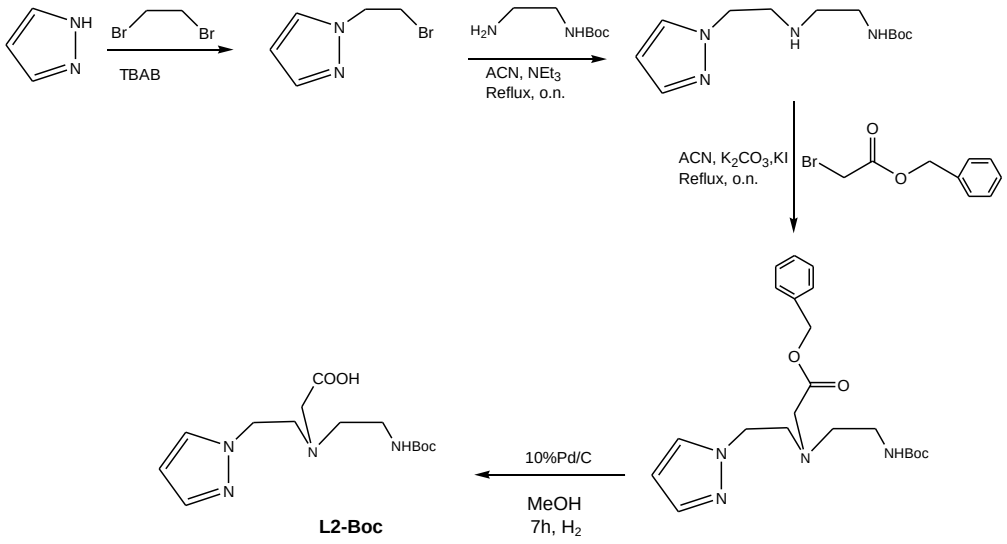

Scheme 3.2 - Synthesis of **L2-Boc** (strategy 1).

All the intermediates and the final BFC, **L2-Boc**, were fully characterized by the usual analytical techniques, namely NMR spectroscopy, electrospray ionization mass spectrometry (ESI–MS) and reverse phase High-Performance Liquid Chromatography (RP-HPLC).

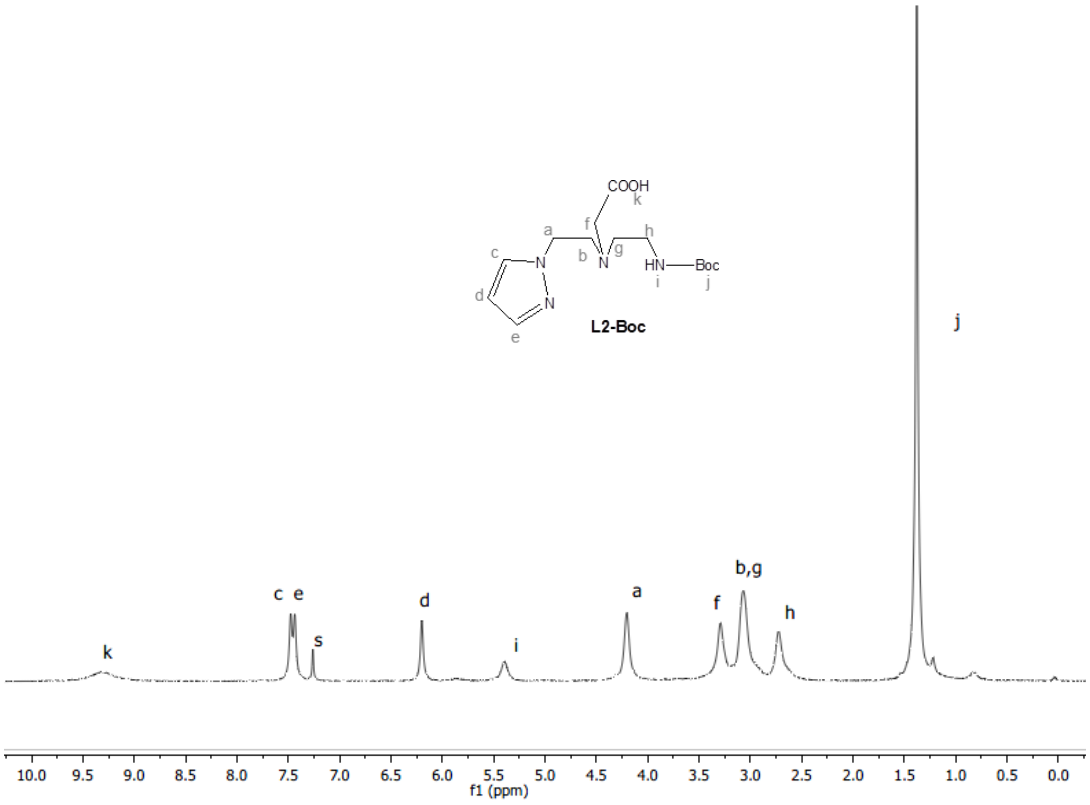

Figure 3.2 - ^{1}H-NMR spectrum of **L2-Boc** in $CDCl_3$. (S= residual $CHCl_3$)

As an example, the ^{1}H-NMR spectrum of **L2-Boc** in $CDCl_3$ is presented in Figure 3.2. The assignment of the peaks present in the ^{1}H-NMR spectrum was made by comparison with the peaks observed for similar compounds and based on the relative areas and chemical shifts of the different peaks. It was found all the expected resonances, namely the typical resonances for the H(3) (H^c; δ **6.15**) H(4) (H^d; δ **6.15**) and H(5) (H^e; δ **7.46**) protons of azolyl ring and the typical singlet for the methyl protons of Boc group.

We also succeeded to obtain **L2-Boc** in a global yield (20%) by reaction of *N*-2-bromoethyl-pyrazole with benzyl 2-(2-(tert-butoxycarbonylamino)ethylamino)acetate, as presented in scheme 3.3. This strategy involved two N-alkylation reactions followed by the the selective deprotection of the benzyl group. This strategy can be useful to obtain BFC's containing carboxylic groups at the 3- and 5- positions of the azolyl ring, aiming at the modulation of the pharmacokinetics of the respective tricabonyl complexes. Preliminary studies have shown that the first strategy does not work for the synthesis of this type of compounds due to side lactamization reaction involving the carboxylic substituents from the azolyl rings (data not shown).

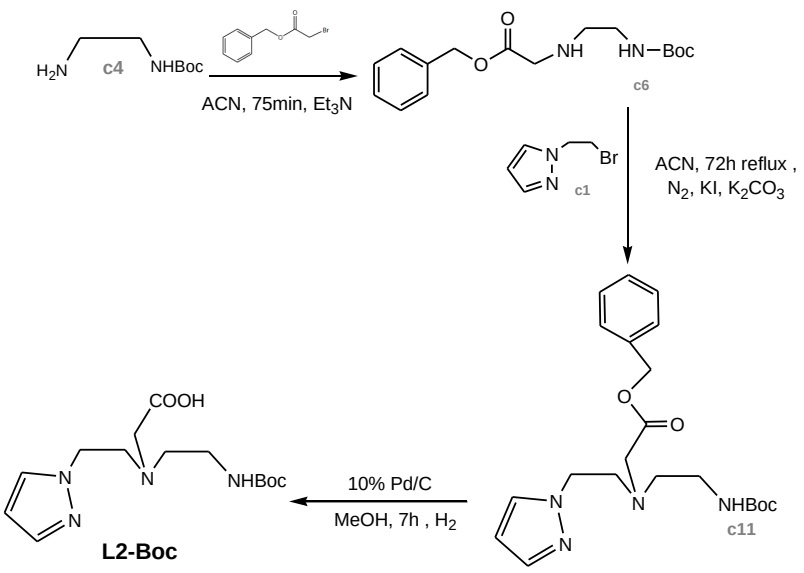

Scheme 3. 3 - Synthesis of **L2-Boc** (strategy 2).

.

3.1.2 Imidazolyl derivatives

As state above, the imidazolyl BFC was synthesized in order to evaluate the influence of the chelating unit on the biological profile of the correspondent bioconjugates. Moreover, the imidazolyl ring is also easily functionalized with selected functional groups (*e.g*. carboxylic acid) to further modulated the pharmacokinetics of the correspondent ^{99m}Tc complexes, in the same way as the congener pyrazolyl-based BFC's. To accomplish this goal, we decided to synthesize a model imidazolyl-diamine chelator to evaluate its coordination capability towards *fac*-$[M(CO)_3]^+$ (M = Re, ^{99m}Tc), as this class of ligands was not studied yet with these metallic cores. These studies were expected to partially predict the stability of Re(I) and ^{99m}Tc(I)-bioconjugate stabilized by BFC's designed based on this imidazoyl-diamine backbone.

As shown in scheme 3.4, the new imidazoyl-diamine chelator **L5** was synthetized in a relatively fast and simple way based on the reductive amination of the desired imidazole aldehyde with Boc-protected ethylenediamine. The final compound has been obtained with an overall yield of 64.7%.

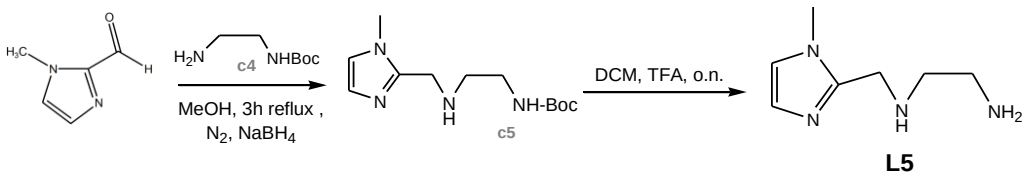

Scheme 3.4 - Synthesis of **L5.**

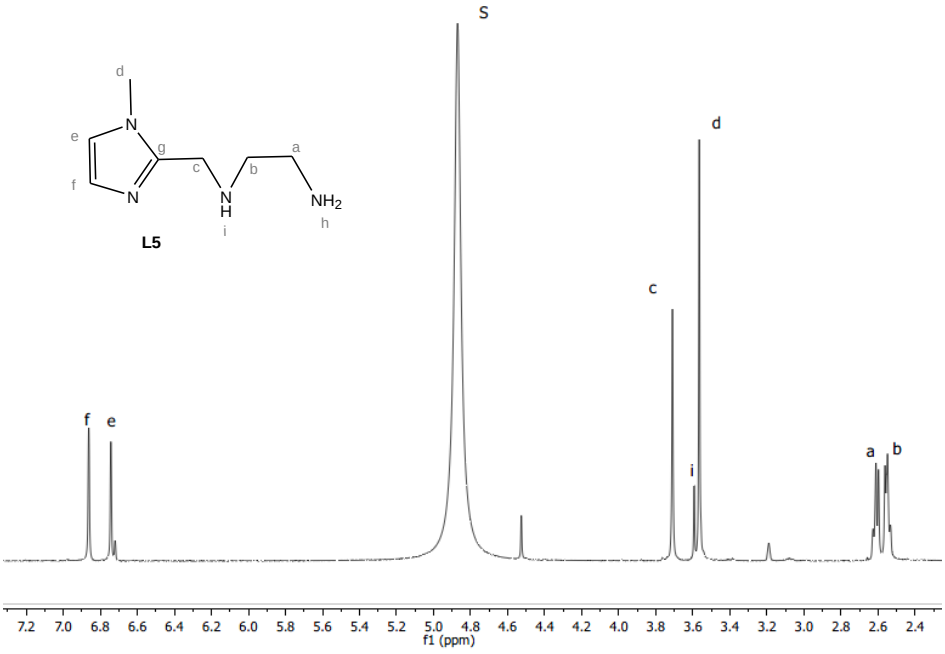

Figure 3.3 - ^{1}H-NMR spectrum of **L5** in CD_3OD or D_2O. (S= residual Water from CD_3OD)

The ^{1}H NMR spectrum of **L5** (Fig. 3.3) shows all the expected protons of the molecule: i) two resonances,integrating for one proton each, due to the CH^{e} and CH^{f} protons of the imidazol ring, are present at low field; ii) a sharp peak integrating to three protons, corresponding to the methyl protons is observed at high field; iii) the methylenic protons H^{a} and H^{b} of the imidazoyl-diamine backbone appear as multiplets, also at high field (δ **2.61** and **2.55**); iv) the remaining methylenic protons (H^{c})emerge as a singlet, at lower field. The two protons from the amines (NH_2^{h} and NH^{i}) are not observed due to the hydrogen–deuterium exchange reaction (also called H–D or H/D exchange) in which the hydrogen atoms are replaced by a deuterium atom, from the deuterated solvent. (98)

Based on the chelating backbone of **L5**, we have studied the possibility of synthesizing imizadoyl-containing BFC's similar to **L1-Boc** and **L2-Boc**. We could not explore the same synthetic pathway as in the case of the pyrazolyl congeners, since the N-alkylation of the imidazolyl-diamine backbone would be accompanied by the quaternization of the tertiary nitrogen atom from the imidazolyl ring. (99) Therefore, we have devised alternative procedures for the synthesis of the imidazolyl-containing BFC's. Such strategies lied on the reductive amination of 1-methyl-2-imidazolecarboxaldehyde with 4-(2-tert-Butoxycarbonylamino-ethylamino)-butyric acid ethyl ester (**c9**), using sodium triacetoxyborohydride as the reducing agent (Scheme 3.3). Compound **c9** has been prepared by mono-alkylation of the primary

amine of tert-butyl 2-aminoethylcarbamate (**c4**). **c9** was obtained in very low yield, due to competition of lactamization reactions, between the formed secondary amine and the ester of the ethyl 4-bromobutyrate arm. The occurrence of such lactamization reactions have precluded the synthesis of the final BFC, 4-[(2-tert-Butoxycarbonylamino-ethyl)-(1-methyl-1H-imidazol-2-ylmethyl)-amino]-butyric acid ethyl ester (**L3.2-Boc**) (Scheme 3.5).

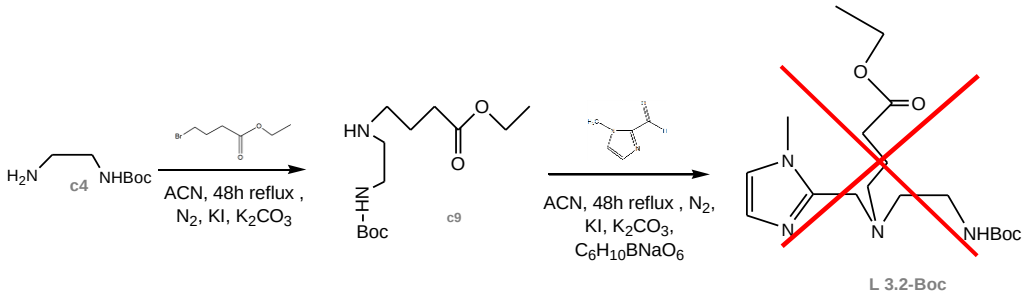

Scheme 3.5 – Synthetic pathway to attain 3-phenylpropyl 2-((2-tert-butoxycarbonylamino)ethyl)(1-metyl-1H-imidazol-2-yl)methyl)amino)acetate

The difficulties found on the synthesis of **L3.2-Boc** were avoided by using a shorter methylenic linker. This allowed the synthesis of **L4-Boc** (Scheme 3.6), which is the imidazolyl-containing congener of the above described **L2-Boc**. To synthesize **L4-Boc** we have started with the mono-alkylation of the primary amine of **c4** with benzyl bromoacetate. As described above, this reaction gave **c6** that was transformed into **c7** upon reductive amination of 1-methyl-2-imidazolaldehyde. Finally, removal of the protecting benzyl group with Pd/C in the presence of H_2 gave **L3-Boc**, which was obtained with an overall yield of 20%.

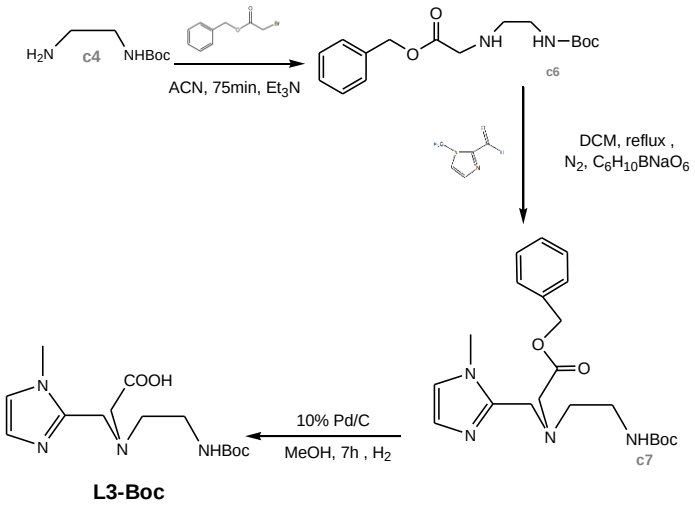

Scheme 3.6 - Synthesis of **L3-Boc.**

L3-Boc was fully characterized by the usual analytical techniques, namely ^{1}H and ^{13}C NMR spectroscopy, and electrospray ionization mass spectrometry (ESI–MS). The spectroscopic characterization corroborated the formulation proposed for **L3-Boc**. As an example, the ^{13}C NMR spectrum of this new BFC is presented in figure 3.4. In this spectrum are present all the expected resonanecs, namely the C=O of Carbon C^{i} and C^{j} at down field (δ **176.85** and **156.42** ppm, respectively)

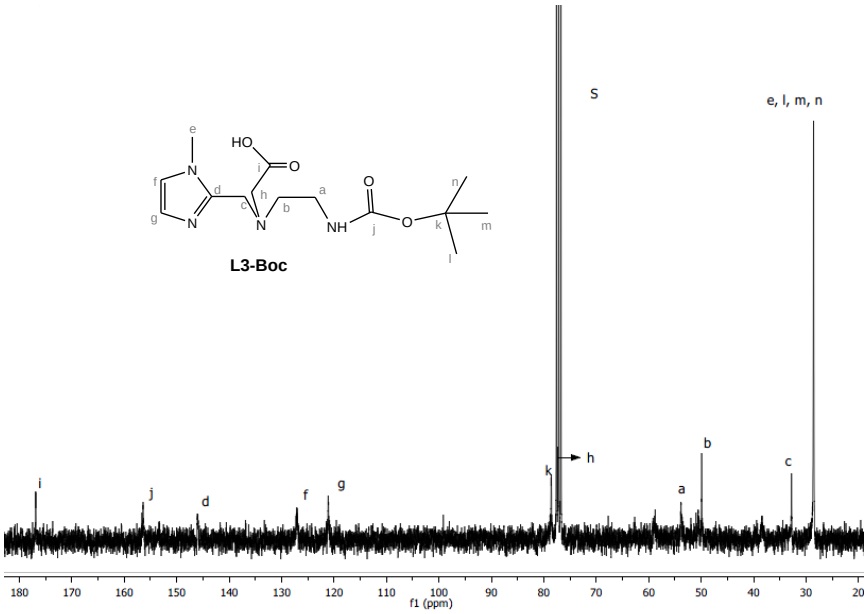

Figure 3.4 - ^{1}H-NMR spectrum of **L3-Boc** in $CDCl_3$ (S= Residual $CHCl_3$, from $CDCl_3$)

3.2. Synthesis, characterization and Biological evaluation of $M(CO)_3L5$ (M= Re, ^{99m}Tc)

3.2.1. Synthesis and Characterization of the Re surrogate: $Re(CO)_3L5$

As mentioned before, owing to the low concentration (10^{-8} – 10^{-10} M) of $[^{99m}TcO_4]^-$ in the saline solution extracted from the generator, it is impossible to characterize the resulting ^{99m}Tc complexes by the normal methods used in chemistry. Therefore, such complexes are often characterized by HPLC comparison with surrogate complexes syntehsized with the natural rhenium ("cold metal"), which present similar coordination chemistry.

The imidazoyl derivative **L5** was reacted with equimolar amount of the precursor *fac*-$[Re(CO)_3(H_2O)]^{Br}$, in refluxing methanol during 3 h (scheme 3.7). This reaction yielded $[Re(CO)_3(\kappa^3\text{-}\mathbf{L5})]^+$ (**Re5**), which was isolated in high yield after purification by preparative RP-HPLC.

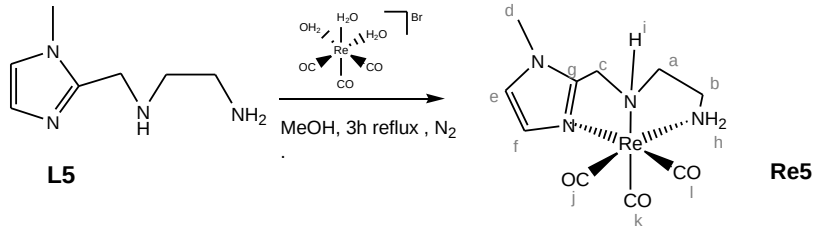

Scheme 3.7 - Synthesis of the complex **Re5**.

Re5 was characterized by ^1H, ^{13}C and 2D-NMR spectroscopy, ESI-MS and RP-HPLC. In the ESI-MS spectrum we identified a peak with m/z=425.2 which the pattern of isotopic distribution is corresponding to the molecular peak $[M+H]^+$ of the rhenium complex. As despicted in Figure 3.5, the tridentate coordination mode of the chelator was confirmed by the splliting pattern and chemical shifts of the several resonances ^1H NMR. The $H^{e,f}$ and the methyl protons of the imidazoyl ring are shifted downfield ($H^{e,f}$, $\Delta\cong0.36$ ppm ; H^d $\Delta\cong0.19$ ppm) relatively to the same resonances in **L5**. The methylenic protons of the coordinating backbone are also downfield shifted and, due to the diastereotopic character of these methylenic protons after coordination to the metal center, they appears as multiplets. The H^c protons emerges as a false singlet and the $H^{a,b}$ protons as two multiplets, one integrating for one proton and the other for three protons. This behavior, which is a strong evidence of ligand coordination, has been already observed in other tricarbonyl complexes of the same type previously described. (60,99–101)

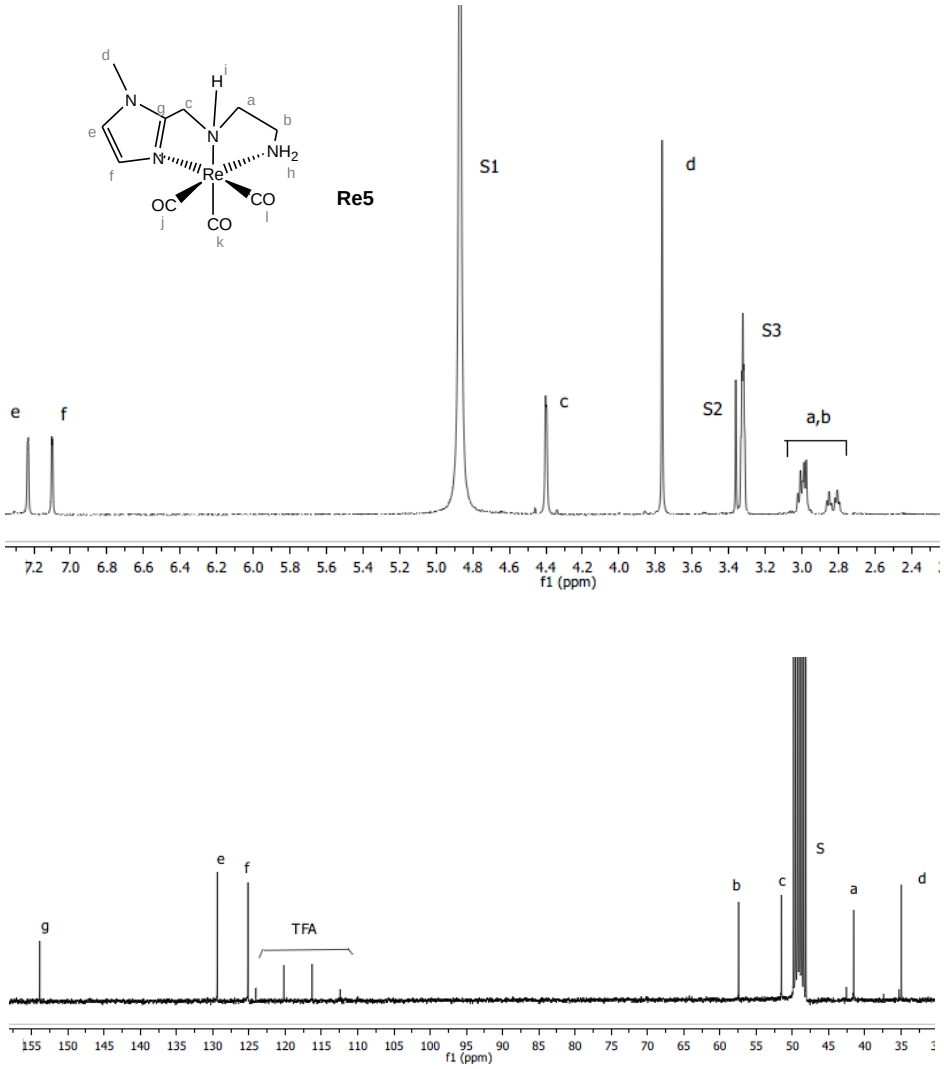

Figure 3.5 - ^{1}H-NMR spectrum (Top) and ^{13}C-NMR spectrum (bottom) of **Re5** in CD_3OD. (S= solvent peak; S1= Residual Water from CD_3OD; S2=Residual MeOH; S3= CD_3OD)

The ^{13}C-NMR spectra showed all the resonances for the imidazoyl backbone and two resonances for the C≡O ligands at downfield.

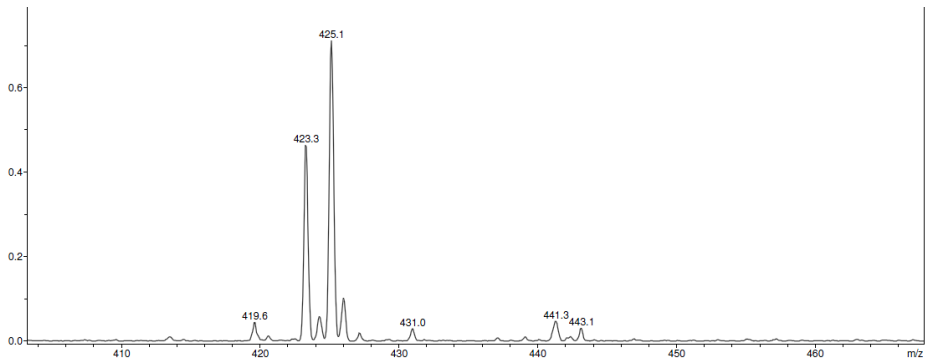

Figure 3.6 – ESI-MS spectrum of **Re5**.

The analysis of the 2D-experiment besides allowing the assignment of the peaks in the ^{1}H spectra, give us information about the correlations between protons. In this case, we observe that the H^{h} and H^{i} are correlated with each other. Also, protons from the aromatic ring of Imz, H^{e} is correlated with H^{d} and H^{c}.

Analysing the ESI-MS spectra, presented in Figure 3.6, we identified a peak with m/z=425.1 that is $[M+H]^{+}$ with a teorical MW calculated for 424.45. And also, by the RP-HPLC chromatogram we found that 18.57 min was the characteristic retention time of **Re 5.**

3.2.2. Synthesis and characterization of the $^{99m}Tc(CO_3)$L5 Complex

To synthesis of *fac*-$[^{99m}Tc(CO)_3(\kappa^3$-**L5**$)]^{+}$ (**Tc5**) was done by reacting **L5** with the tricarbonyl precursor, $[^{99m}Tc(CO_3)(H_2O)_3]^{+}$ (103), which has been obtained by labeling the Isolink kit (IsoLink® kit, Mallinckrodt-Covidien, Petten, The Netherlands) with $[^{99m}TcO_4]^{-}$, as described in detail in the experimental section. The formation of the precursor was controlled by RP-HPLC (figure 3.8), using method 2 (section 2.2.2).

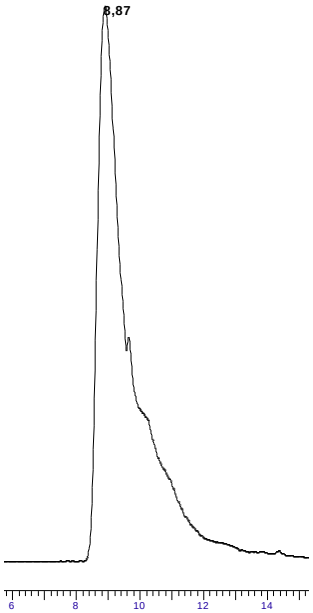

Figure 3.7 – RP-HPLC chromatogram of the tricarbonyl precursor. (Method 2)

As shown in scheme 3.8, an aqueous solution of **L5** (500 µL, [**L5**] = 10^{-4} M) was reacted with the organometallic precursor *fac*-$[^{99m}Tc(CO)_3(H_2O)_3]^{+}$ (500 µL) at 100^{O}C for

30 min, affording *fac*-[^{99m}Tc(CO)$_3$(κ^3-**L5**)]$^+$ (**Tc5**) in high yield and high radiochemical purity (> 95 %).

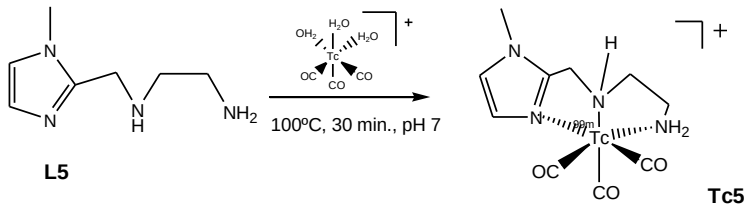

Scheme 3.8 – Synthesis of **Tc5**

The formation of *fac*-[^{99m}Tc(CO)$_3$(κ^3-**L5**)]$^+$ (**Tc5**) has been confirmed by HPLC comparison (Fig. 3.8) with the Re congener, *fac*-[Re(CO)$_3$(κ^3-**L5**)]$^+$ (**Re5**), which has been fully characterized, as above discussed. The difference found in the retention times of the Re and ^{99m}Tc(I) complexes is due to the different paths involved in the detection of the complexes. The Re complex is detected with a UV-vis detector while the ^{99m}Tc complex is with a γ detector. These two detectors are connected in line.

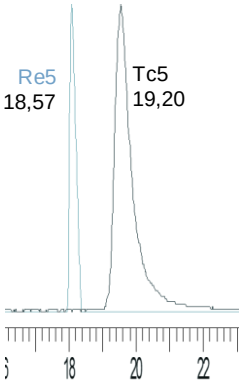

Figure 3.8 - RP-HPLC chromatograms of **Tc5**(γ - detection) and **Re5** (UV detection).

The characterization of *fac*-[^{99m}Tc(CO)$_3$(κ^3-**L5**)]$^+$ (**Tc5**) involved also the assessment of its lipophilicity by measurement of the **log $P_{o/w}$** value at pH = 7.4. **Tc5** has a slightly lipophilic character (log $P_{o/w}$ = + 0.153 ± 0.06), contrarily to the analogous ^{99m}Tc pyrazolyl-diamine complex that is hydrophilic (log $P_{o/w}$ =-0.93± 0.01) (63).

3.2.3 BIODISTRIBUTION STUDIES

The biological behavior of **Tc5** was studied in CD-1 mice, to evaluate its biodistribution, pharmacokinetics and *in vivo* stability. Animals were intravenously injected in the tail. The biodistribution was evaluated at 1 h and 4 h post injection (p.i.). In particular, we were interested in the evaluation of blood clearance, route of elimination and eventual retention in some organs. In fact, the ideal

radiopharmaceutical should be obtained in high yield and radiochemical purity and, after intravenous administration, should be rapidly excreted from non-target organs, preferably by the kidneys, avoiding the hepatobiliar pathway, which compromise their capacity to effectively image solid tumors and metastatic lesions in the abdomen. Moreover, the blood clearance must be fast enough to avoid long exposure to radiation, and slow enough to allow the radioactive compound to reach the target organ.

Table 3.1 - Biodistribution studies of **Tc5** at 1 h and 4 h p.i. (*n* = 3).

Tissue/organ	% AI/g ± SD	
	1 h	4 h
Blood	0.22 ± 0.03	0.07 ± 0.01
Liver	3.82 ± 0,11	0.88 ± 0.07
Intestine	9.03 ± 1.53	6.22 ± 2.48
Spleen	0.22 ± 0.00	0.15 ± 0.01
Heart	0.40 ± 0.07	0.13 ± 0.02
Lung	0.37± 0.20	0.18 ± 0.03
Kidney	2.59 ± 0.04	1.03 ± 0.27
Muscle	0.10 ± 0.01	0.05 ± 0.01
Bone	0.10 ± 0.01	0.05 ± 0.01
Stomach	1.32 ± 0.34	0.26 ± 0.07

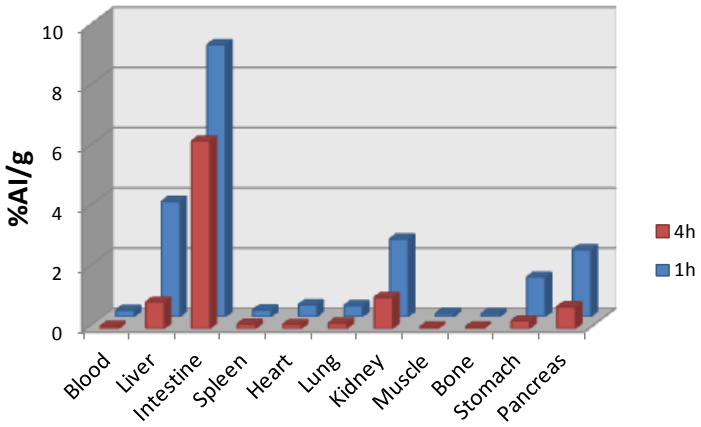

Figure 3.9– Graphic representation of **Tc5** Biosdistribution

Tc5 presented a favorable pharmacokinetic, it was rapidly cleared from the bloodstream (0.22 ± 0.03 to 0.07 ± 0.01 % IA/g, from 1h to 4h p.i.) and major organs, except those related to the excretion pathways. There is no significant uptake in the stomach, indicating a high stability of the complex to reoxidation.

3.2.4 *IN VIVO* STABILITY STUDIES

To study the *in vivo* stability of **Tc5**, urine and blood samples were collected from CD-1 mice injected with the radiotracer, at 1 h p.i. and 4h p.i. After appropriate treatment, the biological samples were analyzed by RP-HPLC. The blood was analyzed after precipitation of proteins, while urine was just centrifuged prior to the HPLC analysis. The chromatograms obtained are shown in figure 3.10 in comparison wih that of **Tc5** (injected solution). The radiochromatograms showed no pertechnetate or other decomposition products, being **Tc5** the only species present, demonstrating the high *in vivo* stability of the radiocomplex.

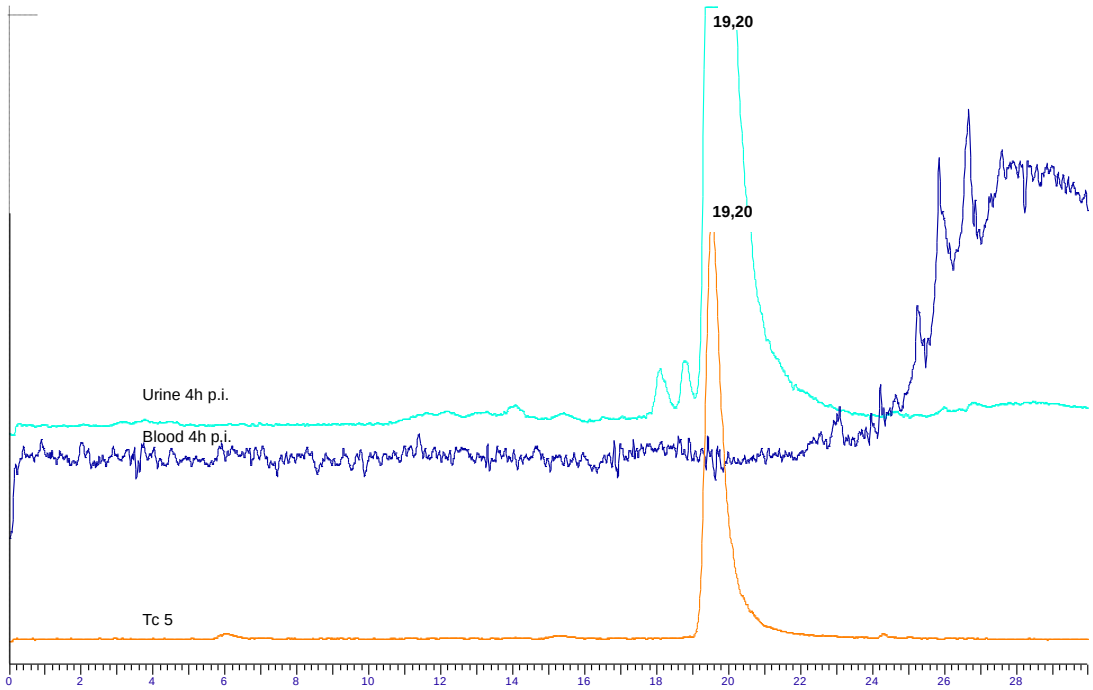

Figure 3.10 - RP-HPLC chromatograms of **Tc5** (injected preparation), blood serum and urine samples collected at 4 h p.i. (γ - detection/Method 2)

The favorable biological behavior of **Tc5** indicated that chelators of the imidazolyl-diamine type have the necessary requirements to be used in the design of BFC's for the labeling of peptides with *fac*-$[^{99m}Tc(CO)_3]^+$ and prompted us to proceed with its conjugation to BN antagonists.

3.3. SYNTHESIS AND PURIFICATION OF BOMBESIN ANTAGONIST DERIVATIVES

The solid phase peptide synthesis methodology (SPPS) was first developed by Bruce Merrifield (Nobel Prize in Chemistry 1984) in the 1950s and 1960s, through the introduction of functionalized solid supports that enable amino acid coupling.(104)

The principle of SPPS is briefly illustrated in Figure 3.11. SPPS is based on the sequential addition (C→N direction) of Nα- and side-chain protected amino acids to a functionalized insoluble polymeric support, the resin. Typically, the C-terminal amino acid is first anchored by the carboxylate to the resin via a linker. Then, the Nα-protecting group can be removed without affecting the side-chain protecting groups and the peptide chain is prepared for the next coupling cycle. (105) The Nα-protecting groups most used in SPPS are the fluoren-9- ylmethyloxycarbonyl (Fmoc) and the tert-butoxycarbonyl (Boc), each a different and defining an overall strategy for SPPS. The Boc strategy, initially introduced by Merrifield, requires trifluoroacetic acid (TFA) or a similar acid for repetitive removal of the Boc groups, and hydrofluoric acid (HF) for peptide cleavage from the solid support, while the Fmoc group can be removed under mild conditions with secondary amines, typically piperidine.(105)

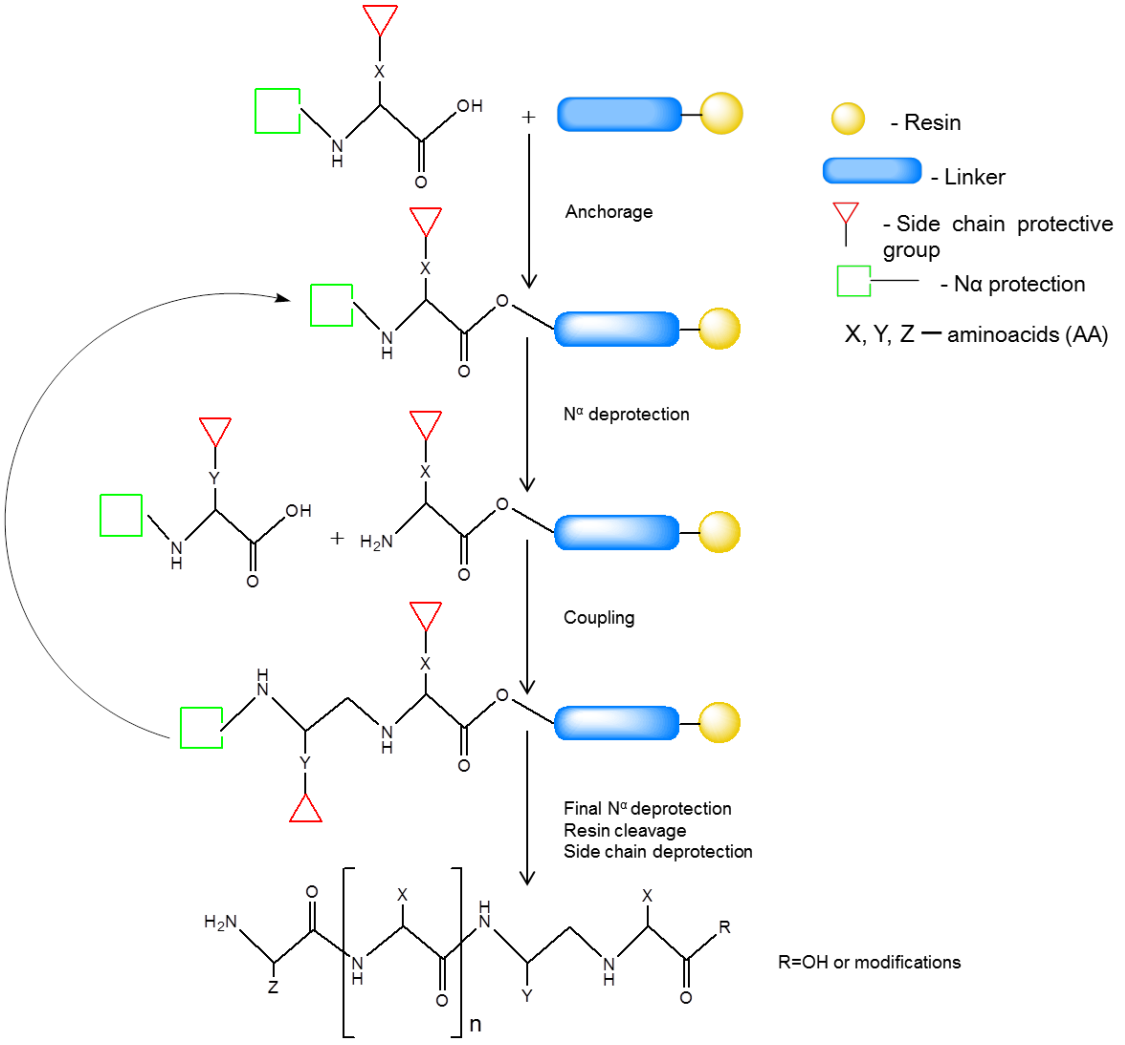

Figure 3.11 – Principle of peptide synthesis in Solid Phase.

In 2003, the first dedicated microwave-assisted peptide synthesizer was introduced (Liberty, CEM), which is a completely automated valve-based system. (106) The Microwave Technology /Chemistry have the fundamental mechanism of heating and involve the agitation of polar molecules or ions that oscillate under the effect of an oscillating electric or magnetic field. (Figure 3.12)

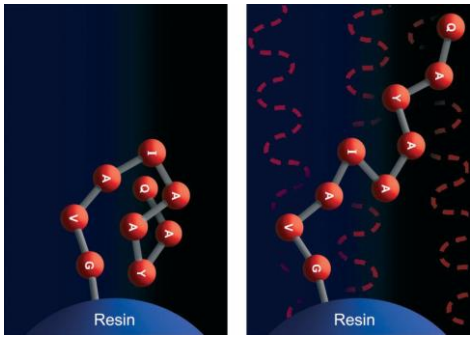

Figure 3.12 - Electromagnetic effect of microwave in Peptide synthesis.

The Microwave can overcome same disadvantages from the SPPS it allow faster reactions, better yield and purity of peptide, better technology for difficult sequences, heating efficiency, solvent less synthesis is possible, less solvent and reagents use with the importance of greater reproducibility. However, Microwave strategy itself has problems as heating under elevated temperatures, the possibility of racemization of the Histidine and Cysteine, lack of scalability and the safety hazards associated with microwave. (107)

We synthesized a bombesin-analogue peptide (Sta)based antagonist (AR) with an oligoethyleneglycol (PEG) spacer, in the N-terminal of the peptide. Briefly, the **AR** peptide sequence DPhe^{1}-Gln^{2}-Trp^{3}-Ala^{4}-Val^{5}-Gly^{6}-His^{7}-Sta^{8}-Leu^{9}-NH_2, shown in figure 3.13, was assembled to the MBHA rink Amide resin by Fmoc-based Solid Phase Peptide Synthesis in a microwave-assisted peptide synthesizer, CEM 12-Channel Automated Peptide Synthesizer, using HOBT/HBTU/HATU as coupling agents, DMF as solvent and Dipea as base. In order to verify the main products formed in this synthesis, the peptide was cleaved from a small portion of the resin and, after appropriate work-up and purification by RP-HPLC, the peptide **AR** was characterized by ESI-MS (Figure 3.14). The peak found at m/z = 557.7 corresponds to $[M+2H]^{2+}$ of the desired peptide and the peak found at m/z = 1130.4 could correspond to the species $[M+NH_3]^{+}$. It is also observed a peak at m/z = 976.9 with significant intensity, which correspondns to the peptide sequence without the His amino acid. This synthesis was repeated one more time and once again we observed the same reesult. This could indicate that the production of the AR

Peptide by SPPS is hampered by the use of microwave associated with the introduction of the His aminoacid.

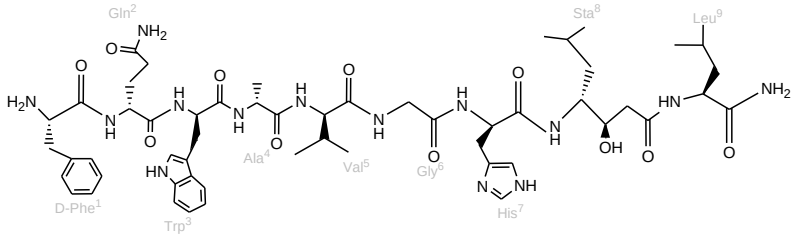

Figure 3.13 - Structural configuration of AR peptide after resin deprotection.

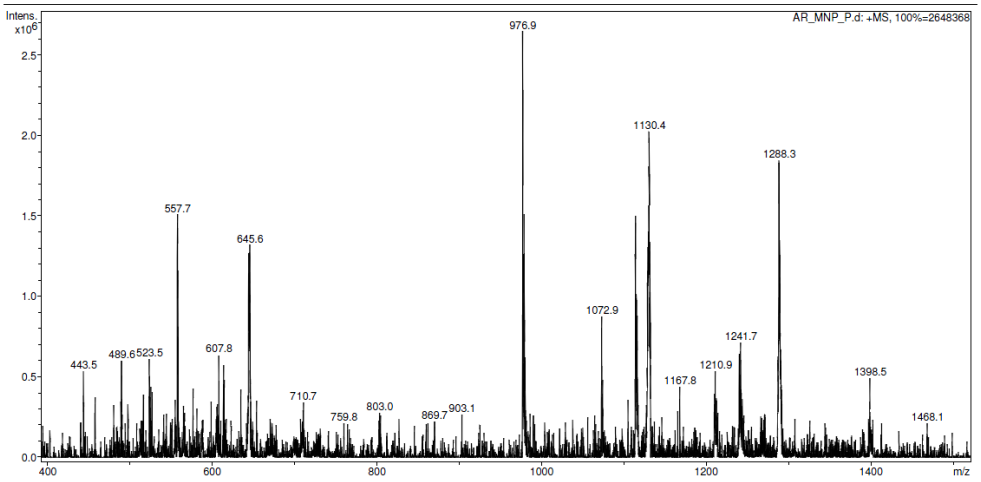

Figure 3. 14 - ESI-MS spectrum of **AR** peptide.

Recently the use of PEG's with Bombensin antagonists derivatives was investigated. In a study made by James M. *et al* it was studied the influence of PEG with different length, on the biological profile of the AR peptide conjugate with different chelators and radionuclides. (82). They conclude that the PEG_4 and PEG_6 showed significantly better properties, then PEG_{12} . They present a very high tumor-to-non-target organ ratios, in particular tumor-to-kidney ratios, that are important in regard to safety concerning kidney toxicity. However, shorter oligo-PEG derivatives have not been evaluated yet; the autors wonder if these small PEGs still maintain high binding affinity and concomitantly suitable pharmacokinetics (82).

In order to answer this question and aiming to provide a more hydrophilic character to our bioconjugates, we decide to couple a small PEG to the previously described **AR** peptide. To the **AR** peptide, still attached to the resin and without any purification, was coupled with success a PEG_2 linker, using the same methodologies involved in the synthesis of the peptide itself (Scheme 3.9).

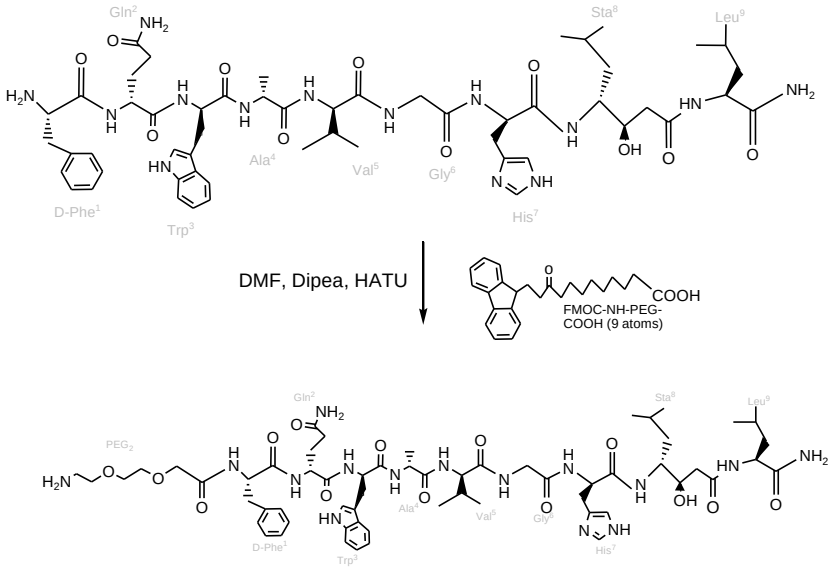

Scheme 3.9 – Synthesis of **ARPEG$_2$**

As showed in scheme 3.9, this coupling was done manually by SPPS with a commercial Fmoc protected PEG$_2$, using HATU as coupling agent, DMF as solvent and Dipea as base. After two cycles of coupling we could verify by Kaiser Test that all amine bonds were consumed. For characterization purposes, only a small part of the resin was deprotected. As showed in Figure 3.15, the ESI-MS analysis revealed a peak at m/z = 1258.9 corresponding to $[M+H]^+$ of the desired peptide conjugate (**ARPEG$_2$**) and a more intense peak at m/z = 1123.1 corresponding to $[M+H]^+$ of the PEG$_2$ conjugate without the His amino acid, in agreement with the ESI-MS results obtained in the synthesis of the AR peptide.

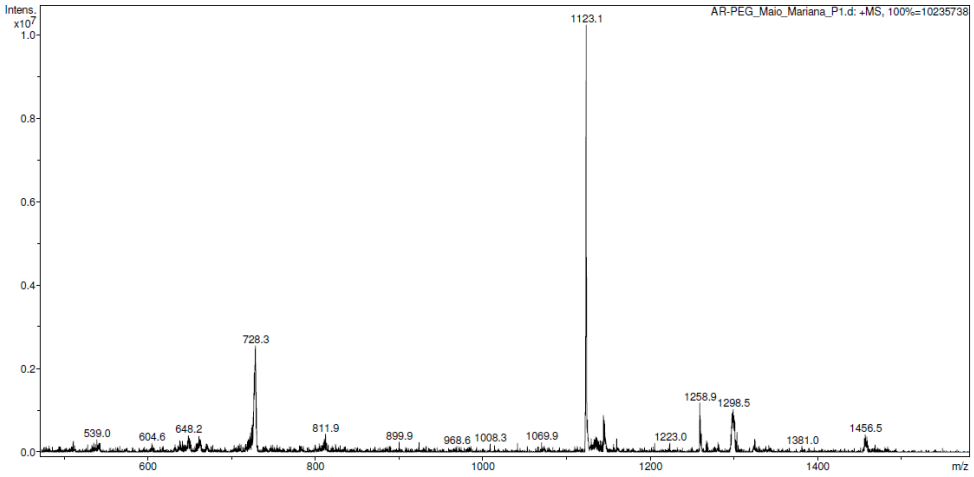

Figure 3.15 - ESI-MS spectrum of **ARPEG$_2$** peptide.

3.4. CONJUGATION OF THE BOMBESIN ANTAGONIST TO THE BFC'S

L1-Boc was conjugated to **ARPEG$_2$**, via HATU activation in the presence of DIPEA in a DMF solution and with microwave irradiation (Scheme 3.10).

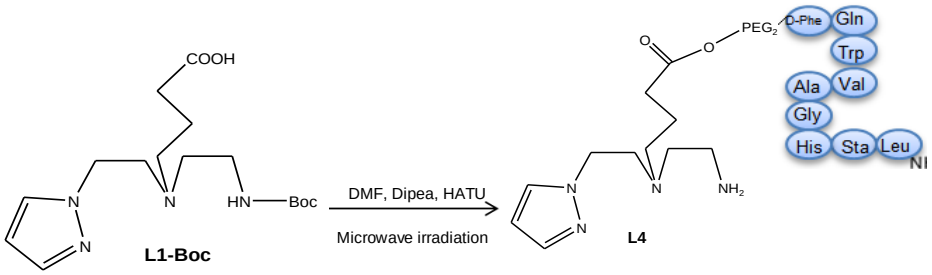

Scheme 3.10 - Synthesis of **L4**, the conjugate of ARPEG$_2$ with L1-Boc.

After removal of the protecting groups, with a standard deprotection cocktail, appropriate work-up and purification by RP-HPLC, the final conjugate was characterized by ESI-MS. The peak found at m/z = 1481.5 have the isotopic pattern corresponding to the $[M+H]^+$ of the desired bioconjugate. The ESI-MS spectrum and the RP-HPLC chromatogram of **L4** peptide conjugate are shown in figures 3.16 and 3.17, respectively

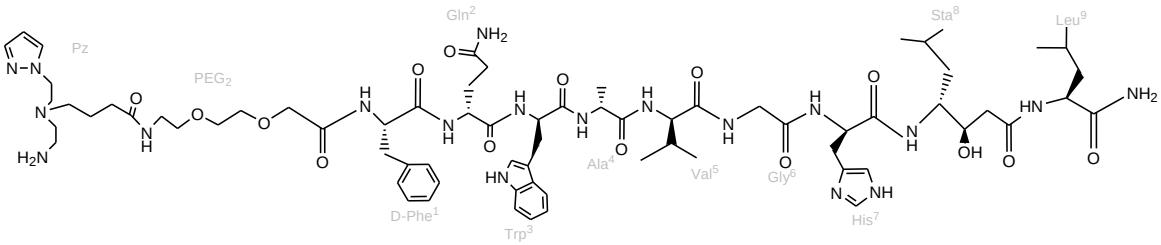

Figure 3.16 - Structural configuration of **L4** peptide conjugate after resin deprotection.

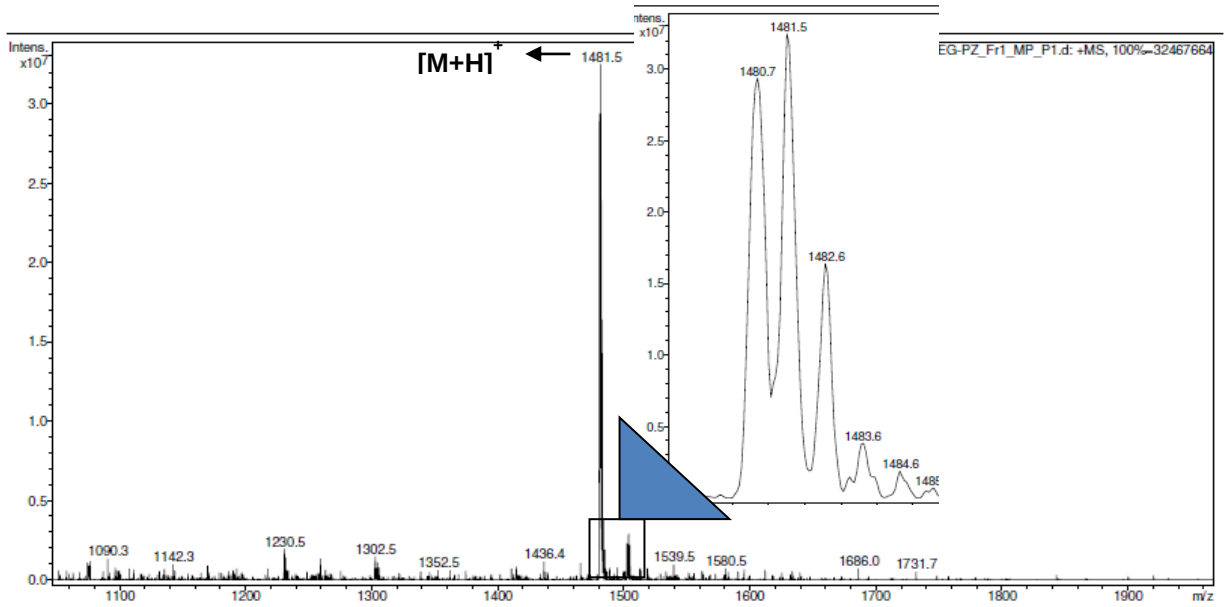

Figure 3.17 - ESI-MS spectrum of **L4** peptide conjugate.

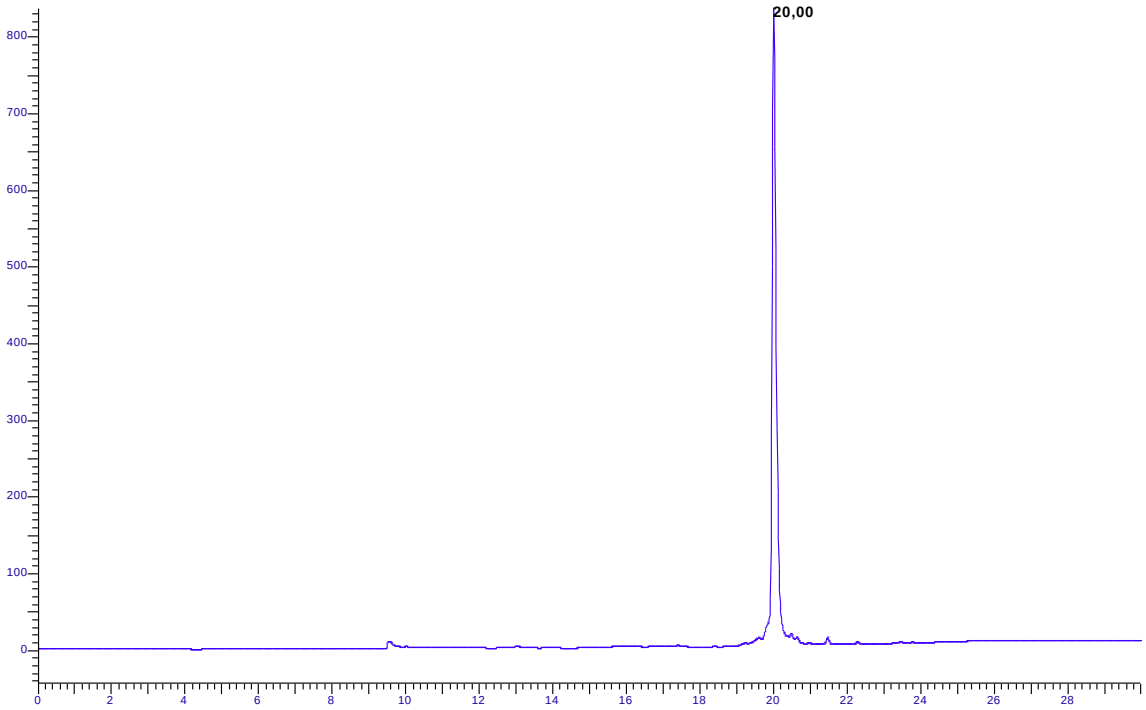

Figure 3.18 – HPLC chromatogram of **L4** peptide conjugate. (Method 1, section 2.2.2)

It has been attempted the conjugation of **ARPEG$_2$** with the pyrazolyl and imidazolyl-based BFC's having a shorter linker, **L2-Boc** and **L3-Boc**, respectively, based on the methodology that has been used to obtain **L4**: i.e. conjugation reaction via HATU activation in the presence of DIPEA in a DMF solution and with microwave irradiation (Scheme 3.11). After resin deprotection, the resulting mixtures were analyzed by ESI-MS before purification.

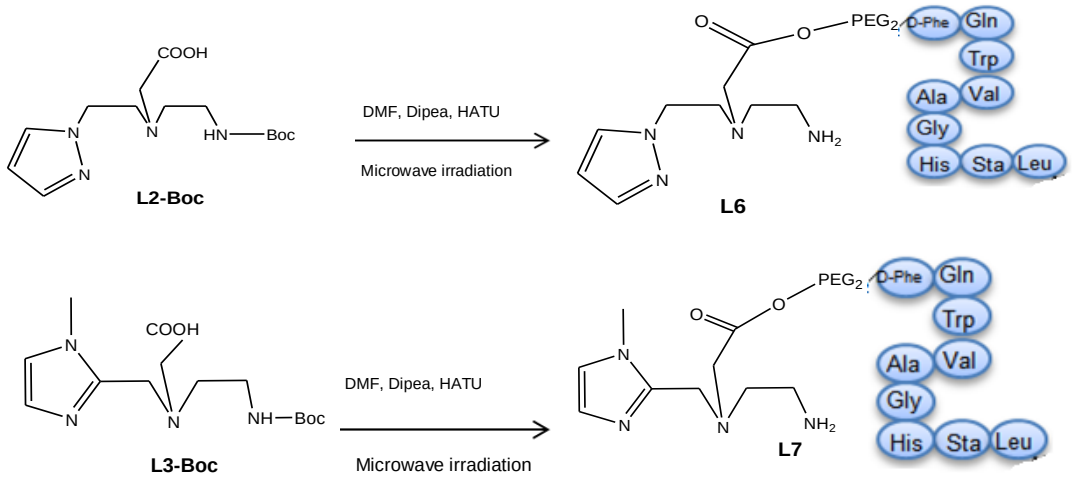

Scheme 3.11 – Attempts to synthesize **L6** and **L7** by conjugation of ARPEG$_2$ with the desired BFC.

In the case of the synthesis of **L6**, the ESI-MS results were ambiguous. The spectrum did not reveal the presence of the m/z peak of the desired peptide conjugate, while the peak found at m/z= 1298.5 $[M+ACN]^+$ certainly corresponds to ARPEG$_2$. For **L7**, the results from the ESI-MS spectrum also did not reveal the presence of a m/z peak of the desired peptide conjugate. So, the conjugation reactions to obtain **L6** and **L7** need to be performed with other experimental conditions in order to obtain the desired products.

3.5. Synthesis and Characterization of Metalated Peptides: *fac*-$[M(CO)_3(L4)]^+$ (M=Re, ^{99m}Tc)

As previously stated, to characterize the $^{99m}Tc(CO)_3$-complexes is necessary to synthesize the natural "cold" rhenium complexes, which present similar physico-chemical properties. Moreover, in the case of metalated peptides the cold Re complexes are useful to determine the *in vitro* binding affinity towards the respective receptors. The

metalopeptide with **L4**, **Re4,** was synthesized via a direct method as displayed in Scheme 3.12.

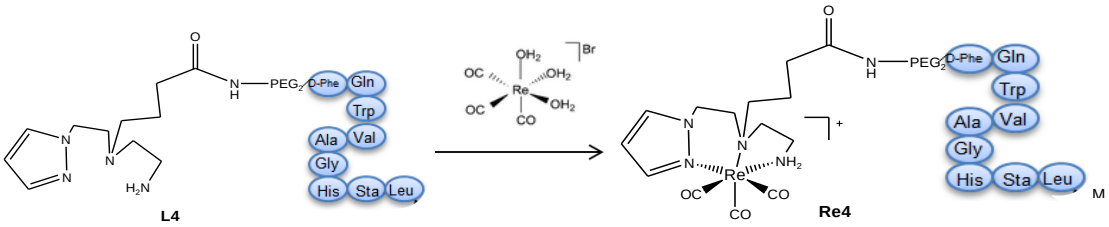

Scheme 3.12 - Synthesis of the metallated peptide **Re4.**

The peptide conjugate **L4** reacted with equimolar amounts of the precursor *fac*-$[Re(CO)_3(H_2O)_3]^{Br}$, in refluxing MeOH during 72 h. After purification by preparative RP-HPLC (Method 2, section 2.2.2), the **Re4** complex of the peptide conjugate **L4** was characterized by ESI-MS and RP-HPLC. The analysis of the ESI-MS revealed a peak at m/z = 1751 corresponding to $[M+H]^+$. The peak found in RP-HPLC (method 2) had a retention time of 23.17 min.

Peptide conjugate **L4** was labeled with ^{99m}Tc(I), following the methodology above described for the labeling of **L5**. As is shown in Scheme 3.12, reaction of the peptide analogue **L4** (40 µL, [**L4**] = 1,65 x 10^{-4} M) with the organometallic precursor *fac*-$[^{99m}Tc(CO)_3(H_2O)_3]^+$ (360 µL), after 45 min at 90^{0}C, gave the desired radiometalated peptide *fac*-$[^{99m}Tc(CO)_3(\kappa^3$-**L4**$)]^+$ (**Tc4**) (t_R = 24.07 min) in a reduced yield and contaminated with a major unidentified radiochemical impurity (figure 3.19).

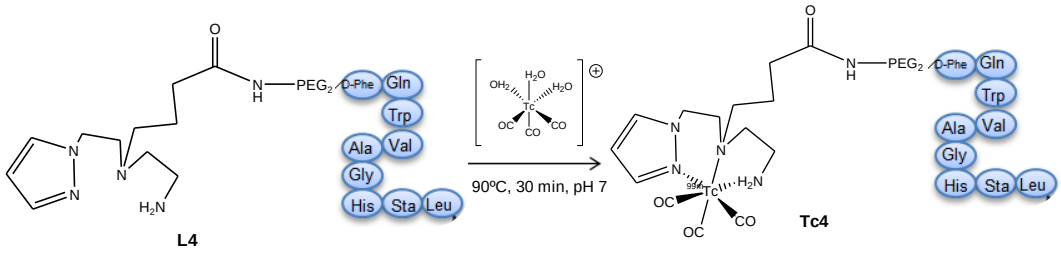

Scheme 3.13 – Synthesis of **Tc4**.

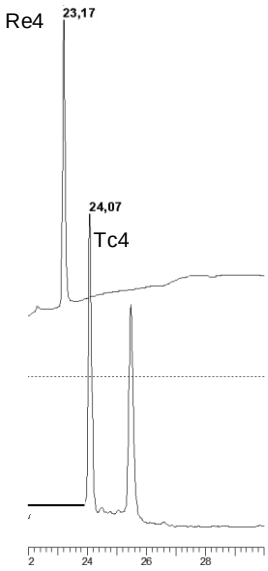

Figure 3.19 – RP-HPLC chromatograms of **Tc4**(γ - detection)/**Re4** (U.V. detection).

We tried to radiolabel the conjugate peptide **L4** using other experimental conditions, namely higher concentration of **L4** and higher temperature, longer reaction time, different pH. We also tried to dissolve **L4** in ethanol to avoid its eventual precipitation during the labeling reaction, since **L4** has poor solubility in aqueous solution. To improve the dissolution of **L4**, with a consequent higher concentration of the peptide conjugate in solution, we have used a solution of acetic acid in water (10:90). However, under all the tested conditions, it was not possible to improve the yield and purity of this radioconjugate. In summary, further work is necessary to improve the radiolabeling yield and to perform the subsequent *in vitro*/*in vivo* studies with this radioconjugate.

4. Concluding Remarks and Outlook

The main goal of this thesis was contribute for the development of radiopharmaceuticals based on $[^{99m}Tc(CO)_3]^+$ for the *in vivo* imaging of tumors overexpressing the Gastrin Releasing peptide-receptor (GRP-r,), particularly prostate cancer.

To accomplish this main goal, three different BFC's containing pyrazolyl (**L1**, **L2**) and imidazolyl (**L3**) coordinating groups were synthesized, characterized and conjugated to a bombesin antagonist (**AR**) peptide, with known ability to target GRP-r. In general, all the BFC's were obtained with high purity and reasonable yields. The investigated BFC's contain N,N,N donor atom sets in order to be applied within the tricarbonyl approach. Both types of chelators have a pendant arm with a terminal carboxylate group for conjugation to the AR peptide.

The coordination behaviour of imidazolyl-diamine ligands, corresponding to the chelating backbone of **L3**, towards the *fac*-$[M(CO)_3]^+$ (M = Re, ^{99m}Tc) core was not studied yet. Therefore, it has been synthesized a model ligand (**L5**) without pendant carboxylate group, which allowed the synthesis of the organometallic complexes *fac*-$[M(CO)_3(\kappa^3\text{-}\mathbf{L5})]^+$ (M = Re (**Re5**), ^{99m}Tc (**Tc5**)). **Tc5** presented a favorable biological profile and a high, stability *in vivo,* which showed that imidazolyl-diamine ligands have the necessary requisites to be used in the desugn of BFC's for labeling of peptides with *fac*-$[M(CO)_3]^+$.

Peptide synthesis and its PEGylation were successfully accomplished, although a significant amount of conjugates without the histidine residue were obtained. This point need to be improved by changing the coupling conditions. Nevertheless, the non-purified conjugate **ARPEG$_2$** was functionalized with the pyrazolyl-containing BFC having the larger linker, affording **L4** that was obtained with high purity after RP-HPLC purification. However, the efficient conjugation of the peptide to the BFC required microwave technology. In our hands, such technology did not allow the coupling of **ARPEG$_2$** to the pyrazolyl- and imidazolyl-containing BFC's having a shorter linker between the ligand backbone and the pendant carboxylic group.

The new peptide conjugate **L4** was radiolabeled with *fac*-$[^{99m}Tc(CO)_3]^+$ but the resulting radiometalated peptide, identified by HPLC comparison with the Re congener, was obtained with low yield and unsatisfactory radiochemical purity. More studies are foreseen to optimize the radiolabeling of **L4**.

The tricarbonyl approach allows the use of the matched pair Tc(I)/Re(I), taking advantage of the therapeutic applications of Re radionuclides. This might open the way for

the development of a theranostic radiolabeled peptide, having at the same time imaging and therapeutic properties. To achieve this goal it is necessary to improve the pharmacokinetic of the conjugates in order to have high ratio between target and non-target organs. It is known that ^{99m}Tc/^{188}Re-tricarbonyl-based radiometalated peptides can be lipophilic, and structural modification are necessary to improve their biological profile. As proposed in this work such modification can comprise the use of PEG moieties and/or the modification of the BFC's. Unfortunately, we weren't able to finish all the proposed studies, and evaluate the effect of different structural alterations on the binding affinity, cellular uptake, tumor uptake and target/non-target ratio of the final radiopeptides.

In future studies is essential to continue with the purification and radiolabelling of **L6** and **L7**. More importantly, the radiolabelling yield of **L4** must be improved. In this way, the biological evaluation of the different compounds can be accomplished, which is expected to show if the devised strategy is adequate to improve the performance of $M(CO)_3$-labeled bombesin antagonists as theranostic tools for the management of GRR-r positive tumors, particularly prostate cancer.

Concerning the Budget (See annex), the work involved in this Thesis it's a expensive labor. Nevertheless, to conclude, we can definitely consider that the majority of the described processes can be improved towards the use of less solvents and reagents, with consequent lower investment.

.

5. Appendix

	Products	Molecular Formula	Manufacturer	Cas-number	Quantity for unit		Price per unit /€	Amount used		Price/€
Solvents	*Diclomethane(DCM)*	CH_2Cl_2	*Sigma-Aldrich*	75-09-2	1,00	L	25,90	2,00	L	**51,80**
	chloroform	$CHCl_3$	*scharlau*	67-66-3	2,50	L	72,50	2,50	L	**72,50**
	Petroleum ether	C_7H_7BrMg	Sigma-Aldrich	8032-32-4	2,50	L	85,00	0,05	L	**1,70**
	Ethyl Acetate(EtOAc)	$CH_3COOC_2H_5$	Carlo-Erba	141-78-6	2,50	L	81,80	0,02	L	**0,65**
	Acetone	$(CH_3)COCH_3$	Carlo-Erba	67-64-1	45,00	L	1120,00	0,01	L	**0,25**
	n-hexane	$CH_3(CH_2)_4CH_3$	Sigma-Aldrich	110-54-3	2,50	L	81,20	0,50	L	**16,24**
	Tetrahydrofurane (THF)	C_4H_8O	Carlo-Erba	109-99-9	2,50	L	74,40	0,10	L	**2,98**
	Ethanol (EtOH)	CH_3CH_2OH	*Panreac*	64-17-5	1,00	L	121,35	0,03	L	**3,64**
	Methanol (MeOH)	CH_3OH	*Carlo-Erba*	67-56-1	5,00	L	84,60	0,50	L	**8,46**
	Diethylether	$(CH_3CH_2)_2O$	Sigma-Aldrich	60-29-7	2,50	L	67,10	0,01	L	**0,27**
	Acetonitrile (ACN)	CH_3CN	*Sigma-Aldrich*	75-05-8	2,50	L	157,50	2,50	L	**157,50**
	N,N-Dimethylformamide (DMF)	$HCON(CH_3)_2$	*Carlo-Erba*	68-12-2	2,50	L	124,00	2,50	L	**124,00**
	Trifluoroacetic acid (TFA)	CF_3COOH	*Sigma-Aldrich*	76-05-1	100,00	mL	128,50	50,00	mL	**64,25**
	Water	H_2O	*In house*	.	.	.	.	.	.	**0,00**
	N,N-Diisopropylethylamine (Dipea)	$[(CH_3)_2CH]_2NC_2H_5$	Sigma-Aldrich	7087-68-5	500,00	mL	132,50	25,00	mL	**6,63**
	Piperidine	$C_5H_{11}N$	*Sigma-Aldrich*	110-89-4	500,00	mL	60,10	15,00	mL	**1,80**
	1,4-Dioxane	$C_4H_8O_2$	*Sigma-Aldrich*	123-91-1	2,50	L	197,00	0,18	L	**14,18**
	Triethylamine	$(C_2H_5)_3N$	*Sigma-Aldrich*	121-44-8	100,00	mL	21,60	1,51	mL	**0,33**
Deuterated Solvents	*Deuterochloroform*	$CDCl_3$	*Sigma-Aldrich*	865-49-6	5,00	mL	38,80	10,00	mL	**77,60**
	Tetradeuteromethanol	CD_3OD	*Euriso-top*	811-98-3	5,00	mL	159,50	3,00	mL	**95,70**
								Total costs of Solvents =		**700,48 €**
Reagents	Benzyl Bromoacetate	$C_9H_9BrO_2$	*Sigma-Aldrich*	5437-45-6	50,00	g	21,80	1,28	g	**0,56**

	Di-*tert*-butyl dicarbonate (Boc protective group)	$[(CH_3)_3COCO]_2O$	*Sigma-Aldrich*	24424-99-5	25,00	g	85,70	14,00	g	**47,99**
	1,2-dibromoethane	$BrCH_2CH_2Br$	*Sigma-Aldrich*	106-93-4	200,00	mL	46,20	95,00	mL	**21,95**
	Ethyl 4-bromobutyrate	$C_6H_{11}BrO_2$	*Sigma-Aldrich*	2969-81-5	50,00	g	32,60	1,40	g	**0,91**
	Ethylenediamine	$NH_2CH_2CH_2NH_2$	*Sigma-Aldrich*	107-15-3	500,00	mL	25,60	27,00	mL	**1,38**
	Hydrochloric acid	HCl	*Sigma-Aldrich*	7647-01-0	2,50	L	133,50	0,007	L	**0,37**
	Magnesium sulfate anhydrous 96%	$MgSO_4$	*Panreac*	7487-88-9	500,00	g	81,20	5,00	g	**0,81**
	1-Methyl-2-imidazolecarboxaldehyde	$C_5H_6N_2O$	*Sigma-Aldrich*	13750-81-7	5,00	g	136,00	0,42	g	**11,42**
	Pyrazol	$C_3H_4N_2$	*Sigma-Aldrich*	288-13-1	25,00	g	45,20	10,50	g	**18,98**
	Palladium on Carbon (Pd/C)	Pd	*Sigma-Aldrich*	MFCD03457879	10,00	g	156,50	1,00	g	**15,65**
	Potassium Iodide	KI	*Sigma-Aldrich*	7681-11-0	100,00	g	33,60	0,03	g	**0,01**
	Potassium Carbonate	K_2CO_3	*Sigma-Aldrich*	584-08-7	25,00	g	122,00	3,10	g	**15,13**
	Sodium Hidroxide	NaOH	*Sigma-Aldrich*	1310-73-2	500,00	g	38,50	16,50	g	**1,27**
	sodium triacetoxyborohydride	$(CH_3COO)_3BHNa$	*Sigma-Aldrich*	56553-60-7	25,00	g	61,00	0,22	g	**0,54**
	Sodium borohydride	NaBH4	*Sigma-Aldrich*	16940-66-2	25,00	g	43,00	0,35	g	**0,60**
	Tetrabutylammonium bromide (TBAB)	$(CH_3CH_2CH_2CH_2)_4N(Br)$	*Sigma-Aldrich*	1643-19-2	25,00	g	25,80	1,20	g	**1,24**
								Total costs of Reagents =		**138,82 €**
Peptide Synthesis	HATU	$C_{10}H_{15}F_6N_6OP$	*Sigma-Aldrich*	148893-10-1	25,00	g	414,50	0,42	g	**7,01**
	FMOC-Ala-OH	$C_{18}H_{17}NO_4$	*Novabiochem*	35661-39-3	5,00	g	50,00	0,37	g	**3,72**

	FMOC-D-Phenylanine-OH	$C_{24}H_{21}NO_4$	*Novabiochem*	86123-10-6	5,00	g	50,00	0,46	g	**4,63**
	FMOC-Gln(Trt)-OH	$C_{39}H_{34}N_2O_5$	*Sigma-Aldrich*	132327-80-1	5,00	g	41,80	1,99	g	**16,64**
	FMOC-Gly-OH	$C_{17}H_{15}NO_4$	*Novabiochem*	29022-11-5	5,00	g	11,00	1,99	g	**4,38**
	FMOC-His(Trt)-OH	$C_{10}H_{15}NO_4$	*Sigma-Aldrich*	109425-51-6	5,00	g	41,80	0,37	g	**3,09**
	FMOC-His(Trt)-OH	$C_{40}H_{33}N_3O_4$	*Novabiochem*	109425-51-6	5,00	g	35,00	1,36	g	**9,55**
	FMOC-Leu-OH	$C_{27}H_{23}NO_4$	*Novabiochem*	35661-60-0	5,00	g	11,00	0,43	g	**0,95**
	FMOC-NH-PEG-COOH (9 atoms)	$C_{21}H_{23}NO_6$	*Novabiochem*	166108-71	1,00	g	300,00	0,40	g	**119,70**
	FMOC-Trp(Boc)-OH	$C_{31}H_{30}N_2O_6$	*Sigma-Aldrich*	143824-78-6	5,00	g	50,00	2,28	g	**2,28**
	FMOC-Sta-OH	$C_{23}H_{27}NO_5$	*Novabiochem*	158257-40-0	25,00	mg	44,30	460,00	mg	**815,12**
	FMOC-Val-OH	$C_{20}H_{21}NO_4$	*Novabiochem*	68858-20-8	5,00	g	11,00	1,54	g	**3,39**
	Rink Amide-MBHA Resin		*Novabiochem*	431041-83-7	5,00	g	212,00	0,97	g	**40,92**
								Total cost of peptide synthesis=		**1.031,36 €**
Materials	silica 230-400 mesh	SiO_2	*Merck*	7631-86-9	5,00	kg	425,50	2,00	kg	**170,20**
	TLC Silica gel 60 F_{254}	.	*Merck*	.	25,00	un/box	63,76 €	10,00	un	**25,50**
	pasteur pipets	.	*Normax*	.	250,00	un/box	5,46 €	350,00	un	**7,64**
	Filter Paper	.	*Sigma-Aldrich*	Whatman Article No. 28413929	1,00	un/box	27,90 €	2,00	un	**55,80**
	Aluminium Foil	.	*Supermarkets*	.	1,00	un/box	1,27 €	1,00	un	**1,27**
	glass Material (new and repairs)	.	.	.	.	.	.	.	.	**150,80**
	Parafilm	.	*Parafilm*	.	0,04	m	566,00	0,004	m	**59,58**
								Total costs of Laboratory Material =		**470,80 €**

			Estimated price/€
Other costs	Nitrogen gas (N_2)	used to dry solvents and do reaction under N_2 atmosphere (considering 10 months)	**400,00 €**
	Water	used in reactions with reflux (considering 10 months)	**200,00 €**
	electricity	used in all the electric equiment, namely Microwave (considering 10 months)	**200,00 €**

TOTAL = **3.141,46 €**

Bibliographic References

1. General Information About Prostate Cancer [Internet]. 2014. Available from: http://www.cancer.gov/cancertopics/pdq/treatment/prostate/Patient/page1

2. Dumont R a, Tamma M, Braun F, Borkowski S, Reubi JC, Maecke H, et al. Targeted radiotherapy of prostate cancer with a gastrin-releasing peptide receptor antagonist is effective as monotherapy and in combination with rapamycin. J Nucl Med [Internet]. 2013 May [cited 2014 Mar 9];54(5):762–9. Available from: http://www.ncbi.nlm.nih.gov/pubmed/23492884

3. Kowalsky R, Falen S. Radiopharmaceuticals in Nuclear Pharmacy and Nuclear Medicine. 2nd Ed. Washington DC: American Pharmacists Association; 2004.

4. Liu S. Bifunctional coupling agents for radiolabeling of biomolecules and target-specific delivery of metallic radionuclides. Adv Drug Deliv Rev [Internet]. 2008 Sep [cited 2014 Jun 20];60(12):1347–70. Available from: http://www.pubmedcentral.nih.gov/articlerender.fcgi?artid=2539110&tool=pmcentrez&rendertype=abstract

5. Blawer P. Towards molecular imaging and treatment of disease with radionuclides: the role of inorganic chemistry. Dalt Trans. (2006):1705–11.

6. Liu S. The role of coordination chemistry in the development of target-specific radiopharmaceuticals. Chem Soc Rev [Internet]. 2004 Sep 10;33(7):445–61. Available from: http://www.ncbi.nlm.nih.gov/pubmed/15354226

7. Saha GB. Fundamentals of Nuclear Pharmacy, Fifth Edition. Fifth Edit. New York: Springer; 2004.

8. Nijsen JFW, Krijger GC, Van het Schip AD. The bright future in Radionuclides for Cancer Therapy. Anticancer Agents Med Chem. 2007;7:271–90.

9. Buchegger F, Perillo-Adamer F, Dupertuis YM, Delaloye AB. Auger radiation targeted into DNA: a therapy perspective. Eur J Nucl Med Mol [Internet]. 2006;33(11):1352–63. Available from: http://clinicaltrials.gov/show/NCT00699751

10. Pysz MA, Gambhir SS, Willmann JK. Molecular imaging: current status and emerging strategies. Clin Radiol. 2010;65(7):500–16.

11. Histed SN, Lindenberg ML, Mena E, Turkbey B, Choyke PL, Kurdziel KA. Review of functional/anatomical imaging in oncology. Nucl Med Commun. 2012;33(4):349–61.

12. Jaffer FA, Weissleder R. Molecular imaging in the clinical arena. J Am Med Assoc. 2005;293(7):855–62.

13. Massoud TF, Gambhir SS. Molecular imaging in living subjects: seeing fundamental biological processes in a new light. Genes Dev [Internet]. 2003 Mar 1 [cited 2014 May 23];17(5):545–80. Available from: http://www.ncbi.nlm.nih.gov/pubmed/12629038

14. Kobayashi H, Longmire MR, Ogawa M, Choyke PL. Rational chemical design of the next generation of molecular imaging probes based on physics and biology: mixing modalities, colors and signals. Chem Soc Rev. 2011;40(9):4626–48.

15. Wadas TJ, Wong EH, Weisman GR, Anderson CJ. Coordinating Radiometals of Copper, Gallium, Indium, Yttrium, and Zirconium for PET and SPECT Imaging of Disease. Chem Rev. 2010;110:2858–902.

16. Hicks RJ, Hofman MS. Is there still a role for SPECT–CT in oncology in the PET–CT era? Nat Rev Clin Oncol. 2012;9:712–20.

17. Bartholoma MD, Louie AS, Valliant JF, Zubieta J. Technetium and Gallium Derived Radiopharmaceuticals: Comparing and Contrasting the Chemistry of Two Important Radiometals for the Molecular Imaging Era. Chem Rev. 2010;110(5):2903–20.

18. Ametamey SM, Honer M, Schubiger PA. Molecular imaging with PET. Chem Rev. 2008;108(5):1501–16.

19. Ido T, Wan CN, Casella V, Fowler JS, Wolf AP, Reivich M, et al. Labeled 2-Deoxy-D-Glucose Analogs - F-18-Labeled 2-Deoxy-2-Fluoro-D-Glucose, 2-Deoxy-2-Fluoro-D-Mannose and C-14-2-Deoxy-2-Fluoro-D-Glucose. J Label Compd Rad. 1978;14(2):175–83.

20. Liu S. Bifunctional Coupling Agents for Radiolabeling of Biomolecules and Target-Specific Delivery of Metallic Radionuclides. Adv Drug Deliv Rev [Internet]. 2008 Sep [cited 2014 Jun 20];60(12):1347–70. Available from: http://www.pubmedcentral.nih.gov/articlerender.fcgi?artid=2539110&tool=pmcentrez&rendertype=abstract

21. Wester HJ. Nuclear imaging probes: From bench to bedside. Clin Cancer Res. 2007;13(12):3470–81.

22. Schwaiger, M.; Wester HJ. How Many PET Tracers Do We Need? J Nucl Med. 2011;52:36s–41s.

23. Volkert WA, Hoffman TJ. Therapeutic radiopharmaceuticals. Chem Rev. 1999;99(9):2269–92.

24. Kassis AI, Adelstein SJ. Radiobiologic principles in radionuclide therapy. J Nucl Med. 2005;46:4S–12S.

25. Kwekkeboom DJ, de Herder WW, Kam BL, van Eijck CH, van Essen M, Kooij PP, et al. Treatment with the radiolabeled somatostatin analog [Lu-177-DOTA(0), Tyr(3)] octreotate: Toxicity, efficacy, and survival. J Clin Oncol. 2008;26(13):2124–30.

26. Kam BLR, Teunissen JJM, Krenning EP, de Herder WW, Khan S, van Vliet EI, et al. Lutetium-labelled peptides for therapy of neuroendocrine tumours. Eur J Nucl Med Mol. 2012;39:103–12.

27. Rösch F. AEF. Radiolanthanides in Nuclear Medicine. In: Siegel and H. Siegel E, editor. In Metal Ions in Biological Systems: Metal Complexes in Tumor Diagnosis and as Anticancer Agents. 42nd ed. New York: Marcel Decker, Inc.; 2004. p. 77–108.

28. Nilsson S, Larsen RH, Fossa SD, Balteskard L, Borch KW, Westlin JE, et al. First clinical experience with alpha-emitting radium-223 in the treatment of skeletal metastases. Clin Cancer Res. 2005;11(12):4451–9.

29. Nilsson S, Franzen L, Parker C, Tyrrell C, Blom R, Tennvall J, et al. Bone-targeted radium-223 in symptomatic, hormone-refractory prostate cancer: a randomised, multicentre, placebo-controlled phase II study. Lancet Oncol. 2007;8(7):587–94.

30. Stepanek J, Ilvonen SA, Kuronen AA, Lampinen JS, Savolainen SE, Valimaki PJ. Radiation spectra of In-111, In-113m and In-114m. Acta Oncol. 2000;39(6):667–71.

31. Tavares AAS, Tavares JMRS. Tc-99m Auger electrons - Analysis on the effects of low absorbed doses by computational methods. Appl Radiat Isot. 2011;69(3):607–8.

32. Reilly RM. Monoclonal Antibody and Peptide-targeted Radiotherapy of Cancer. John Wiley & Sons I ed., editor. 2010.

33. R. Dilworth J, J. Parrott S. The biomedical chemistry of technetium and rhenium. Chem Soc Rev [Internet]. 1998;27(1):43. Available from: http://xlink.rsc.org/?DOI=a827043z

34. Jurisson S, Berning D, Jia W, Ma D. Coordination compounds in Nuclear Medicine. Chem Rev. 1993;93:1137–56.

35. Liu S, Edwards DS. 99mTc-Labeled Small Peptides as Diagnostic Radiopharmaceuticals. Chem Rev [Internet]. 1999 Sep 8;99(9):2235–68. Available from: http://www.ncbi.nlm.nih.gov/pubmed/11749481

36. Abram U, Alberto R. Technetium and rhenium - Coordination chemistry and nuclear medical applications. J Brazil Chem Soc. 2006;17(8):1486–500.

37. Horn RK, Kutzeenellenbogen JA. Technetium-99m-Labeled Radiopharmaceuticals : Recent Developments and Encouraging Results Integrated Design. Nucl Med Biol. 1997;24(112):485–98.

38. Cantorias MV, Howell RC, Todaro L, Cyr JE, Berndorff D, Rogers RD, et al. MO Tripeptide Diastereomers (M = 99/99mTc, Re): Models To Identify the Structure of 99mTc Peptide Targeted Radiopharmaceuticals. Inorg Chem. 2007;46(18):7326–40.

39. Roberta S, Grallert M, Rangel-yagui CDO, Fernanda K, Pasqualoto M, Tavares LC. Polymeric micelles and molecular modeling applied to the development of radiopharmaceuticals. Brazilian J Pharm Sci. 2012;48(1):1–16.

40. Richard J. Kowalsky SWF. Radiopharmaceuticals in nuclear pharmacy and nuclear medicine. 2nd editio. APhA, American Pharmacists Association, 2004;

41. Alberto R. The Chemistry of Technetium-Water Complexes within, the Manganese Triad: Challenges and Perspectives. Eur J Inorg Chem. 2009;1:21–31.

42. Richards P, Tucker WD, Srivastava SC. Technetium-99m - an Historical-Perspective - Introduction. Int J Appl Radiat Is. 1982;33(10):793–9.

43. Eckelman WC. Unparalleled Contribution of Technetium-99m to Medicine Over 5 Decades. Jacc-Cardiovasc Imag. 2009;2(3):364–8.

44. Knapp FF, Mirzadeh S. The Continuing Important Role of Radionuclide Generator Systems for Nuclear Medicine. Eur J Nucl Med. 1994;21(10):1151–65.

45. Zolle I. Technetium-99m Pharmaceuticals [Internet]. Zolle I, editor. Berlin, Heidelberg: Springer Berlin Heidelberg; 2007. Available from: http://www.springerlink.com/index/10.1007/978-3-540-33990-8

46. Schibli R. Synthetic and Structural Considerations of Organometallic Compounds of the Elements Technetium and Rhenium for Use in Radiopharmacy. ETH Zürich; 2003.

47. Lazarova, N., James, S., Babich, J., Zubieta J. A convenient synthesis, chemical characterization and reactivity of [Re(CO)3(H2O)3]Br: the crystal and molecular structure of [Re(CO)3(CH3CN)2Br]. Inorg Chem Commun. 2004;9(7):1023–6.

48. Waibel R, Alberto R, Willuda J, Finnern R, Schibli R, Stichelberger A, et al. Stable one-step technetium-99m labeling of His-tagged recombinant proteins with a novel Tc(I)-carbonyl complex. Nat Biotechnol. 1999;17(9):897–901.

49. Schibli R, Schubiger PA. Current use and future potential of organometallic radiopharmaceuticals. Eur J Nucl Med Mol Imaging. 2002;29(11):1529–42.

50. Bartholomä MD, Louie AS, Valliant JF, Zubieta J. Technetium and gallium derived radiopharmaceuticals: comparing and contrasting the chemistry of two important radiometals for the molecular imaging era. Chem Rev. 2010;110(5):2903–20.

51. Oliveira BL, Morais M, Figueira F, Palma E, Gano L, Santos IC, et al. Oliveira, B. L.; Morais, M.; Figueira, F.; Palma, E.; Gano, L.; Santos, I. C.; Santos, I.; Correia, J. D. G. Unpubl results.

52. Mundwiler S, Kundig M, Ortner K, Alberto R. A new [2+1] mixed ligand concept based on [Tc-99(m)(OH2)(3)(CO)(3)](+): a basic study. Dalt T. 2004;9:1320–8.

53. Van Staveren DR, Benny PD, Waibel R, Kurz P, Pak JK, Alberto R. S-functionalized cysteine: Powerful ligands for the labelling of bioactive molecules with triaquatricarbonyltechnetium-99m(1+) ([Tc-99m(OH2)(3)(CO)(3)](+)). Helv Chim Acta. 2005;88(3):447–60.

54. Schibli R, La Bella R, Alberto R, Garcia-Garayoa E, Ortner K, Abram U, et al. Influence of the denticity of ligand systems on the in vitro and in vivo behavior of Tc-99m(I)-tricarbonyl complexes: A hint for the future functionalization of biomolecules. Bioconjugate Chem. 2000;11(3):345–51.

55. Van Staveren DR, Mundwiler S, Hoffmanns U, Pak JK, Spingler B, Metzler-Nolte N, et al. Conjugation of a novel histidine derivative to biomolecules and labelling with [Tc-99m(OH2)(3)(CO)(3)](+). Org Biomol Chem. 2004;2(18):2593–603.

56. Zobi F, Spingler B, Alberto R. Syntheses, Structures and Reactivities of [CpTc(CO)(3)X](+) and [CpRe(CO)(3)X](+). Eur J Inorg Chem. 2008;27:4205–14.

57. James S, Maresca KP, Allis DG, Valliant JF, Eckelman W, Babich JW, et al. Extension of the single amino acid chelate concept (SAAC) to bifunctional biotin analogues for complexation of the M(CO)(3)(+1) core (M = Tc and Re): Syntheses, characterization, biotinidase stability, and avidin binding. Bioconjugate Chem. 2006;17(3):579–89.

58. Jiang H, Kasten BB, Liu H, Qi S, Liu Y, Tian M, et al. Novel Cysteine-Modified Chelation Strategy for the Incorporation of [MI(CO)3]+ (M = Re, 99mTc) in an α-MSH Peptide. Bioconjugate Chem. 2012;

59. Suzuki K, Shimmura N, Thipyapong K, Uehara T, Akizawa H, Arano Y. Assessment of macrocyclic triamine ligands as synthons for organometallic Tc-99m radiopharmaceuticals. Inorg Chem. 2008;47(7):2593–600.

60. Correia J, Paulo A, Santos I. Re and Tc Complexes with Pyrazolyl-Containing Chelators: from Coordination Chemistry to Target-Specific Delivery of Radioactivity. Curr Radiopharm [Internet]. 2009 Oct 1;2(4):277–94. Available from: http://www.eurekaselect.com/openurl/content.php?genre=article&issn=1874-4710&volume=2&issue=4&spage=277

61. Alves, S., Paulo, A., Correia, J.D.G, Domingos, A., Santos I. Coordination capabilities of pyrazolyl containing ligands towards the fac-[Re(CO)3]+ moiety. J Chem Soc, Dalt Trans. 2002;24:4714–9.

62. Vitor RF, Alves S, Correia JDG, Paulo A, Santos I. Rhenium(I)- and technetium(I) tricarbonyl complexes anchored by bifunctional pyrazole-diamine and pyrazole-dithioether chelators. J Organomet Chem. 2004;689(25):4764–74.

63. Alves S, Paulo A, Correia JDG, Gano L, Smith CJ, Hoffman TJ, et al. Pyrazolyl derivatives as bifunctional chelators for labeling tumor-seeking peptides with the fac-[M(CO)(3)](+) moiety (M=Tc-99m, Re): Synthesis, characterization, and biological behavior. Bioconjugate Chem. 2005;16(2):438–49.

64. Alves S, Correia JDG, Santos I, Veerendra B, Sieckman GL, Hoffman TJ, et al. Pyrazolyl conjugates of bombesin: a new tridentate ligand framework for the stabilization of fac-[M(CO)(3)](+) moiety. Nucl Med Biol. 2006;33(5):625–34.

65. Garcia R, Paulo A, Domingos A, Santos I, Ortner K, Alberto R. Re and Tc complexes containing B-H center dot center dot center dot M agostic interactions as building blocks for the design of radiopharmaceuticals. J Am Chem Soc. 2000;122(45):11240–1.

66. Morais GR, Paulo A, Santos I. Organometallic Complexes for SPECT Imaging and/or Radionuclide Therapy. Organometallics [Internet]. 2012;31(16):5693–714. Available from: http://pubs.acs.org/doi/ipdf/10.1021/om300501d

67. Schroeder A, Heller DA, Winslow MM, Dahlman JE, George WP, Langer R, et al. Treating metastatic cancer with nanotechnology. Nat Rev Cancer. 2012;(12):39–50.

68. Schwaiger M, Beer A, Ziegler S, Wester HJ. Functional Imaging. Eur J Cancer. 2012;48:S13–S14.

69. Weissleder R, Pittet MJ. Imaging in the era of molecular oncology. Nature. 2008;452(7187):580–9.

70. Maecke HR. Radiolabeled peptides in nuclear oncology: influence of peptide structure and labeling strategy on pharmacology. Radiolabeled Peptides in Nuclear Oncology [Internet]. 2005. p. 43–72. Available from: http://www.ncbi.nlm.nih.gov/pubmed/15524210

71. Melis M. Radiopeptides for Targeted Tumour Therapy and the Kidney. Oud-Beijerland, The Netherlands; 2010.

72. Ambrosini V, Fani M, Fanti S, Forrer F, Maecke HR. Radiopeptide imaging and therapy in Europe. J Nucl Med [Internet]. 2011 Dec [cited 2014 Apr 17];52 Suppl 2(12):42S–55S. Available from: http://www.ncbi.nlm.nih.gov/pubmed/22144555

73. G-Protein Coupled Receptors Market Report By Transparency Market Research [Internet]. Available from: http://www.scoop.it/t/market-research-industry/p/2687274926/2012/09/14/g-protein-coupled-receptors-market-report-by-transparency-market-research

74. Reubi JC, Wenger S, Schmuckli-maurer J, Schaer J, Gugger M. Bombesin Receptor Subtypes in Human Cancers : Detection with the Universal Radioligand 125I-[D-TYR6, -ALA11, PHE13, NLE14] Bombesin(6–14). Clin Cancer Res. 2002;8(April):1139–46.

75. Ladenheim EE, Knipp S. Capsaicin treatment differentially affects feeding suppression by bombesin-like peptides. Physiol Behav [Internet]. 2007 May 16 [cited 2014 May 12];91(1):36–41. Available from: http://www.pubmedcentral.nih.gov/articlerender.fcgi?artid=2075355&tool=pmcentrez&rendertype=abstract

76. Schober O, Riemann B, editors. Molecular Imaging in Oncology. 1st ed. Munster: Springer; 2013.

77. Van de Wiele C, Dumont F, Vanden Broecke R, Oosterlinkck W, Cocquyt V, Serreyn R et al. Technetium-99m RP527, a GRP analogue for visualisation of GRP receptor-expressing malignancies: a feasibility study. Eur J Nucl Med [Internet]. 2000;27(11):1694–9. Available from: http://hdl.handle.net/1854/LU-128311

78. Lantry LE, Cappelletti E, Maddalena ME, Fox JS, Feng W, Chen J, et al. Synthesis and Characterization of a Systemic Radiotherapy of Prostate Cancer. 2006;47(7):1144–52.

79. Kroll C, Mansi R, Braun F, Dobitz S, Maecke HR, Wennemers and H. Hybrid Bombesin Analogues: Combining an Agonist and an Antagonist in Defined Distances for Optimized Tumor Targeting. J Am Chem Soc. 2013;135:16793–6.

80. Mansi R et al. Targeting GRPR in urological cancers—from basic research to clinical application. Nat Rev Urol. 2013;

81. Zhang H, Schuhmacher J, Waser B, Wild D, Eisenhut M, Reubi, Jean Claude Maecke HR. DOTA-PESIN, a DOTA-conjugated bombesin derivative designed for the imaging and targeted radionuclide treatment of bombesin receptor-positive tumours. Eur J Nucl Med Mol Imaging. 2007;34(8):1198–208.

82. Jamous M, Tamma ML, Gourni E, Waser B, Reubi JC, Maecke HR, et al. PEG spacers of different length influence the biological profile of bombesin-based radiolabeled antagonists. Nucl Med Biol [Internet]. Elsevier B.V.; 2014 Mar 29 [cited 2014 May 19]; Available from: http://www.ncbi.nlm.nih.gov/pubmed/24780298

83. Mansi R, Wang X, Forrer F, Kneifel S, Tamma M-L, Waser B, et al. Evaluation of a 1,4,7,10-tetraazacyclododecane-1,4,7,10-tetraacetic acid-conjugated bombesin-based radioantagonist for the labeling with single-photon emission computed tomography, positron emission tomography, and therapeutic radionuclides. Clin Cancer Res [Internet]. 2009 Aug 15 [cited 2014 Feb 22];15(16):5240–9. Available from: http://www.ncbi.nlm.nih.gov/pubmed/19671861

84. Abiraj K, Mansi R, Tamma M-L, Forrer F, Cescato R, Reubi JC, et al. Tetraamine-derived bifunctional chelators for technetium-99m labelling: synthesis, bioconjugation and evaluation as targeted SPECT

imaging probes for GRP-receptor-positive tumours. Chem A Eur J [Internet]. 2010 Feb 15 [cited 2014 Feb 21];16(7):2115–24. Available from: http://www.ncbi.nlm.nih.gov/pubmed/20066690

85. Cescato R, Maina T, Nock B, Nikolopoulou A, Charalambidis D, Piccand V, et al. Bombesin receptor antagonists may be preferable to agonists for tumor targeting. J Nucl Med [Internet]. 2008 Feb [cited 2014 May 19];49(2):318–26. Available from: http://www.ncbi.nlm.nih.gov/pubmed/18199616

86. Mansi R, Wang X, Forrer F, Waser B, Cescato R, Graham K, et al. Development of a potent DOTA-conjugated bombesin antagonist for targeting GRPr-positive tumours. Eur J Nucl Med Mol Imaging [Internet]. 2011 Jan [cited 2014 Feb 22];38(1):97–107. Available from: http://www.ncbi.nlm.nih.gov/pubmed/20717822

87. Abiraj K, Mansi R, Tamma M-L, Fani M, Forrer F, Nicolas G, et al. Bombesin antagonist-based radioligands for translational nuclear imaging of gastrin-releasing peptide receptor-positive tumors. J Nucl Med [Internet]. 2011 Dec [cited 2014 Feb 22];52(12):1970–8. Available from: http://www.ncbi.nlm.nih.gov/pubmed/22080443

88. Yang M, Gao H, Zhou Y, Ma Y, Quan Q, Lang L, et al. F-Labeled GRPR Agonists and Antagonists : A Comparative Study in Pros- tate Cancer Imaging. Theranostic. 2011;1(1):220–9.

89. Lane, Stephanie R. Veerendra, Bhadrasetty L. Rold T, Sieckman, Gary L. . Hoffman TJ, Jurisson SS, Smith CJ. 99mTc(CO)3-DTMA bombesin conjugates having high affinity for the GRP receptor. Nucl Med Biol. 2008;35(3):263–72.

90. Armarego, W.L.F., Perrin DD. Purification of Laboratory Chemicals. 4th ed. Elsevier; 1996.

91. Alberto R. New Organometallic Technetium Complexes for Radiopharmaceutical Imaging. In: Krause W, editor. Contrast Agents III Radiopharmaceuticals - From Diagnostics to Therapeutics. Springer; 2005.

92. Fulmer GR, Miller AJM, Sherden NH, Gottlieb HE, Nudelman A, Stoltz BM, et al. NMR Chemical Shifts of Trace Impurities: Common Laboratory Solvents, Organics, and Gases in Deuterated Solvents Relevant to the Organometallic Chemist. Organometallics [Internet]. American Chemical Society; 2010;29(9):2176–9. Available from: http://dx.doi.org/10.1021/om100106e\nhttp://pubs.acs.org/doi/abs/10.1021/om100106e

93. Walker JM, editor. The Protein Protocols Handbook. 2nd Editio. Totowa, New Jersey: HUMANA PRESS; 2002.

94. Liu GZ, Hnatowich DJ. Labeling biomolecules with radiorhenium - A review of the bifunctional chelators. Anti-Cancer Agent Me. 2007;7(3):367–77.

95. Friedman M. Applications of the Ninhydrin Reaction for Analysis of AminoAcids, Peptides, and Proteins to Agricultural and Biomedical Sciences. J Agric Food Chem. 2004;52:385–406.

96. Novabiochem. Peptide synthesis 2012/2013. Merck, editor.

97. Moura C, Vítor RF, Maria L, Paulo A, Santos IC, Santos I. Rhenium(V) oxocomplexes with novel pyrazolyl-based N4- and N3S-donor chelators. Dalt Trans. 2006;(47):5630–40.

98. Englandera SW, Kallenbach NR. Hydrogen exchange and structural dynamics of proteins and nucleic acids, Quarterly. Rev Biophys. 1983;16(04):521–655.

99. Green MD, Long TE. Designing Imidazole-Based Ionic Liquids and Ionic Liquid Monomers for Emerging Technologies. J Macromol Sci Part C Polym Rev [Internet]. 2009 Oct 30 [cited 2014 Jul 11];49(4):291–314. Available from: http://www.tandfonline.com/doi/abs/10.1080/15583720903288914

100. Campello MPC, Lacerda S, Santos IC, Pereira G a, Geraldes CFGC, Kotek J, et al. Lanthanide(III) complexes of 4,10-bis(phosphonomethyl)-1,4,7,10-tetraazacyclododecane-1,7-diacetic acid (trans-H6do2a2p) in solution and in the solid state: structural studies along the series. Chem A Eur J

[Internet]. 2010 Jul 26 [cited 2014 Jun 17];16(28):8446–65. Available from: http://www.ncbi.nlm.nih.gov/pubmed/20540046

101. Esteves T, Marques F, Paulo A, Rino J, Nanda P, Smith CJ, et al. Nuclear targeting with cell-specific multifunctional tricarbonyl M(I) (M is Re, (99m)Tc) complexes: synthesis, characterization, and cell studies. J Biol Inorg Chem [Internet]. 2011 Dec [cited 2014 May 29];16(8):1141–53. Available from: http://www.ncbi.nlm.nih.gov/pubmed/21706254

102. Esteves T, Xavier C, Gama S, Mendes F, Raposinho PD, Marques F, et al. Tricarbonyl M(I) (M = Re, (99m)Tc) complexes bearing acridine fluorophores: synthesis, characterization, DNA interaction studies and nuclear targeting. Org Biomol Chem [Internet]. 2010 Sep 21 [cited 2014 Jun 17];8(18):4104–16. Available from: http://www.ncbi.nlm.nih.gov/pubmed/20648265

103. Frier M, Perkins A. Nuclear Medicine in Pharmaceutical Research. 2002nd ed. E-Library T& F, editor. 1999.

104. Merrifield RB. Solid Phase Peptide Synthesis. I. The Synthesis of a Tetrapeptide. J Am Chem Soc. 1963;85(14):2149–54.

105. Stawikowski M, Fields GB. Introduction to Peptide Synthesis. Curr Protoc Protein Sci. 2002;1–17.

106. Erlélyi M, Gogoll A. Rapid Microwave-Assisted Solid Phase Peptide Synthesis. Synthesis (Stuttg). 2002;1(11):1592–6.

107. Pedersen SL, Tofteng a P, Malik L, Jensen KJ. Microwave heating in solid-phase peptide synthesis. Chem Soc Rev [Internet]. 2012 Mar 7 [cited 2014 Jun 4];41(5):1826–44. Available from: http://www.ncbi.nlm.nih.gov/pubmed/22012213

108. Stokel K. Understanding the Functional Nature of Cancer: The Value of PET [Internet]. Life Extension Magazine. 2012 [cited 2014 Jul 3]. Available from: http://www.lef.org/magazine/mag2012/jul2012_Value-Of-PET_01.htm

109. Karpacho AP, Kuell CS. Mono-protected diamines. N-tert-butoxycarbonyl-α,ω- alkanediamines from α,ω-alkanediamines. Synth Comm. 1990;(20):2559–64.

110. Feagin T a, Shah NI, Heemstra JM. Convenient and scalable synthesis of fmoc-protected Peptide nucleic Acid backbone. J Nucleic Acids [Internet]. 2012 Jan [cited 2014 May 23];2012(6):354549. Available from: http://www.pubmedcentral.nih.gov/articlerender.fcgi?artid=3400375&tool=pmcentrez&rendertype=abstract

111. Enders D, Geibel G, and Osborne S. Diastereo- and Enantioselective Total Synthesis of Stigmatellin A. Chem Eur J. 2000;6:1302–9.